

The Institute for Plant Nutrition and Soil Science
of the Christian-Albrechts-Universität Kiel

**Influence of static and cyclic loading including spatial variation
caused by artificially vertical holes on changes in soil pore function,
gas transport and hydraulic properties**

Dissertation
submitted for the Doctoral Degree
awarded by the Faculty of Agricultural and Nutritional Sciences
of the
Christian-Albrechts-Universität Kiel

submitted

M.Sc. Xiafei Zhai

born in Henan, China

Kiel, 2019

Dean: Prof. Dr. Christian Henning

1. Examiner: Prof. Dr. Rainer Horn

2. Examiner: Prof. Dr. Rainer Duttmann

Day of Oral Examination: 26.06.2019

TABLE OF CONTENT

LIST OF TABLES.....	VII
LIST OF FIGURES.....	VIII
LIST OF ABBREVIATIONS AND SYMBOLS.....	XIII
1 SUMMARY.....	1
2 ZUSAMMENFASSUNG.....	5
3 GENERAL INTRODUCTION.....	9
3.1 Types and causes of soil compaction.....	9
3.2 Impact factors of soil deformation.....	11
3.2.1 soil internal factors, which are influenced by nature of soil properties such as initial bulk density, texture (content and types of clay minerals), soil organic matter, initial water content or matric potential and structure (aggregation).....	12
3.2.2 soil external factors depend on the magnitude, duration, numbers/frequency and the speed of loading.....	14
3.3 The effect of soil compaction on soil properties.....	15
3.3.1 Pore functions.....	16
3.3.2 Gas transport.....	18
3.3.3 Hydraulic properties.....	23
3.4 References.....	30
4 OBJECTIVES.....	41
5 Effect of static and cyclic loading including spatial variation by vertical holes on changes in soil aeration.....	45
5.1 Abstract.....	45
5.2 Introduction.....	46
5.3 Materials and methods.....	47
5.3.1 Soil sampling and properties.....	47
5.3.2 Sample preparation.....	48
5.3.3 Compaction experiment.....	49
5.3.4 Measurements of air permeability and gas diffusivity.....	49
5.3.5 Models for gas transport prediction and pore geometry indexes.....	50
5.3.6 Statistical analyses.....	51
5.4 Results and discussion.....	52
5.4.1 Total porosity.....	52
5.4.2 Air-filled porosity.....	53
5.4.3 Air permeability.....	54
5.4.4 Relative diffusion coefficient.....	56
5.5 Models for gas transport prediction.....	57
5.6 Conclusion.....	58
5.7 Acknowledgement.....	59
5.8 References.....	59
6 Dynamics of pore functions and gas transport parameters in artificially ameliorated soils due to static and cyclic loading.....	63

TBALE OF CONTENT

6.1 Abstract.....	63
6.2 Introduction.....	63
6.3 Material and methods.....	66
6.3.1 Soil sampling and properties.....	66
6.3.2 Sample preparation.....	67
6.3.3 Compaction experiments.....	67
6.3.4 Measurements of gas transport and pore functions.....	68
6.3.5 Statistical analyses.....	69
6.4 Results.....	69
6.4.1 The effect of type and magnitude of loading on pore functions and gas transport.	69
6.4.2 The relationship between pore functions and gas transport under various stress applications.....	73
6.4.3 The effect of artificial vertical pores on pore functions and gas transport for a given stress application.....	75
6.5 Discussion.....	78
6.5.1 The effect of static loading on pore functions and gas transport.....	78
6.5.2 The effect of cyclic loading on pore functions and gas transport.....	81
6.5.3 The effect of loading intensity on pore functions and gas transport.....	81
6.5.4 The effect of soil structure (artificial vertical pores) on pore functions and gas transport.....	82
6.6 Conclusion.....	84
6.7 Acknowledgement.....	84
6.8 References.....	84
7 Influence of static and cyclic loading on mechanical and hydraulic properties of soils with different textures and matric potentials.....	91
7.1 Abstract.....	91
7.2 Introduction.....	92
7.3 Material and methods.....	96
7.3.1 Soil sampling and properties.....	96
7.3.2 Sample preparation.....	96
7.3.3 Compaction experiment.....	97
7.3.4 Measurements of mechanical and hydraulic properties.....	97
7.3.5 Models of hydraulic properties and pore functions.....	97
7.4 Results.....	101
7.4.1 Water retention curve.....	101
7.4.2 Time- and stress-dependent change in mechanical properties (vertical displacement) for each treatment after each stress application.....	103
7.4.3 Time- and stress-dependent change in hydraulic properties for each treatment after each stress application.....	106
7.4.4 The relationships between mechanical and hydraulic deformation for a given treatment.....	110
7.4.5 Consequences of stress application on effective stress.....	113
7.5 Discussion.....	115
7.5.1 The effect of loading type on soil deformation for a given compaction level.....	115

TBALE OF CONTENT

7.5.2 The effect of loading intensity on soil deformation after each stress application.....	119
7.5.3 What are the consequences on soil strength after each stress application.....	120
7.6 Conclusions.....	121
7.7 Acknowledgement.....	122
7.8 References.....	122
8 GENERAL DISCUSSION.....	129
8.1 The effect of static loading on soil physical properties.....	129
8.2 The effect of the further cyclic loading on soil physical properties.....	133
8.3 The effect of soil structure (artificially vertical holes) on soil physical properties.....	134
8.4 References.....	136
9 CONCLUSIONS.....	139
ACKNOWLEDGEMENT.....	141
CURRICULUM VITAE.....	143

LIST OF TABLES

Table 3-1 Three main gas transport mechanisms in soils.....	18
Table 3-2 Classical models for predicting relative gas diffusion coefficient.....	23
Table 5-1 Basic physical and chemical soil properties of studied soils.....	48
Table 5-2 Arithmetic Means and standard deviation of pore continuity (C_2) and tortuosity (τ) indexes for all treatments at each procedure.....	55
Table 6-1 Basic physical and chemical properties of studied arable soils.....	66
Table 7-1 The extent of changes in effective saturation (S_e), pore water pressure (p) and effective stress (σ') for all treatments after each stress application under all applied stresses (50, 100 and 200 kPa).....	114

LIST OF FIGURES

Fig.3-1 Simplified model of soil pores arrangement for gas transport (from Kuncoro et al., 2014b).....19

Fig.3-2 Different zones of typical soil water retention curve.....24

Fig.3-3 Model of hydraulic conductivity as a function of suction.....26

Fig.5-1 Schematic chart of the experiments.....50

Fig.5-2 Stress application and vertical holes effects on changes of (a) total porosity and (b) air-filled porosity (ϵ_a) in each treatment. X axis: B.L. = before loading; A.SL. = after static loading; A.CL. =after cyclic loading; A.Hs&B.SL.= after having drilled holes and before static loading; A.Hs&A.SL. = after having drilled holes and after static loading.....52

Fig.5-3 Stress application and vertical holes effects on changes of (a) air permeability (K_a) and (b) relative gas diffusivity (D_s/D_o) in each treatment. X axis: B.L. = before loading; A.SL. = after static loading; A.CL. =after cyclic loading; A.Hs&B.SL.= after having drilled holes and before static loading; A.Hs&A.SL. = after having drilled holes and after static loading.....54

Fig.5-4 Relationship between air-filled porosity (ϵ_a) and air permeability (K_a) before having drilled vertical holes (a) and after having drilled vertical holes (b). The open symbols represent measured data for all samples. The solid lines represent the linear regression for all data.....57

Fig.5-5 Relationship between air-filled porosity (ϵ_a) and relative gas diffusivity (D_s/D_o) before having drilled vertical holes (a) and after having drilled vertical holes (b). The open symbols represent the measured data for all samples. The solid and dashed lines represent the linear and exponential regression for all data, respectively.....58

Fig.6-1 Schematic diagram of the position of vertical holes on the cross-section of soil core.....68

Fig.6-2 Effects of stress application and vertical holes at three different levels (50, 100 and 200 kPa) for sand soil at the matric potential of -60 hPa on changes of (a) air-filled porosity; (b) pore continuity; (c) pore tortuosity; (d) air permeability and (e) relative gas diffusivity. X axis: B.L. = before loading; A.SL. = after static loading; A.CL. = after cyclic loading, A.Hs +

LIST OF FIGURES

B.SL. = after having drilled holes and before static loading; A.Hs + A.SL. = after having drilled holes and after static loading. Letters indicate significant differences on compaction levels (*P < 0.05).....70

Fig.6-3 Effects of stress application and vertical holes at three different levels (50, 100 and 200 kPa) for clay loam soil at the matric potential of -300 hPa on changes of (a) air-filled porosity; (b) pore continuity; (c) pore tortuosity; (d) air permeability and (e) relative gas diffusivity. X axis: B.L. = before loading; A.SL. = after static loading; A.CL. = after cyclic loading, A.Hs + B.SL. = after having drilled holes and before static loading; A.Hs + A.SL. = after having drilled holes and after static loading. Letters indicate significant differences on compaction levels (*P < 0.05).....72

Fig.6-4 The relationships among air-filled porosity, pore continuity or pore tortuosity for all the measured data in sand soil at the matric potential of -60 hPa.....73

Fig.6-5 Gas transport parameters (air permeability and relative gas diffusivity) as a function of pore functions properties (air-filled porosity, pore continuity and pore tortuosity) for all the measured data in sand soil at the matric potential of -60 hPa.....74

Fig.6-6 Pore continuity and pore tortuosity as a function of air-filled porosity for all treatments under all compaction levels after static loading before and after having drilled vertical holes.....75

Fig.6-7 Air permeability as a function of air-filled porosity and pore continuity for all treatments under all compaction levels after static loading before and after having drilled vertical holes. The solid line represents the linear regression for all data in Fig.6-7a. The linear regressions for sand (solid line), silt loam (dash line) and clay loam (dot line) soil at -300 hPa matric potential are shown in Fig.6-7c, respectively.....76

Fig.6-8 Relative gas diffusivity as a function of air-filled porosity and pore tortuosity for all treatments under all compaction levels after static loading before and after having drilled vertical holes. The solid line represents the linear regression for all data in Fig.6-8a and 6-8b.....77

Fig.6-9 Air permeability as a function of relative gas diffusivity for all treatments under all compaction levels after static loading before and after having drilled vertical holes. The solid line represents the linear regression for all data in Fig.6-9a.....78

LIST OF FIGURES

Fig.7-1 The effect of compaction levels (50, 100 and 200 kPa) on soil water retention curve (volumetric water content as a function of matric suction) for five different treatments (sand soil (-60 hPa), silt loam soil (-60 hPa), sand soil (-300 hPa), silt loam soil (-300 hPa), clay loam soil (-300 hPa)) after static loading (A.SL.), cyclic loading (A.CL.) and static loading with vertical holes (A.Hs).....100

Fig.7-2 The effect of compaction levels (50, 100 and 200 kPa) on van Genuchten parameter α for (a) sand soil (-60 hPa), (b) silt loam soil (-60 hPa), (c) sand soil (-300 hPa), (d) silt loam soil (-300 hPa) and (e) clay loam soil (-300 hPa) before loading (B.L.) and after static loading (A.SL.), cyclic loading (A.CL.) and static loading with vertical holes (A.Hs).....101

Fig.7-3 The effect of compaction levels (50, 100 and 200 kPa) on van Genuchten parameter n for (a) sand soil (-60 hPa), (b) silt loam soil (-60 hPa), (c) sand soil (-300 hPa), (d) silt loam soil (-300 hPa) and (e) clay loam soil (-300 hPa) before loading (B.L.) and after static loading (A.SL.), cyclic loading (A.CL.) and static loading with vertical holes (A.Hs).....102

Fig.7-4 The effect of compaction levels (50, 100 and 200 kPa) on volumetric water content θ_w for (a) sand soil (-60 hPa), (b) silt loam soil (-60 hPa), (c) sand soil (-300 hPa), (d) silt loam soil (-300 hPa) and (e) clay loam soil (-300 hPa) before (B.SL.) and after (A.SL.) static loading, before (B.CL.) and after (A.CL.) cyclic loading, before (B.Hs) and after (A.Hs) static loading with vertical holes.....103

Fig.7-5 Time- and stress-dependent change in vertical displacement for (a) sand soil (-60 hPa), (b) silt loam soil (-60 hPa), (c) sand soil (-300 hPa), (d) silt loam soil (-300 hPa) and (e) clay loam soil (-300 hPa) during static loading (S.L.), cyclic loading (C.L.) and static loading with vertical holes (Hs). Vertical solid and dotted lines distinguish different type of stress application and loading and unloading process for a given stress application, respectively.....104

Fig.7-6 Vertical displacement (a) and pore water pressure (b) as a function of the first 5 cycles under three compaction levels (50, 100 and 200 kPa) for sand soil at the matric potential of -60 hPa.....105

Fig.7-7 Time- and stress-dependent change in pore water pressure for (a) sand soil (-60 hPa), (b) silt loam soil (-60 hPa), (c) sand soil (-300 hPa), (d) silt loam soil (-300 hPa) and (e) clay loam soil (-300 hPa) during static loading (S.L.), cyclic loading (C.L.) and static loading with

LIST OF FIGURES

vertical holes (Hs). Vertical solid and dotted lines distinguish different type of stress application and loading and unloading process for a given stress application, respectively.....106

Fig.7-8 Time- and stress-dependent change in saturated hydraulic conductivity K_s for (a) sand soil (-60 hPa), (b) silt loam soil (-60 hPa), (c) sand soil (-300 hPa), (d) silt loam soil (-300 hPa) and (e) clay loam soil (-300 hPa) during static loading (S.L.), cyclic loading (C.L.) and static loading with vertical holes (Hs). Vertical solid and dotted lines distinguish different type of stress application and loading and unloading process for a given stress application, respectively.....108

Fig.7-9 Time- and stress-dependent change in unsaturated hydraulic conductivity K for (a) sand soil (-60 hPa), (b) silt loam soil (-60 hPa), (c) sand soil (-300 hPa), (d) silt loam soil (-300 hPa) and (e) clay loam soil (-300 hPa) during static loading (S.L.), cyclic loading (C.L.) and static loading with vertical holes (Hs). Vertical solid and dotted lines distinguish different type of stress application and loading and unloading process for a given stress application, respectively.....109

Fig.7-10 Relationship between vertical displacement Δx and the absolute value of the change in pore water pressure $\Delta\psi$ after compaction compared to before under different compaction levels (50, 100 and 200 kPa) for five different treatments (sand soil (-60 hPa), silt loam soil (-60 hPa), sand soil (-300 hPa), silt loam soil (-300 hPa), clay loam soil (-300 hPa)) during static loading (A.SL.), cyclic loading (A.CL.) and static loading with vertical holes (A.Hs).....111

Fig.7-11 Relationship between vertical displacement Δx and water flux q after compaction compared to before under different compaction levels (50, 100 and 200 kPa) for five different treatments (sand soil (-60 hPa), silt loam soil (-60 hPa), sand soil (-300 hPa), silt loam soil (-300 hPa), clay loam soil (-300 hPa)) during static loading (A.SL.), cyclic loading (A.CL.) and static loading with vertical holes (A.Hs).....112

Fig.7-12 Degree of saturation χ (a-c) and effective stress σ' (d-f) as a function of stress applications (before loading (B.L.) and after static loading (A.SL.), cyclic loading (A.CL.) and static loading with vertical holes (A.Hs)) for five different treatments (sand soil (-60 hPa),

LIST OF FIGURES

silt loam soil (-60 hPa), sand soil (-300 hPa), silt loam soil (-300 hPa), clay loam soil (-300 hPa) under different compaction levels (50, 100 and 200 kPa).....113

LIST OF ABBREVIATIONS AND SYMBOLS

ABBREVIATIONS:

B.L.	Before loading
A.SL.	After static loading
A.CL.	After cyclic loading
A.Hs & B.SL.	After having drilled holes and before static loading
A.Hs & A.SL.	After having drilled holes and after static loading
WRC	Water retention curve
HFC	Hydraulic conductivity function

SYMBOLS:

K_a	Air permeability (m^2)
q'	Volumetric flow rate ($m^3 s^{-1}$)
η	Air dynamic viscosity (Pa s)
Δp	Pneumatic pressure difference (Pa)
L_s	Length of the sample (m)
A_s	Cross sectional area of the cylindric sample (m^2)
V_s	Volume of the sample (m^3)
D_s	Apparent soil gas diffusion coefficient ($m^2 s^{-1}$)
D_s/D_o	Relative gas diffusion coefficient
ΔC	Oxygen concentration difference between two chambers ($g m^{-3}$)
C_{eq}	Final oxygen concentration at equilibrium ($g m^{-3}$)
t	Time (s)
C_2	Pore continuity index (m^2)
L	Average capillary tube length (m)
L_e	Porous media (soil sample) length (m)
τ	Index of tortuosity

LIST OF ABBREVIATIONS AND SYMBOLS

θ_s	Saturated water content ($\text{cm}^3 \text{ cm}^{-3}$)
θ_r	Residual water content ($\text{cm}^3 \text{ cm}^{-3}$)
h	Matric suction (the negative value of matric potential) (hPa)
α, n and m	Empirical fitting parameters of soil water retention curve (WRC)
$S_e(h)$	Effective saturation at matric suction h
K_s	Saturated hydraulic conductivity (cm s^{-1})
$K(h)$	Unsaturated hydraulic conductivity (cm s^{-1})
g	Unit weight of permeant
μ	Viscosity of permeant
C_{K-C}	Kozeny-Carman empirical coefficient
S_o	Specific surface area per unit volume of particles (cm^{-1})
e	void ratio ($\text{cm}^3 \text{ cm}^{-3}$)
q	Hydraulic flux (cm s^{-1})
Δh	Difference in matric suction between after and before loading
Δx	Vertical displacement after loading
σ'	Effective stress (kPa)
σ	Normal stress (kPa)
u_a	Pore air pressure (kPa)
u_w	Pore water pressure (kPa)
χ	Factor which depends on the degree of saturation

1 SUMMARY

Soil compaction is regarded as one of the most serious problems resulting in soil degradation in modern agriculture. The overuse of machinery (an increase in weight and frequency of wheeling) has been identified as the main reason contributing to soil compaction. Soil structure has a major influence on the ability of soil functions (e.g. soil aeration and water transport). Therefore, in this study, we hypothesized that soil compaction under static and cyclic loading and the amelioration of soil structure by artificially drilled vertical holes can obviously affect soil physical properties.

To better understand the interaction between soil physical properties and the stress strain behavior as well as their influence on pore functions, soil aeration and gas fluxes, the capacity (total porosity and air-filled porosity ε_a) and intensity (pore continuity index C_2 and tortuosity τ , air permeability K_a and gas diffusion coefficient D_s/D_o) properties of pore functions were investigated. Repacked, homogenized soils (bulk density of 1.4 g cm^{-3}) with three different textures (sand, silt loam and clay loam) at two matric potential (-60 and -300 hPa) under two types of loading (static and cyclic loading) and three compaction levels (50, 100 and 200 kPa) were analyzed. Plastic soil deformation is a reaction of a soil to an applied stress, if the internal soil strength is exceeded. Mechanical or hydraulic processes can either cause it, while the extent of soil deformation depends on the external stress/internal strength ratio. Therefore, vertical displacement and pore water pressure were also detected by our experiment.

In the case of static loading, there was a close relationship between soil pore functions and gas transport. Soil deformation resulted in the reduction of the quantity and quality of air-filled pores, and thus restricted the ability of soil aeration (a decrease in K_a and D_s/D_o). Vertical displacement and changes in pore water pressure increased with the applied vertical stress for treatments at a given soil texture and initial matric potential. Under the same compaction level, soil mechanical deformation was more obvious at high matric potential (-60 hPa) than at low matric potential (-300 hPa). Regardless of initial matric potential, the finer-textured soils tended to have a higher vertical displacement, especially under a higher compaction level. The time-dependent vertical displacement curves for all treatments at all compaction levels were similar in shape but different in scale. An intensive vertical

displacement was observed in the beginning of stress application, while it tended to constantly slightly decline with increasing loading time. However, different situations of time-dependent change in pore water pressure were found due to different soil internal strength resulting from soil texture and initial matric potential. In the case of subsequent cyclic loading, the volume of macropores (ε_a) decreased, but the functional quality of air-filled pores was improved (an increase in pore continuity index C_2 and a decrease in pore tortuosity τ). Therefore, a combined effect of soil pore capacity and intensity properties resulted in a minor change in K_a and D_s/D_o after cyclic loading. Vertical displacement increased during loading but an elastic rebound was observed to some extent (depending on the treatments) during unloading, which principally resulted in an increase in pore water pressure during loading and a decrease during unloading. The frequency of loading also played an important role in soil deformation, e.g. soil deformation increased with increasing number of cycles.

In the case of changes in soil structure, the preparation of artificially vertical holes caused an increase in pore continuity C_2 and a significant decrease in pore tortuosity τ , while air-filled porosity ε_a remained almost the same because the total volume of holes was only 0.4 cm³. Consequently, the negative effect of soil compaction on K_a and D_s/D_o was alleviated. The deterioration of soil pore functions, and especially capacity properties occurred after static loading. Due to the existence of highly conductive macropores for preferential mass flow resulting from the artificially vertical holes, there were minor differences in K_a but distinct differences in D_s/D_o among all treatments. Due to an increase in soil strength caused by previous stress applications (static and subsequent cyclic loading), soils became stronger to withstand the applied stresses, which resulted in a reduction of the extent of soil deformation (vertical displacement and changes in pore water pressure) during static loading with vertical holes compared to without.

A combined effect of the degree of pore water saturation and changes in pore water pressure, resulted in weakened soils which reduced the resistance to external forces for treatments at -60 hPa matric potential. However, soils became more stable to external stresses for treatments at -300 hPa matric potential after each stress application, which can be reflected by an increased effective stresses.

1 SUMMARY

Hence, appropriate management of soils under favourable soil conditions can ameliorate the negative effects resulting from soil compaction. For example, the agricultural field operations should be employed during the more negative matric potential (at least -300 hPa). Meanwhile, the frequency and duration of the usage of agricultural field operations should be also minimized. In addition, improving soil structure (such as adding artificially vertical holes in soils) can improve the ability of soil aeration and water transport for the compacted soils.

2 ZUSAMMENFASSUNG

In der modernen Landwirtschaft ist Bodenverdichtung als ein schwerwiegendes Problem anzusehen, das mit für die Degradation der Böden verantwortlich ist. Die Überbeanspruchung von Maschinen hinsichtlich steigender Maschinengewichte und Überfahungshäufigkeit ist einer der Hauptursache für die Entstehung von Bodenverdichtung. Die Bodenstruktur hat einen maßgeblichen Einfluss auf die Bodenfunktionalität (z.B. Bodenluft- und -wasserhaushalt). In dieser Arbeit werden daher die Veränderungen der bodenphysikalischen Eigenschaften durch Bodenverdichtung (statische und dynamische mechanische Belastungen) und Strukturmeliormationsmaßnahmen in Form von künstlich erzeugten vertikalen Röhren näher betrachtet.

Um die Zusammenhänge zwischen bodenphysikalischen Eigenschaften und dem Spannungs-Verformungsverhalten sowie deren Einfluss auf die Bodenfunktionseigenschaften wie Bodenbelüftung und Gasflüsse besser zu verstehen, wurden Porenkapazitäts- (Gesamtporosität und luftgefülltes Porenvolumen) und Porenintensitätsgrößen (Porenkontinuität Index C_2 , Porentortuosität τ , Luftleitfähigkeit K_a und Sauerstoffdiffusionskoeffizient D_s/D_0) untersucht. Die Untersuchungen wurden an homogenisierten Bodenproben (Lagerungsdichte = $1,4 \text{ g cm}^{-3}$) unterschiedlicher Textur (Sand sowie schluffiger und toniger Lehm) und variierendem Vorentwässerungsgrad (Matrixpotential von - 60 und -300 hPa) anhand von mechanischen Belastungsversuchen (statisch und zyklisch) mit 3 Laststufen (50, 100 und 200 kPa) durchgeführt. Plastische Bodenverformungen sind Folge von Spannungseinträgen, die die interne Bodenstabilität überschreiten. Das Ausmaß der Bodendeformation hängt daher von dem Verhältnis zwischen externem Spannungseintrag und interner Bodenstabilität ab, das wiederum durch mechanische und hydraulische Prozesse beeinflusst wird.

Unter statischer Belastung besteht ein enger Zusammenhang zwischen den Porenfunktionen und Gastransporteigenschaften des Bodens. Die Bodendeformation führte zu einer Reduzierung der Quantität und Qualität von luftgefüllten Poren und damit zu einer Einschränkung der Bodenbelüftung. Vertikale Verformungsprozesse und Änderungen der Porenwasserdrücke verstärkten sich mit zunehmendem vertikalen Spannungseintrag bei

2 ZUSAMMENFASSUNG

gegebener Bodentextur und Matrixpotential der verschiedenen Versuchsvarianten. Bei gleicher Laststufe nahm die Bodendeformation bei höherem (-60 hPa) im Vergleich zum geringeren Matrixpotential (-300 hPa) zu. Unabhängig vom Matrixpotential wiesen die feinkörnigeren Böden eine höhere vertikale Verformung, insbesondere bei hohen Laststufen, auf. Das zeitabhängige vertikale Verformungsverhalten ähnelte sich dabei für die unterschiedlichen Versuchsvarianten im Verlauf, jedoch nicht in der Dimension (Ausmaß der Deformation). Eine deutliche Setzungszunahme wurde dabei zu Beginn der Lastaufbringung beobachtet, während nachfolgend konstant geringere Setzungszunahmen über die Belastungszeit auftraten. Bedingt durch Unterschiede in der internen Bodenstabilität, in Abhängigkeit von der Bodentextur und dem Matrixpotential, konnten allerdings unterschiedliche Szenarien der zeitabhängigen Änderung von Porenwasserdrücken ausgemacht werden.

Unter zyklischer Belastung reduziert sich das Volumen an Makroporen (ϵ_a), während sich die Funktionalität von luftgefüllten Poren verbessert hat (Zunahme des Porenkontinuitätsindex C_2 und Abnahme der Porentortuosität τ). Durch diesen gekoppelten Effekt von Porenkapazitäts- und -intensitätsänderungen sind nur geringe Auswirkungen auf die Parameter K_a und D_s/D_0 festzustellen. Die vertikale Verformung nimmt während der Belastung zu, während bei Entlastung eine unterschiedlich hohe elastische Rückverformung (abhängig von der Variante) eintrat. Dies führte prinzipiell dazu, dass die Porenwasserdrücke während der Belastung anstiegen und während der Entlastung wieder abklagen. Auch die Belastungsfrequenz spielte eine wichtige Rolle für das Verformungsverhalten, was sich in einer zunehmenden Bodendeformation mit steigender Anzahl an Belastungszyklen äußerte.

Hinsichtlich der Bodenstrukturänderungen führte die Präparation von vertikalen Röhren zu einer Zunahme der Porenkontinuität und einer signifikanten Abnahme der Porentortuosität τ , während das luftgefüllte Porenvolumen nahezu konstant blieb, da das Gesamtporenvolumen der vertikalen Röhren nur $0,4 \text{ cm}^3$ beträgt. Dadurch ließ sich der negative Effekt der Bodenverdichtung auf die Parameter K_a und D_s/D_0 mindern. Eine Verschlechterung der Porenfunktionen und insbesondere der Kapazitätskenngrößen erfolgte unter statischer Belastung. Aufgrund des Vorhandenseins von leitfähigen Makroporen für den präferenziellen Massenfluss in Form der vertikalen Röhren konnten geringe Unterschiede in

der K_a , nicht aber in den D_s/D_o -Werten zwischen den Versuchsvarianten festgestellt werden. Durch die durchgeführten statischen und zyklischen Belastungen wurden die untersuchten Bodenproben widerstandsfähiger gegenüber weiteren mechanischen Spannungseinträgen (höhere interne Bodenstabilität), wodurch sich das Ausmaß der Bodendeformation (vertikale Verformung und Änderung der Porenwasserdrücke) für die Versuchsvariante mit künstlichen vertikalen Röhren im Vergleich zu der ohne Röhren verringerte.

Das Zusammenwirken von Porenwassersättigungsgrad und Änderungen der Porenwasserdrücke führte zu instabilen Bodenverhältnissen mit geringerem Widerstand gegenüber externen Spannungseinträgen bei einem Matrixpotential von -60 hPa. Demgegenüber erhöhte sich die Stabilität der Böden bei einem Matrixpotential von -300 hPa nach jeder Belastungsphase, was mit einer Zunahme der effektiven Spannung einherging.

Das bedeutet, ein angepasstes Bodenmanagement kann unter günstigen Bedingungen dazu beitragen den negativen Effekten der Bodenverdichtung entgegenzuwirken. So sollten u.a. Bodenbearbeitungsmaßnahmen auf landwirtschaftlich genutzten Böden unter stärker negativem Matrixpotential (mindestens -300 hPa) durchgeführt werden. Genauso sollte die Überfahungshäufigkeit und -dauer mit landwirtschaftlichen Maschinen reduziert werden. Zusätzlich kann durch Bodenstrukturmeliorationsmaßnahmen (z.B. durch künstlich hergestellte vertikale Röhren) die Bodenbelüftung und der Wassertransport in verdichteten Böden wieder verbessert werden.

3 GENERAL INTRODUCTION

3.1 Types and causes of soil compaction

Globally, soil compaction is one of most harmful processes to threaten soil quality. About 33 million ha of arable land in Europe and 68 million ha worldwide are seriously degraded by soil compaction (Peth et al., 2010). It can be caused naturally due to freezing-thawing (Defosseze and Richard, 2002), swelling-shrinkage (Pagliai et al., 2003) and chemical precipitation (like in Gleysols or Podzols) processes. Soil compaction by anthropogenic processes are induced by external forces such as animal trampling (Hamza and Anderson, 2005) and farm machinery traffic (Horn et al., 1995b). Among these factors, the overuse of machinery has been recognized as the most common reason of soil compaction in agriculture (Saffih-Hdadi et al., 2009; Kuncoro et al., 2014a). Meanwhile, the problem of soil compaction has been also worsened by inappropriate management of soil in unfavourable soil conditions (Hamza and Anderson, 2005).

Two types of loading events can lead to soil compaction. Static loading is defined as a given load, which is constant with time (no change in magnitude and position). However, cyclic (or dynamic) loading reflects a loading path that exhibits a degree of regularity in terms of both time and magnitude. In the laboratory, the test procedure is employed with a constant loading frequency and magnitude. If considering field conditions, the time between loading-unloading events is usually not at all constant. Hence, the term “repeated loading” is used instead of “cyclic loading” in the field situation (Peth and Horn, 2006).

Soil compaction caused by traffic loading may result in a change in volume of the soil under both normal and shear stresses, below the contact surface between soil and tire (Horn and Rostek, 2000). Two different processes may cause the volume changes due to mechanical stress: according to Dexter and Tanner, (1974) and Cambi et al., (2015), compaction is defined as the process when soil deformation occurs with expulsion of air. This process mostly leads to the decrease of air-filled voids, while the reduction of water content is negligible small. Consolidation is the process when soil deformation coincides with the expulsion of water. This process mainly happens by gradual drainage of water from the soil

pores under continuous stress application. It mainly happens in soils with higher water content, especially at or near saturation. Hydraulic stresses can result in soil shrinkage, which is defined as the specific volume change of soil relative to its water content and is mainly due to the existence of swelling clay. The opposite process is swelling due to changes in water content (Glinski et al., 2011). The relationship between the change of soil volume and the mechanical or hydraulic stresses is expressed as soil strain-stress relation and soil shrinkage-swelling relation, respectively (Peng et al., 2012). In contrast, soil shearing results in no change in soil total porosity, but it changes the angles between soil particles and destroys the continuity of macropores (Horn et al., 1995b; Alaoui et al., 2011). It is mainly caused by the slipping effect of the driving tires or chains or by kneading strains from animals (hoof treading, scratching) (Blume et al., 2016).

Soil compaction not only can change many properties and processes in the topsoil, e.g. retention, saturated and unsaturated hydraulic conductivity, air content and transport of gases, root growth and function, nutrient transport and uptake and soil workability. As the weight of agricultural machinery and wheeling frequency increases, this may also lead to stress propagation down to deeper soil layers (subsoil). Botta et al. (2006) found that the maximum depth of subsoil compaction attainable by conventional equipment was about 600 mm. Wiermann et al. (2000) reported that increasing wheel loads and repeated passes resulted in increasing structural degradation of the subsoil. Zink et al. (2011) documented a significantly stronger decrease in the subsoil (40 and 60 cm) air-filled pore space after ten compared to a single wheel pass. The effect of topsoil compaction may be partly ameliorated by tillage managements and natural regeneration processes such as drying-wetting cycles (Bullock et al., 1985; Werner and Werner, 2001; van den Akker and Hoogland, 2011) while subsoil compaction can persist for decades (Alakukku, 1996b; Berisso et al., 2012). Since subsoil compaction is cumulative and permanent (Håkansson and Reeder, 1994; Horn et al., 1995b), the irreversible deterioration of subsoil structure and pore functions will take place for a very long time (Zink et al., 2011; Naveed et al., 2016).

Compaction by traffic has been identified as a major process that affects the production and the environment by changing the soil physical properties. Quantifying the soil damage by compaction is therefore of importance when establishing strategies for farming and forest

management on a local scale and for environmental protection measures on a larger scale. The evaluation of the soil compaction effects on soil physical properties is generally based on the consideration of the changes in soil mechanical strength, aeration and hydraulic properties (Horn et al., 1995b; Lipiec and Hatano, 2003; Schäfer- Landefeld et al., 2004).

3.2 Impact factors of soil deformation

Soil deformation comprises the process of soil compaction and the change in the structure of the soil's three-phase system caused by shearing (Blume et al., 2016). Therefore, soil deformation is the response of a soil to an applied stress, which could be either mechanical or hydraulic. Compaction and deformation are coupled processes: soil deformation is a function of soil stress and soil strength (Glinski et al., 2011). If the internal soil strength is exceeded by external stresses, soil deformation is considered as plastic, i.e. irreversible and permanent, even when the external stresses are removed. When soil is subjected to the external stresses smaller than the internal soil strength, soils react with elastic deformation, which means that the majority of soil deformation is recoverable when the external stresses are removed (Keller et al., 2013; Peth et al., 2010; Destain et al., 2016). However, during cyclic loading, a slight plastic deformation may also take place (Peth and Horn, 2006; Larson and Gupta, 1980; Krümmelbein et al., 2008).

Our understanding of deformation processes in arable soil is still limited. One reason might be that in soil compaction research, the major focus has been on the agronomic and environmental impacts of compaction, rather than on the soil deformation process itself. In order to understand the impacts of soil compaction on soil functions and crop response, knowledge of the cause and process of soil deformation is needed. Furthermore, improved understanding of the soil deformation processes will promote better predictions of the impact of soil management practices on soil functions (Keller et al., 2013).

Before discussing the impact factors of soil deformation by compaction, some terms used to define dynamic compressive properties should be differentiated.

Stress is defined as force applied to a soil per area. If soil is non-rigid, stress can lead to a change in the volume and/or shape of soil, which is expressed as deformation or strain. In quantitative terms, strength is the maximal stress a given soil can bear without undergoing

failure, or the minimal stress that will cause soil to fail (Glinski et al., 2011). Soil strength can be either increased due to compaction or decreased because of destruction of existing aggregation due to shearing (Horn et al., 1995b). Soil deformation depends on two categories of factors:

3.2.1 soil internal factors, which are influenced by nature of soil properties such as initial bulk density, texture (content and types of clay minerals), soil organic matter, initial water content or matric potential and structure (aggregation).

Every soil or soil horizon has its own inherent strength corresponding to the previous history. In general, the soil is more stable under a given load,

1) the coarser the texture with the same bulk density. In general, clay or silt soils are more sensitive to soil compaction than sandy soils (Hillel, 1998). Horn et al. (1995b) found that silt loam soils with low colloid contents are more susceptible than medium or fine textured loamy and clayey soils at low water contents, while sandy soils are only slightly susceptible to soil compaction.

2) the lower the content and the swelling capacity of clay minerals. The physical properties of soils changes with increasing clay content until the clay content reaches about 30 %. Saffifih-Hdadi et al. (2009) found that the higher the clay content, the higher the soil's capacity to bear greater stresses at higher initial water contents without severe compaction. Among the types of clay minerals, soils dominated by 1:1 type of clay minerals, e.g., kaolinite were less compactible than soils with predominantly 2:1 type clay minerals, e.g. smectite and vermiculite. the higher the valency of the adsorbed cations (monovalent < divalent < trivalent), and the higher the ionic strength, the greater the shearing resistance under a given condition (Warrick, 2002).

3) the higher the organic matter content. Increasing organic matter may increase soil strength and shearing resistance by increasing aggregation formation and stability through organic binding agents, and improving aggregate strength through altering the cohesiveness of inter- and intra-aggregate structure and increasing the friction between particles. However, higher organic matter may reduce maximum soil compactibility through lowering bulk density and increasing rebounding forces and elastic properties to soil, and increasing critical

water content at maximum compactibility by increasing soil water absorption capacity (Logsdon et al., 2013; Ekwue, 1990; Soane, 1990; Hamza and Anderson, 2005).

4) the lower soil water content. As the soil gets drier, the lower its deformability (Soehne, 1958; Richard et al., 1999). Increasing soil water content results in a decrease in the frictional forces between soil particles (Sumner, 1999), and causes a reduction in the permissible ground pressure (Medvedev and Cybulko, 1995), hence soils become more susceptible to compaction. If the soil is too wet, the load support capacity of the soil decreases (Kondo and Dias Junior, 1999), and leads to higher risk of plastic deformation (Hamza and Anderson, 2005; van Asselen et al., 2009).

5) the lower initial matric potential. The effect of matric potential (pore water pressure) on soil strength is governed by the theory of the effective stress, which quantifies the actual forces between the solid particles in the soil per unit area, which have a stabilizing effect.

In saturated soils, the effective stress σ' is defined as the difference between the total stress, σ , and the pore water pressure, u_w .

$$\sigma' = \sigma - u_w \quad (1)$$

In unsaturated soils, the most widely used relationship for the effective stress, σ' , is expressed as (Bishop, 1959):

$$\sigma' = (\sigma - u_a) + \chi(u_a - u_w) \quad (2)$$

where σ' is the effective stress, σ is the normal stress, u_a and u_w is the pore air and water pressure, respectively, and χ is the factor which depends on the degree of saturation (for completely dry soils, $\chi = 0$; while for fully saturated soils, $\chi = 1$).

The pore air pressure is always neglected, because the air fraction generally immediately escapes at the moment the load is exerted. It only plays a role in rare cases, e.g. if air is trapped in pores due to flood irrigation or refilling from a great height during recultivation. Hence, the effective stress mainly depend on the pore water pressure (or matric potential) and the degree of saturation at a given total stress. Soil becomes more sensitive against external stress when the effective stress decreases due to an increase in pore water pressure (positive value). It is in contrast more stable to compaction when the effective stress increases if the reduction of the degree of saturation caused by the decrease in the water-filled pore space

induced by desiccation is lower than the corresponding reduction in the pore water pressure (negative value).

6) the more structured soil or the stronger the aggregation. The less structured soils are more susceptible to soil compaction. Baumgartl and Horn (1991) found that the homogenized soil shows lower shear strength, and smaller cohesion and angle of internal friction values than the structured soil. At a given soil type, soil strength increases with aggregation (i.e., coherent < prismatic < blocky < crumbly, platy < subangular blocky) (Warrick, 2002). Słowińska-Jurkiewicz and Domzła (1991) observed that the effect of soil compaction on sandy soil is less pronounced, which is related to its homogeneous granular composition which easily reaches the densest particle configuration.

3.2.2 soil external factors depend on the magnitude, duration, numbers/frequency and the speed of loading.

Soil deformation caused by compaction depends not only on soil internal strength but also on the externally applied load. Once the applied load exceeds soil internal strength, soil plastic deformation will take place, because of soil particle displacement and rearrangement. The more complete load-dependent rearrangement of soil structure, the higher is the final soil strength during consecutive loading, and the smaller is the corresponding changes in soil physical properties (Horn and Hartge, 1990). There is a positive linear log-log relationship between the vertical displacement and the applied stress if the soil undergoes virgin compression behavior (Naveed et al., 2016). Furthermore, at the same loading magnitude, soil deformation could be very different with different loading time: the shorter the loading duration, the higher the elastic deformation and the lower the viscous deformation (Ghezzehei and Or, 2001; Keller et al., 2013).

Soil deformation also strongly depends on the speed of wheeling (Hartge, 1994). With increasing speed, the duration of loading and the magnitude of stress decrease, and this means that less compaction effects are produced (Dexter and Tanner, 1974; Horn et al., 1989; Alakukku et al., 2003; Mordhorst et al., 2012). At lower wheeling speed, the shape of the vertical stress curve becomes more smoothly. The higher the wheeling speed at the same high water content, the more stresses could be transmitted to deeper depth, and the more likely

aquaplaning to happen (Horn and Hartge, 1990).

Frequency of wheeling passes plays an important role in soil deformation. During compaction, soil deformation increases with the number of passes (Bakker and Davis, 1995; Hamza and Anderson, 2005; Horn et al., 2003; Keller et al., 2004). According to Peth and Horn (2006), a linear regression curve was found between the decreasing void ratio and increasing the number of cycles. The slope is referred as cyclic compressibility (C_n), where the higher C_n value indicates more pronounced sensitivity against cyclic loading. Peth et al. (2010), Mordhorst et al. (2012) and Reszkowska et al. (2011) have further used this concept. The only first pass has a significant effect on changes in soil stress state, due to soil strength increasing after first loading event. This leads to highest irreversible changes in soil volume and soil structure, and then a significant deformation occurs, especially in the topsoil (Arvidsson and Ristic, 1996; Håkansson, 1994; Lipiec et al., 1992; Mordhorst et al., 2012; Pytka, 2005). Therefore, during cyclic loading, soil deformation is more pronounced during the first pass than after the subsequent passes. Since cyclic loading creates cumulative effects, irreversible soil deformation may be induced by even using a light vehicle with increasing number of passes (Botta et al., 2006). Alakukku et al. (2003) found that a higher loading frequency with a lower applied stress can result in the same effect of soil compaction as a lower loading frequency with a higher applied stress. Campbell et al. (1986) found that even for light-weight traffic, crop yield decreased for each additional wheel pass, due to the alteration of topsoil properties on plant growth. Horn et al. (2003) outlined the complicated processes for soils exposed to repeated wheeling. Pagliai et al. (2003) stated that repeated wheel traffic resulted in further compaction, which occurred due to the strain processes in further stabilization and more pronounced stress attenuation with an increasing number of passes.

3.3 The effect of soil compaction on soil properties

It is well known that compaction not only results in soil deformation but also in a change of pore functions, soil aeration and water transport. To improve our understanding of the impact of compaction on these properties which is necessary to quantify soil structure quality (Pagliai et al., 2003). Both capacity (total porosity, macroporosity and pore size distribution)

and intensity (pore continuity, pore tortuosity, air permeability, gas diffusion and hydraulic conductivity) properties will be discussed as follows.

3.3.1 Pore functions

Soil pore systems can be defined as the ensemble of the voids or spaces existing in a given volume of soil, which guarantees the water, gas and heat exchange, nutrient transport and adsorption as well as an optimal rootability (Glinski et al., 2011).

The soil bulk density and associated total porosity is the most general and frequently used parameter to characterize the state of compactness and physical properties of soil (Assouline, 2006). Soil compressibility described by the shape of the stress-strain curve, is defined as a resistance to a volume decrease, when the soil is subjected to a mechanical load (Warrick, 2002). If soil strength is exceeded, its ability to overcome the external loading vanishes, which results in an increase in the number of contacts between soil particles. However, the relative movement and rearrangement of solid particles finally results in a more dense soil (Krümmelbein et al., 2008). Hence, with increasing the levels of compaction, soil dry bulk density increases significantly, which consequently leads to a decrease in total porosity. In term of cyclic loading, total porosity is greatly reduced by the first loading, and the further loading also decreased total porosity, but in a much smaller magnitude (Peth et al., 2010). However, its usefulness in characterizing compaction effects on storage and transport of water and air in terms of connectivity and continuity is not obvious. This is due to the fact that at given bulk density for the same soil, the pore geometry and continuity can differ due to soil management practices. Otherwise, soil shearing results in no change in bulk density, while the pore continuity alters at the identical pore volume. For these reasons bulk density alone is not always a sensitive indicator of soil compaction effects, particularly with respect to transport properties (Gebhardt et al., 2009; Horn et al., 2003; Lipiec et al., 2003).

Macropores in soil are mainly formed in three ways: 1) Biopores such as decayed roots channels and earthworm burrows; 2) Fissures and cracks as a consequence of volumetric changes in swell-shrink soils; 3) Macropores originating due to management practices (e.g. tillage) (DVWK, 1995; Glinski et al., 2011). Macropores play an important role in some physical processes such as gas transport and water flow, even though they only represent a

small part of the soil total porosity (Katuwal et al., 2015).

Generally, macroporosity is more sensitive to compaction than total porosity, because the macropores decrease firstly during compaction (Alakukku, 1996a). Kim et al. (2010) found that the CT-measured number of pores decreased by 71%, the number of macropores (>1000 mm diameter) by 69% and coarse mesopores (200-1000 mm diameter) by 75% for silt loam soils on the compacted plot. Schäffer et al. (2007) found that macro-porosity was reduced by about 20% after two and by up to 74% after 10 passes. Horn et al. (2003) noted full homogenization of the pore system with increasing wheeling. Lipiec and Håkansson (2000) reported that the number of passes reduced the macroporosity from 13.4 to 5.6 (% v/v). Although compaction can result in the decrease of macropores ($\text{Ø} \geq 30 \mu\text{m}$), micropores ($\text{Ø} < 30 \mu\text{m}$) are little affected or even increased by compaction (Horn et al., 1995b; Etana et al., 2013; Schäffer et al., 2007; Kuncoro et al., 2014b; Matthews et al., 2010; Gebhardt et al., 2009).

Compaction can also affect the quality of soil pores (e.g. pore continuity and tortuosity), which is an important factor for predicting air flow (Arthur et al., 2013; Dörner et al., 2012; Schjønning and Rasmussen, 2000) and water transport (Dörner et al., 2010; Osunbitan et al., 2005). Compaction may result in the decrease in pore continuity, which is probably related to the reduction of the volume of air-filled pores. Ball et al. (1988) found that at -60 hPa matric potential, pore continuity index decreased in direct drilled clay loam soil after one pass of an unladen tractor applied. Munkholm et al. (2002) observed that at the matric potential of -30 and -100 hPa, pore continuity index decreased significantly after compaction with a 6-8 t tractor, which indicated a relatively poorer continuity of macropores in the compacted soil. However, the experimental data of the effect of compaction on pore tortuosity have yet rarely been documented. The tortuosity factor is typically used to describe the longer connecting pore channels and affected by various obstacles within the porous paths. It means to depend mainly on the pores geometry and not on the contribution of gas and water transport mechanisms. Thus low porosity pore networks tend to be having higher tortuosity and vice versa. Connectivity, the number of throats/bonds that are connected to the same pore body/node, influences the nature of the interconnecting pores and therefore the tortuosity factors themselves. In theory, the two parameters should be inversely related, with highly

connected porous solids having low tortuosities and vice versa (Vogel, 1997). The use of X-ray microtomography provides more detailed descriptions of soil compaction processes, including local changes in soil structural pore space characteristics and deformation (Peth et al., 2010) and decreases in connectivity of macropores (Schäffer et al., 2007, 2008).

3.3.2 Gas transport

There are three main mechanisms of gas transport in soils: mass flow or advection/convection, molecular diffusion, and the Knudsen flux. Air permeability is the governing parameter for mass flow induced by pressure gradients. While relative gas diffusivity is the governing parameter for molecular diffusion induced by concentration gradients (Glinski et al., 2011). A third gas transport mechanism is the Knudsen flux. In soil science, Knudsen flux is normally considered negligible small. It only takes places when gas molecules collide with soil particles, which may happen in very dense soils (Uteau et al., 2013; Allaire et al., 2008).

Table 3-1 Three main gas transport mechanisms in soils

Gas transport mechanisms	Mass flow	Molecular diffusion	Knudsen flux
Governing parameter	Air permeability (K_a)	Relative gas diffusivity (D_s/D_o)	Knudsen diffusion (N)
Trigger mechanism	Pressure gradient	Concentration gradient	Molecule-wall collisions
Governing law	Darcy's law	Fick's law	Knudsen diffusion
Usual measuring method	Steady state method	Double chamber method	Models
Equation	$K_a = \frac{q' L_s \eta}{A_s \Delta p}$	$D_s = \frac{-\ln(\Delta C / (2 \times C_{eq})) \times V_s \times L_s}{A_t \times t \times 2}$	$N = -CD\Delta x$
Ranges of values	0.01-500*10 ⁻¹² m ²	< 1	--

The volume and arrangement/organization of the soil macropores are determinants of the state of soil aeration (Fig.3-1) (Blackwell et al., 1990; Kuncoro et al., 2014b; Schjønning et al., 2000). Gas transport process is the easiest through pore arrangements of 'a'. Compared to 'a' arrangement, air permeability and gas diffusion is more influenced by 'c' and 'b' arrangement, respectively. In the case of 'd' arrangement, it is considered inactive for gas transport at wetter

conditions (high soil matric potential), but it may be connected at drier conditions (low soil matric potential) through which the soil air can be transported. The transport process, however, does not take place for the dead-end or confined pores ('e' arrangement). Therefore, soil pore functions have a direct effect on the quality of soil gas transport.

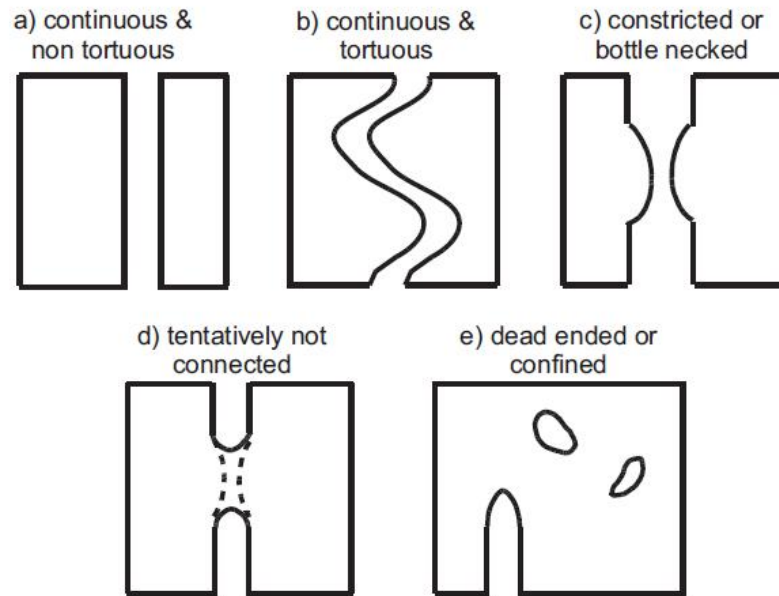


Fig.3-1 Simplified model of soil pores arrangement for gas transport (from Kuncoro et al., 2014b)

3.3.2.1 Air permeability

Air permeability is an easily measured parameter both in the laboratory and in situ by using undisturbed or remoulded soil samples (Moldrup et al., 2003). According to Glinski and Stepniewski (1985), the values of air permeability in soil are within the range of $0.01-500 \cdot 10^{-12} \text{ m}^2$. Air permeability depends on the quantity and quality of air-filled pores. The latter term relates to the pore size distribution and continuity which depends on bulk density, water content, organic matter and soil texture (Ball, 1981; Glinski et al., 2011; Mentges et al., 2016; Groenevelt et al., 1984; Lipiec and Hatano, 2003). Therefore, air permeability is a good indicator for identifying soil pore characteristics (Granovsky and McCoy, 1997; Moldrup et al., 2003; Iversen et al., 2001), and evaluating the changes in soil structure (Fish and Koppi, 1994; Moldrup et al., 2001, 2003). Furthermore, the intensity and the number of loading influence it (Mosaddeghi et al., 2007). Tanner and Wengel (1957)

reported that soil air permeability was the most sensitive measure of compaction on pasture soils by animal traffic among all tested parameters, which included bulk density, total porosity, pore size distribution, aggregate stability and penetrability. The effect factors of air permeability will be discussed below.

1) Internal properties

It is well known, that air permeability depends on the amount of air-filled pores. Berisso et al. (2013) found that at three different matric potential and at four different depth, there is a strong positive linear log-log relationship between K_a and ε_a in the control and compacted blocks. This is in agreement with Ball et al. (1988), Dörner and Horn (2006), Schjønning et al. (2002) and Kuncoro et al. (2014a).

Furthermore, pore continuity is also an important variable affecting the values of air permeability (Moldrup et al., 2003; Chamindu Deepagoda et al., 2011; Kuncoro et al., 2014a). The role of macropore continuity in controlling K_a may be illustrated by considering the potential effect of the bottle-necks formed by water menisci in the macropore system (the inter-aggregate pore system) at air-filled condition, by which K_a may be restricted. As air-filled porosity increased, the lower increase rate of air permeability in clay soil was found due to lower pore continuity and higher water content at similar matric potential (Mosaddeghi et al., 2007; Chamindu Deepagoda et al., 2011). Chen et al. (2014) also found that air permeability in 0-12 cm soil depth decreased with the level of compaction and this reduction was related to the increase of pore tortuosity and the decrease of pore continuity. Mosaddeghi et al. (2007) found that the rate of decrease in K_a and air-filled porosity with increasing stress was larger at low matric suctions, because soil water content was directly related to pore continuity responsible for air flow and blocking of airspace (Mentges et al., 2016). Seyfried and Murdock (1997) found that blocked porosity increased due to increase in volumetric water content, which was significantly reduced soil K_a in a soil contained 97% sand-sized particles. Peth et al. (2010) observed that the correlation coefficient of air conductivity and the change in total pore volume was relatively low, which may be because the differences in the pore geometry (continuity and tortuosity) between individual samples. The presence of soil organic matter was likely to block soil pores and might also facilitate the formation of bottle-necks by water menisci, which results in lower air permeability in soils mixed with organic matter than

in the control soil for a given air content (Kuncoro et al. 2014a).

2) External stress

Several investigators have reported the effect of compaction on soil air permeability (Mordhort et al., 2012; Peth et al., 2010; Reszkowska et al., 2011; Berisso et al., 2013; Simojoki et al., 1991; Mosaddeghi et al., 2007; Kuncoro et al., 2014a; Tang et al., 2011; Chamindu Deepagoda et al., 2011). The results varied among these studies depending upon the different prevailing conditions. Naveed et al. (2016) observed that air permeability was reduced by 55-80% for topsoils (5-25 cm depth) and by 10-20% for subsoils (25-35 cm depth) under 620 kPa stress at the matric potential of -5 hPa after static loading (15 min). This reduction was associated with lower total porosity and macroporosity. Semmel (1993) reported the stress-dependent changes in air permeability from tests on soil samples from 0.4 m deep in a Luvisol derived from loess, at a matric potential potential of -6 kPa. Upon additional loading, it was observed that K_a decreased sharply as soon as the precompression stress value (100 kPa) was exceeded. In the work of Mosaddeghi et al. (2007), K_a was measured on five remoulded soils from sandy loam to clay at four matric potentials (-10, -20, -50 and -80 kPa) and three axial stresses (200, 400, and 600 kPa). The results showed that cyclic loading was not always accompanied by significant irrecoverable strain but could result in up to 10 times decrease in air permeability at low matric suctions. Linear regression was applied to the relationship between the logarithm of K_a and the logarithm of vertical stress. Peng et al. (2004) observed that air permeability was not significantly reduced at higher initial bulk density (1.45 g cm^{-3}) during compaction, while it was reduced obviously at lower initial bulk density (1.25 g cm^{-3}) on repacked soils with the load of 400 kPa. Air conductivity was measured on undisturbed soils at the matric potential of -300 hPa by Reszkowska et al. (2011). They found that the air conductivity decreased only slightly after the first load (40 kPa), and the following loads led to a further, stepwise decline in air conductivity at the ungrazed site. At the continuously grazed site, the air conductivity declined strongly after the first load, and further loading did not lead to more pronounced changes in air conductivity.

3.3.2.2 Gas diffusion

Relative gas diffusion coefficient (D_s/D_o), is the ratio of gas diffusion coefficient in soil (D_s) to that of the same gas in the same free air (D_o) taken at the same pressure and temperature (Glinski et al., 2011). The value of D_s/D_o in soil is usually below 1, due to tortuosity and limited connectivity of air-filled pores in soil (Uteau et al., 2013). With the intensity of compaction, soil porosity decreased with an accompanying greater resistance to gas transport, especially mass flow, since air permeability depends on the fourth power of pore radius while gas diffusion on the second power (Ball et al., 1981). Therefore, gas diffusion is not strongly affected by soil structure, compared to air permeability (Moldrup et al., 2001, 2003; Schjønning et al., 2013).

The degradation of the pore functions due to compaction may result in reduced or even zero gas diffusion (Zink et al., 2011). Air-filled porosity is the most important variable for gas diffusion. There is the positive relationship between values of ϵ_a and values of D_s/D_o (Kuncoro et al., 2014a). The higher values of D_s/D_o are mainly ascribable to higher values of ϵ_a , that is, a greater volume of macropores. Ball and Ritchie (1999) described a decrease of the relative gas diffusivity of undisturbed soils with textures between loam and sandy loam after compaction. Currie et al. (1960) proposed that D_s/D_o was affected by not only porosity, but also pore tortuosity. Other researchers (Ball, 1981; Moldrup et al., 2001; Hamamoto et al., 2009) further used this concept. At the same air-filled porosity, gas diffusivity in wet media was lower than in dry media. This is probably due to a change of pore shape and configuration of air-filled pores when the porous media become wet, which leads to an increase in pore tortuosity for restricted gas diffusion (Papendick and Runkles, 1965). Fujikawa and Miyazaki (2005) reported that soil compaction led to an increase in D_s/D_o at the same air-filled porosity, probably due to lower volumetric water content. Lower water blockage effects resulted in the increase in active air-filled pore space for gas diffusion. Therefore, the reduction of soil relative gas diffusivity after compaction is mainly attributed to the decrease in both the capacity and intensity of air-filled pores.

Since measuring methods are time consuming, several models are currently available for estimating D_s/D_o . The most frequently used models are showed in Table 3-2. In Buckingham (1904) and Penman (1940) models, D_s/D_o follows a function of the air-filled porosity (ϵ_a). In Millington and Quirk (1961) models, they considered the effects of soil type by including soil

total porosity (Φ). Next generation models related to another soil physical properties, such as matric potential/water content (Chamindu Deepagoda, 2012; Moldrup, 2000) and bulk density (Chamindu Deepagoda et al., 2011) are developed.

Table 3-2 Classical models for predicting relative gas diffusion coefficient

Model	Reference
$\frac{D_s}{D_o} = \varepsilon^2$	Buckingham (1904)
$\frac{D_s}{D_o} = 0.66\varepsilon$	Penman (1940)
$\frac{D_s}{D_o} = \frac{\varepsilon^{10/3}}{\Phi^2}$	Millington and Quirk (1961)

Note that: D_s/D_o is relative gas diffusivity. ε is air-filled porosity. Φ is total porosity.

3.3.2.3 Knudsen flux

Knudsen diffusion is dominant compared with molecular (gas) diffusion when the mean pore diameter of a porous medium is smaller than the mean free path of gas molecules, collisions take place between the diffusing molecules (Clifford and Hillel, 1986; Fen et al., 2011). The frequency of pore wall collisions increases with decreasing pore size or decreasing pressure, small pores and low gas pressure can substantially reduce the efficiency of this transport process. The Knudsen diffusion coefficient is commonly assessed through a Klinkenberg parameter, which is usually related to the permeability of the porous medium and varies with the moisture content of the porous medium (Reinecke and Sleep, 2002). Massmann and Farrier (1992) stated that Knudsen diffusion can be pronounced for soil systems with permeabilities $< 10^{-14} \text{ m}^2$. Abu-El-Sha'r (1993) found that Knudsen diffusion could be a significant flux mechanism in fine sands at high levels of water saturation, due to a reduction of the mean pore diameter and an increase in the tortuosity.

3.3.3 Hydraulic properties

Compaction and shearing, as well as the rearrangement of soil particles due to shrinkage, can strongly influence the pore functions (i.e. total porosity, pore shapes, pore size distributions, and pore continuity) of agricultural, forest and grassland soils. Changes in these soil structural properties directly affect soil vadose zone flow and water transport processes

by altering the hydraulic properties that are commonly described by the soil water retention curve (WRC) and the saturated/unsaturated hydraulic conductivity function (HCF) (Horton et al., 1994; Green et al., 2003; Alaoui et al., 2011; Assouline, 2006).

3.3.3.1 Water retention curve (WRC)

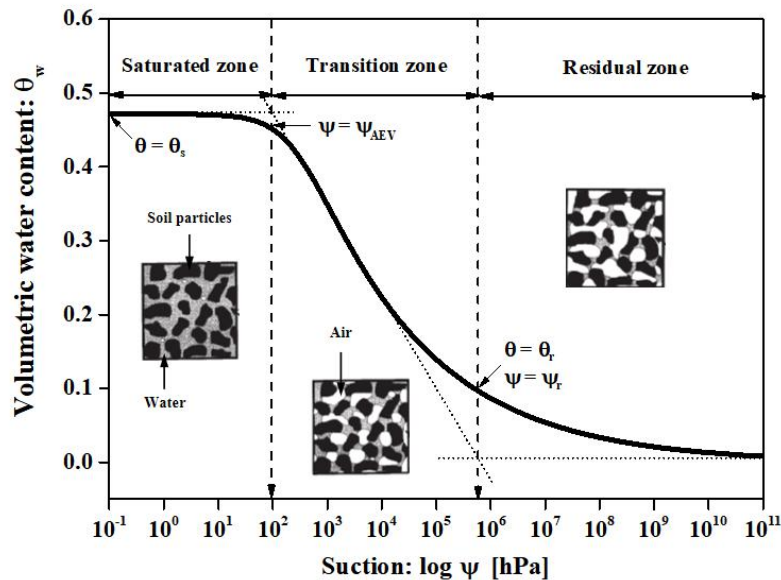


Fig.3-2 Different zones of typical soil water retention curve

Soil-water characteristic curves can be divided into three main zones (Fig.3-2), namely:

Saturated zone: The zone extends up to the air-entry value ψ_{AEV} . All soil pores are filled with water (assuming no vapor phase) with the water-phase continuous and the gas-phase non-continuous.

Transition zone: The air-entry value is the matric potential where air starts to enter the largest pores in the soil. The zone between the air-entry value ψ_{AEV} and the residual state matric potential ψ_r is termed the transition zone. During transition zone, the pores become increasingly occupied by air and the amount of water at the soil particle contacts reduces with desaturation. This part of the WRC is represented by a steep-sloped linear relationship, indicating a significant reduction in θ_a with decreasing ψ_m . In this zone, the pore water is retained mainly by capillary forces. Both the water- and gas-phases can be continuous.

Residual zone: The residual zone follows after the transition zone. In this zone, the pore water is retained in form of thin films on the soil particles, leading to minor variations in θ

with increasing ψ due to the immobile of the pore water. Water transport mainly occurs as vapor flow. The water-phase becomes non-continuous.

Compaction affects soil water retention by altering pore size distributions, because the decrease in soil total volume only occurs as a result of the compression of pore space. Most of the decreases in water retention take place at high matric potentials due to the preferential loss of larger pores resulting from compaction. Soil water retention at lower matric potential may not be affected or may increase due to an increase in smaller pores at the expense of larger pores that are compressed during compaction (Startsev and McNabb, 2001; Hill and Sumner, 1967). The two processes are linked by an “inflection point” (Dexter, 2004) above which, for soil drying, mainly structural pores are emptying and below which mainly textural pores are emptying. Consequently, compacted soils present flattened water retention curve (WRC), with a reduction of the slope of the WRC at the inflection point (Dexter, 2004; Assouline et al., 1997; Alaoui et al., 2011).

Often the water retention function is not available for a test soil over the whole water content range. Van Genuchten (1980) suggested that the fitting function in equations (3), using the available incomplete data, can provide good estimates of the water retention.

$$\theta(h) = (\theta_s - \theta_r) \left[1 + (\alpha h)^n \right]^{-m} + \theta_r \quad (3)$$

where θ_s and θ_r are the saturated and residual water content ($\text{cm}^3 \text{cm}^{-3}$), respectively. In general, θ_s is assumed to be equal or close to soil total porosity. h is matric suction (the negative value of matric potential) (hPa). α , n and m are empirical fitting parameters which affect the shape of soil water retention curve (WRC).

The parameter α is the pivot point of the curve, and its value is directly related to the value of the air-entry value. As α increases, the air-entry value also increases. The parameter n controls the slope of WRC. As n increases, the sloping portion of the curve between ψ_{AEV} and the knee of the WRC becomes steeper. Horn et al. (1995a) found that the smaller the α value at a given n , the smaller is the slope and the smaller is the amount of coarse pores. Increasing n at a given α value results in more pronounced changes in the pore size distribution. The parameter m rotates the sloping portion of the curve. As m increases, the range of the curve between ψ_{AEV} and the knee of the WRC decreases.

Dry bulk density is an important physical property influencing the estimated van Genuchten's parameters. The value of α is the most sensitive to soil compaction. With increasing the bulk density, value of α decreases (Horn et al., 1995a; Startsev and McNabb, 2001; Stange and Horn, 2005). Conflicting evidence exists in the literature about the influence of soil compaction on the van Genuchten parameter n . Assoline et al. (1997) assumed a linear decrease in n with bulk density, Horn et al. (1995a) found that n can both increase or decrease with increased mechanical stress at a given initial bulk density.

3.3.3.2 Hydraulic conductivity function (HCF)

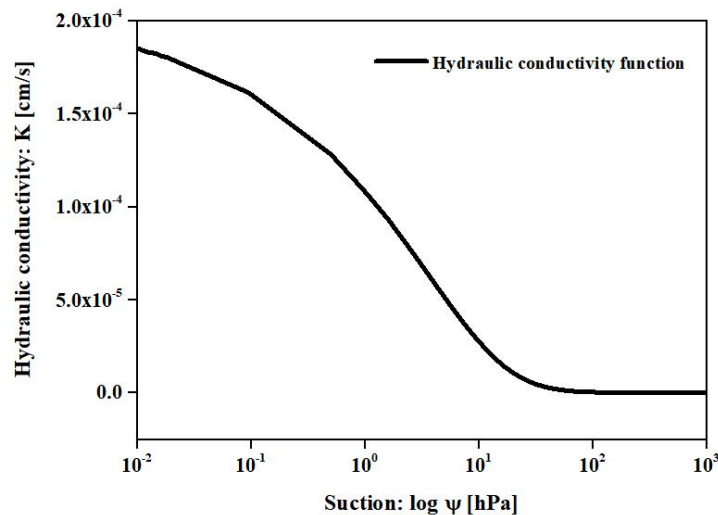


Fig.3-3 Model of hydraulic conductivity as a function of suction

When the soil is saturated, all of the pores are water-filled and the hydraulic conductivity (K_s) is maximal. When the soil starts to desaturate, some of the pores become air-filled, leading to cross-sectional area available for water flow. Furthermore, as suction develops, the larger pores are emptied first which are the most conductive according to Poiseuille's law. At the same time, the large empty pores have to be circumvented, hence with progressive desaturation, more tortuous pathways of water flow occur, resulting in a reduction of unsaturated hydraulic conductivity.

1) Saturated hydraulic conductivity

Saturated hydraulic conductivity (K_s) has been used to evaluate the effect of soil compaction on water transport, since K_s values are predominantly governed by macropores

and their continuity (Pagliai et al., 2003; Lipiec and Hatano, 2003; Zhang et al., 2006). With increasing the levels of compaction, saturated hydraulic conductivity can become smaller by several orders of magnitude (Horn et al., 2003). A stronger positive linear relationship was observed between macroporosity ($\varnothing \geq 30 \mu\text{m}$) and saturated hydraulic conductivity for all compaction treatments by Kuncoro et al. (2014a). They suggested that the reduced K_s values are probably attributable to the reduction in the volume of macropores after compaction. Kim et al. (2010) also found that compared to non-trafficked treatment, a decrease in K_s by 74% in a silt loam soil at 0-10 cm depths for the trafficked treatment by two passes with a tractor pulling a water wagon (vertical stress on the soil surface approximately 500 to 1000 kPa), and this reduction was associated with the preferential removal of macropores. Gebhardt et al. (2009) found that saturated hydraulic conductivity was significantly reduced at values as low as 70 kPa in case of clayey soils. In contrast, only small differences were detected concerning sandy soils.

2) Unsaturated hydraulic conductivity

Compared to numerous researchers on the changes of saturated hydraulic conductivity due to compaction, there are few experiment data on the effect of compaction on unsaturated flow (Richard et al., 2001; Alaoui et al., 2011). Some studies have shown that soil compaction results in higher unsaturated hydraulic conductivity (K) of soils (Assouline et al., 1997; Richard et al., 2001) and for soil aggregates (Lipiec et al., 2009). This increase was ascribed to increased connectivity between smaller pores filled with water in a compacted soil than in a loose one (Lipiec and Hatano, 2003; Lipiec et al., 2009). Richard et al. (2001) found that for the matric potential less than -15 kPa, unsaturated hydraulic conductivity on silty soils of the compacted layer was higher than that of the uncompacted layer. They suggested that the reduction of soil pore space during compaction increases the contact surface area between the aggregates. On the contrary, Zhang et al. (2006) observed that unsaturated hydraulic conductivity on silty loam soils both at 0-5 cm and 10-15 cm depths were not affected by compaction. In the study of Sillon et al. (2003), unsaturated hydraulic conductivity in soils with two different texture was observed both in non-compacted plot and compacted plot by using a tractor (8.3 t with rear tyres of 65 cm width inflated to 200 kPa) at the matric potential of -5 kPa. They found that in the calcareous soil, the compacted plot had a higher unsaturated

hydraulic conductivity in the whole range of water volume ratio. In the loess soil, unsaturated hydraulic conductivity in the compacted plot was higher in the dry range (water volume ratio $< 0.3 \text{ m}^3 \text{ m}^{-3}$). However, there was no difference between the compacted and non-compacted plot in the wet range (water volume ratio $> 0.3 \text{ m}^3 \text{ m}^{-3}$). Reicosky et al. (1981) found that both saturated and unsaturated hydraulic conductivity decreased markedly with the increase in soil bulk density. They explained that this decrease in the water movement through the soil may be attributed to the reduction in the number of larger pores that resulted in a reduction of cross-sectional area for water flow. At the same time the number of contacts between these individual soil particles increased with increasing soil bulk density which resulted in increased tortuosity.

3.3.3.3 Pore water pressure

Compactive processes affect soil hydraulic properties and associated soil water potential (pore water pressures). Direct influences of compaction on hydraulic properties may control infiltration and redistribution of water in the soil profile. This water flow process has many indirect and important influences on plant rooting and growth, such as aeration status, soil mechanical resistance to rooting, root extension and uptake of water and plant nutrients. Limited water transport in tightly compacted zones may promote water fluxes towards preferential pathways as wormholes or activated macropores (provided that water ponding occurs at the soil surface) (Kulli et al., 2003) and more permeable zones (Coquet et al., 2005).

Variations in soil water potential change and soil structural integrity with load application time have been inadequately characterized. During loading, pore water pressure changes (depending on internal soil strength and the time-dependent settlement) as the cross-sections of pore channels are deformed. In the case of static loading, for water saturated soils, each height change coincides with the adequate water loss by drainage. If such a drainage is however prevented by the simultaneously decreasing hydraulic conductivity, an increasing pore water pressure, starting from the initial values up to even positive values, must be considered as responsible for further internal soil processes. For the initially unsaturated soil, air-filled coarse pores is mechanically stressed but remains still unsaturated after compaction, even more negative pore water pressure values can be determined because

of newly formed finer but at present still air-filled pores. The disequilibrium results in a redistribution of the actual water and finally results in more negative pore water pressure values (Hartge and Horn, 2016; Larson and Gupta, 1980). Higher loads and longer loading times will produce even positive pore water pressure due to water saturation of finer pores and concurrent lower hydraulic conductivity. Once an equilibrium between internal soil strength and the applied stress is achieved, there are no further changes in soil deformation (Horn and Hartge, 1990) and a new equilibrium between applied stress and soil strength is formed, but physical, physico-chemical or biological properties and functions have been already altered.

In the case of cyclic loading, the changed pore water pressure due to the height loss can be explained by the combined stress strain and rebound processes. In one cycle event, a less negative pore water pressure was found during loading compared to during unloading. When the applied stress was removed, water menisci were stretched and less curved and thus the shape became more concave, leading to a decrease in pore water pressure (more negative) during unloading. Similar effect was also reported by Peth and Horn (2006), Mordhorst et al. (2012), Reszkowska et al. (2011) and Krümmelbein et al. (2008). Zhang et al. (2005) stated that fluctuations of settlement and matric potential during cyclic loading determine the resistance (to loading) and resilience (to unloading) of the soil. Furthermore, they found an increase in the height of rebound with applied stress and stated that the rebound can be used to quantify the soil mechanical resilience, i.e., the recovery of the soil pore structure after mechanical disturbance.

The higher and more frequent cyclic loading, the more soil structure weakening occurs, and the more pore water gets more fluid. Krümmelbein et al. (2008) found that cyclic loading not only resulted in soil structure degradation by deformation, but also pumped additional water from deeper soil horizons under in situ conditions, which further enhanced soil deformation. This leads to hydraulic dis-equilibrium and the more moist samples are subject to permanent, plastic deformation until they ultimately liquify especially at high cyclic loading frequencies. In soil mechanics this effect is called liquefaction. Peth et al. (2010) observed that pore water pressure increased during cyclic loading and reached positive values in most cases for the topsoil layers (12-15 cm) due to an increase in degree of saturation

resulting from the loss of macropores under the high applied stress.

Although pore water pressure is not a typical variable used for soil compaction measurements, it is often included and considered in soil strength calculations (Ajayi et al., 2009; Severiano et al., 2013). Cui et al. (2010) reported that most of the models used to estimate soil deformation during the passage of machines neglect pore water pressure as an important stress variable for unsaturated soils. Changes in soil water potential have proven to be a useful indicator for evaluating compaction induced changes in soil structure during stress application (Larson and Gupta, 1980). The time dependent change in pore water pressure during the stress strain processes maybe directly coupled with the strain affected reduction in hydraulic conductivity but these interactions are still mostly unknown or not determined in detail (Hartge and Horn, 2016).

3.4 References

- Abu-El-Sha'r, W. Y., 1993. Experimental assessment of multicomponent gas transport flux mechanisms in subsurface systems, PhD. thesis, 119 pp., Dep. of Civ. Eng., Univ. of Michigan, Ann Arbor.
- Ajayi, A. E., Dias Junior, M. S., Curi, N., Araujo Junior, C. F., Souza, T. T. T., Inda Junior, A. V., 2009. Strength attributes and compaction susceptibility of Brazilian Latosols. *Soil Till. Res.* 105, 122-127.
- Alakukku, L., 1996a. Persistence of soil compaction due to high axle load traffic: I. Short-term effects on the properties of clay and organic soils. *Soil Till. Res.* 37(4), 211-222.
- Alakukku, L., 1996b. Persistence of soil compaction due to high axle load traffic II. Long-term effects on the properties of fine-textured and organic soils. *Soil Till. Res.* 37(4), 223-238.
- Alakukku, L., Weisskopf, P., Chamen, W.C., Tijink, F.G., van der Linden, J., Pires, S., Sommer, C., Spoor, G., 2003. Prevention strategies for field traffic-induced subsoil compaction: a review. *Soil Till. Res.* 73, 145-160.
- Alaoui, A., Lipiec, J., Gerke, H.H., 2011. A review of the changes in the soil pore system due to soil deformation: A hydrodynamic perspective. *Soil Till. Res.* 115-116, 1-15.
- Allaire, S.E., Lafond, J.A., Cabral, A.R., Lange, S.F., 2008. Measurement of gas diffusion through soils: comparison of laboratory methods. *J. Environ. Monitor* 10, 1326-1336.
- Arthur, E., Schjønning, P., Moldrup, P., Tuller, M., de Jonge, L.W., 2013. Density and permeability of a

- loess soil: long-term organic matter effect and the response to compressive stress. *Geoderma* 236-245, 193-194.
- Arvidsson, J., Ristic, S., 1996. Soil stress and compaction effects for four tractor types. *J. Terramechan.* 33 (5), 223-232.
- Assouline, S., 2006. Modeling the relationship between soil bulk density and the hydraulic conductivity function. *Vadose Zone J.* 5, 697-705.
- Assouline, S., Tavares-Filho, J., Tessier, D., 1997. Effect of compaction on soil physical and hydraulic properties: experimental results and modelling. *Soil Sci. Soc. Am. J.* 61, 390-398.
- Bakker, D.M., Davis, R.J., 1995. Soil deformation observations in a Vertisol under field traffic. *Aust. J. Soil Res.* 33, 817-832.
- Ball, B. C., O'Sullivan, M. F., Hunter, R., 1988. Gas diffusion, fluid flow and derived pore continuity indices in relation to vehicle traffic and tillage. *J. Soil Sci.* 39, 327-339.
- Ball, B.C., 1981. Pore characteristics of soils from two cultivation experiments as shown by gas diffusivities and permeabilities and air-filled porosities. *J. Soil Sci.* 32, 483-498.
- Ball, B.C., Harris, W., Burford, J.R., 1981. A laboratory method to measure gas diffusion and flow in soil and other porous materials. *J. Soil Sci.* 32, 323-333.
- Ball, B.C., Ritchie, R.M., 1999. Soil and residue management effects on arable cropping conditions and nitrous oxide fluxes under controlled traffic in Scotland: 1. Soil and crop responses. *Soil Till. Res.* 52(3-4), 177-189.
- Baumgartl, T. and Horn, R., 1991. Effect of aggregate stability on soil compaction. *Soil Tillage Res.*, 19, 203-213.
- Berisso, F.E., Schjønning, P., Keller, T., Lamandé, M., Simojoki, A., Iversen, B.V., Alakukku, L., Forkman, J., 2013. Gas transport and subsoil pore characteristics: Anisotropy and long-term effects of compaction. *Geoderma* 195-196, 184-191.
- Berisso, F.E., Schjønning, P., Keller, T., Lamandé, M., Etana, A., de Jonge, L.W., Iversen, B.V., Arvidsson, J., Forkman, J., 2012. Persistent effects of subsoil compaction on pore size distribution and gas transport in a loamy soil. *Soil Till. Res.* 122(3-4), 42-51.
- Bishop, A.W., 1959. The principle of effective stress. *Teknisk Ukeblad* 106 (39), 859-863.
- Blackwell, P.S., Ringrose-Voase, A.F., Jayawardane, N.S., Olsson, K.A., McKenzie, D.C., Mason, W.K., 1990. The use of air-filled porosity and intrinsic permeability to characterize macropore structure

- and saturated hydraulic conductivity of clay soils. *J. Soil Sci.* 41, 215-228.
- Blume, H.P., Brümmer, G.W., Fleige, H., Horn, R., Kandeler, E., Kögel-Knabner, I., Kretzschmar, R., Stahr, K., Wilke, B.M., 2016. *Scheffer/Schachtschabel Soil Science*. Springer.
- Botta, G., Jorajuria, D., Rosatto, H., Ferrero, C., 2006. Light tractor traffic frequency on soil compaction in the Rolling Pampa region of Argentina. *Soil Till. Res.* 86, 9-14.
- Buckingham, E., 1904. Contributions to our Knowledge of the Aeration of Soils. In: Soil, B. (Ed.). US Gov. Print. Office, Washington, DC.
- Bullock, P., Newman, A.C.D., Thomasson, A.J., 1985. Porosity aspects of the regeneration of soil structure after compaction. *Soil Till. Res.* 5, 325-341.
- Cambi, M., Certini, G., Neri, F., Marchi, E., 2015. The impact of heavy traffic on forest soils: A review. *Forest Ecol. Manag.* 338, 124-138.
- Campbell, D.J., Dickson, J.W., Ball, B.C., Hunter, R., 1986. Controlled seedbed traffic after ploughing or direct drilling under winter barley in Scotland, 1980-1984. *Soil Till. Res.* 8, 3-28.
- Chamindu Deepagoda, T.K.K., 2012. Variable pore connectivity model linking gas diffusivity and air-phase tortuosity to soil matric potential. *Vadose Zone J.* 11 (1).
- Chamindu Deepagoda, T.K.K., Moldrup, P., Schjønning, P., De Jonge, L.W., Kawamoto, K., Komatsu, T., 2011. Density-corrected models for gas diffusivity and air permeability in unsaturated soil. *Vadose Zone J.* 10, 226-238.
- Chen, G., Weil, R.R., Hill, R.L., 2014. Effects of compaction and cover crops on soil least limiting water range and air permeability. *Soil Till. Res.* 136, 61-69.
- Clifford, S.M., Hillel, D., 1986. Knudsen diffusion: The effect of small pore size and low gas pressure on gaseous transport in soil. *Soil Sci.* 141, 289-297.
- Coquet, Y., Coutadeur, C., Labata, C., Vachier, P., van Genuchten, M.Th, RogerEstrade, J., Simunek, J., 2005. Water and solute transport in a cultivated silt loam soil. I. Field observations. *Vadose Zone J.* 4, 573-586.
- Cui, K., Defosse, P., Cui, Y. J., Richard, G., 2010. Quantifying the effect of matric potential on the compressive properties of two agricultural soils using an osmotic oedometer. *Geoderma* 156, 337-345.
- Currie, J.A., 1960. Gas diffusion in porous media Part 1. A non-steady state method. *Br. J. Appl. Phys.* 11, 314-317.

- Defossez, P., Richard, G., 2002. Models of soil compaction due to traffic and their evaluation. *Soil Till. Res.* 67 (1), 41-64.
- Destain, M.-F., Roisin, C., Dalcq, A.-S., Mercatoris, B.C.N., 2016. Effect of wheel traffic on the physical properties of a Luvisol. *Geoderma* 262, 276-284.
- Dexter, A.R., 2004. Soil physical quality: Part II: Friability, tillage, tilth and hardsetting. *Geoderma* 120, 215-225.
- Dexter, A.R., Tanner, D.W., 1974. Time dependence of compressibility for remoulded and undisturbed soils. *J. Soil Sci.* 25 (2), 153-164.
- Dörner, J., Dec, D., Feest, E., Vasquez, N., Diaz, M., 2012. Dynamics of soil structure and pore functions of a volcanic ash soil under tillage. *Soil Till. Res.* 125, 52-60.
- Dörner, J., Dec, D., Peng, X., Horn, R., 2010. Effect of land use change on the dynamic behaviour of structural properties of an Andisol in southern Chile under saturated and unsaturated hydraulic conditions. *Geoderma* 159, 189-197.
- Dörner, J., Horn, R., 2006. Anisotropy of pore functions in structured Stagnic Luvisols in the Weichselian moraine region in N Germany. *J. Plant Nutr. Soil Sci.* 169 (2), 213-220.
- Ekwe, E.I., 1990. Organic-matter effects on soil strength properties. *Soil Till. Res.* 16, 289-297.
- Etana, A., Larsbo, M., Keller, T., Arvidsson, J., Schjønning, P., Forkman, J., Jarvis, N., 2013. Persistent subsoil compaction and its effects on preferential flow patterns in a loamy till soil. *Geoderma* 192, 430-436.
- Fen, C.-S., Liang, W., Hsieh, P., Huang, Y., 2011. Knudsen and molecular diffusion coefficients for gas transport in unconsolidated porous media. *Soil Sci. Soc. Am. J.* 75, 456-467.
- Fish, A.N., Koppi, A.J., 1994. The use of a simple field air permeameter as a rapid indicator of functional soil pore space. *Geoderma* 63, 255-264.
- Fujikawa, T., Miyazaki, T., 2005. Effects of bulk density on the gas diffusion coefficient in repacked and undisturbed soils. *Soil Sci.* 170, 892-901.
- Gebhardt, S., Fleige, H., Horn, R., 2009. Effect of compaction on pore functions of soils in a Saalean moraine landscape in North Germany. *J. Plant Nutr. Soil Sci.* 172, 688-695.
- Ghezzehei, T.A., Or, D., 2001. Rheological properties of wet soils and clays under steady and oscillatory stresses. *Soil Sci. Soc. Am. J.* 65, 624-637.
- Glinski, J., Horabik, J., Lipiec, J., 2011. *Encyclopedia of agrophysics*. Springer.

- Glinski, J., Stepniewski, W., 1985. *Soil Aeration and Its Role for Plants*. Boca Raton: CRC Press.
- Granovsky, A.V., E.L. McCoy., 1997. Air flow measurements to describe field variation in porosity and permeability of soil macropores. *Soil Sci. Soc. Am. J.* 61, 1569-1576.
- Green, T.R., Ahuja, L.R., Benjamin, J.G., 2003. Advances and challenges in predicting agricultural management effects on soil hydraulic properties. *Geoderma* 116, 3-27.
- Groenevelt, P.H, Kay, B.D., Grant, C.D., 1984. Physical assessment of soil with respect to rooting potential. *Geoderma* 34, 101-114.
- Håkansson, I., 1994. Subsoil compaction by high axle load traffic. *Soil Till. Res.* 29, 105-306 (special issue).
- Håkansson, I., Reeder, R.C., 1994. Subsoil compaction by vehicles with high axle load extent. Persistence and crop response. *Soil Till. Res.* 29, 277-304.
- Hamamoto, S., Moldrup, P., Kawamoto, K., Komatsu, T., Rolston, D.E., 2009. Unified measurement system for the gas dispersion coefficient, air permeability, and gas diffusion coefficient in variably saturated soil. *Soil Sci. Soc. Am. J.* 73, 1921-1930.
- Hamza, M.A., Anderson, W.K., 2005. Soil compaction in cropping systems: A review of the nature, causes and possible solutions. *Soil Till. Res.* 82 (2), 121-145.
- Hartge, K.H., 1994. Soil Structure, its Development and its Implications for Properties and Processes in Soils - a synopsis based on recent research in Germany. *J. Plant Nutr. Soil Sci.* 157 (3), 159-164.
- Hartge, K.H., Horn, R., 2016. *Essential Soil Physics, An Introduction to Soil Processes, Functions, Structure and Mechanics*. Schweizerbart Science Publishers.
- Hill, J.N.S., Sumner, M.E., 1967. Effect of bulk density on moisture characteristics of soils. *Soil Sci.*, 103, 234-238.
- Hillel, D., 1998. *Environmental Soil Physics*. Academic Press, San Diego.
- Horn, R., Baumgratl, T., Gräsle, W., 1995a. Stress induced changes of hydraulic properties in soils. *Unsaturated soils Volume I*, Alonso & Delage (eds). pp 123-127.
- Horn, R., Blackwell, P.S., White, R., 1989. The effect of speed of wheeling on soil stresses, rut depth and soil physical properties in an ameliorated transitional red-brown earth. *Soil Till. Res.* 13, 353-364.
- Horn, R., Domżzał, H., Słowińska-Jurkiewicz, A., van Ouwerkerk, C., 1995b. Soil compaction processes and their effects on the structure of arable soils and the environment. *Soil Till. Res.* 35

- (1-2), 23-36.
- Horn, R., Hartge, K.H., 1990. Effects of short-time loading on soil deformation and strength of an ameliorated Typic Paleustalf. *Soil Till. Res.* 15, 247-256.
- Horn, R., Rostek, J., 2000. Subsoil compaction processes-state of knowledge. In Horn, R., van den Akker, J.J.H., Arvidsson, J., eds., *Subsoil Compaction-Distribution, Processes, and Consequences. Advances in Geocology* 32, Catena, Reiskirchen, Germany, 44-54.
- Horn, R., Way, T., Rostek, J., 2003. Effect of repeated tractor wheeling on stress/strain properties and consequences on physical properties in structured arable soils. *Soil Till. Res.* 73 (1-2), 101-106.
- Horton, R., Ankeny, M.D., Allmaras, R.R., 1994. Effects of Compaction on Soil Hydraulic Properties. *Developments in Agricultural Engineering* 11, 141-165.
- Iversen, B.V., Moldrup, P., Schjønning, P., Loll, P., 2001. Air and water permeability in differently textured soils at two measurement scales. *Soil Sci.* 166(10), 643-659.
- Katuwal, S., Norgaard, T., Moldrup, P., Lamandé, M., Wildenschild, D., de Jonge, L.W., 2015. Linking air and water transport in intact soils to macropore characteristics inferred from X-ray computed tomography. *Geoderma* 237-238, 9-20.
- Keller, T., Arvidsson, J., Dawidowski, J.B., Koolen, A.J., 2004. Soil precompression stress II. A comparison of different compaction tests and stress-displacement behaviour of the soil during wheeling. *Soil Till. Res.* 77 (1), 97-108.
- Keller, T., Lamandé, M., Peth, S., Berli, M., Delenne, J.-Y., Baumgarten, W., Rabbel, W., Radjaï, F., Rajchenbach, J., Selvadurai, A.P.S., Or, D., 2013. An interdisciplinary approach towards improved understanding of soil deformation during compaction. *Soil Till. Res.* 128, 61-80.
- Kim, H., Anderson, S.H., Motavalli, P.P., Gantzer, C.J., 2010. Compaction effects on soil macropore geometry and related parameters for an arable field. *Geoderma* 160, 244-251.
- Kondo, M.K., Dias Junior, M.S., 1999. Soil compressibility of three latosols as a function of moisture and use. *Revista Brasileira de Ciencia do Solo* 23, 211-218.
- Krümmelbein, J., Peth, S., Horn, R., 2008. Determination of pre-compression stress of a variously grazed steppe soil under static and cyclic loading. *Soil Till. Res.* 99 (2), 139-148.
- Kulli, B., Gysi, M., Flühler, H., 2003. Visualizing soil compaction based on flow pattern analysis. *Soil Till. Res.* 70, 29-40.
- Kuncoro, P.H., Koga, K., Satta, N., Muto, Y., 2014a. A study on the effect of compaction on transport

- properties of soil gas and water I: Relative gas diffusivity, air permeability, and saturated hydraulic conductivity. *Soil Till. Res.* 143, 172-179.
- Kuncoro, P.H., Koga, K., Satta, N., Muto, Y., 2014b. A study on the effect of compaction on transport properties of soil gas and water. II: Soil pore structure indices. *Soil Till. Res.* 143, 180-187.
- Larson, W.E., Gupta, S.C., 1980. Estimating critical stresses in unsaturated soils from changes in pore water pressure during confined compression. *Soil Sci. Soc. Am. J.* 44, 1127-1132.
- Lipiec, J., Arvidsson, J., Murer, E., 2003. Review of modelling crop growth, movement of water and chemicals in relation to topsoil and subsoil compaction. *Soil Till. Res.* 73, 15-29.
- Lipiec, J., Håkansson, I., 2000. Influences of degree of compactness and matric water tension on some important plant growth factors. *Soil Till. Res.* 53, 87-94.
- Lipiec, J., Hatano, R., 2003. Quantification of compaction effects on soil physical properties and crop growth. *Geoderma* 116, 107-136.
- Lipiec, J., Szustak, S., Tarkiewicz, S., 1992. Soil compaction: responses of soil physical properties and crop growth. *Zeszyty Problemowe Postępow w Nauk Rolniczych* 398, 113-117.
- Lipiec, J., Woźciga, A., Horn, R., 2009. Hydraulic properties of soil aggregates as influenced by compaction. *Soil Till. Res.* 103, 170-177.
- Logsdon, S., Berli, M., Horn, R., 2013. *Advances in Agricultural Systems Modeling 3. Quantifying and Modeling Soil Structure Dynamics.* SSSA.
- Massmann, J., D.F. Farrier. 1992. Effects of atmosphere pressures on gas transport in the vadose zone. *Water Resour. Res.* 28, 777-791.
- Matthews, G.P., Laudone, G.M., Gregory, A.S., Bird, N.R.A., Matthews, A.G., de, G., Whalley, W.R., 2010. Measurement and simulation of the effect of compaction on the pore structure and saturated hydraulic conductivity of grassland and arable soil. *Water Resour. Res.* 46 (5).
- Medvedev, V.V., Cybulko, W.G., 1995. Soil criteria for assessing the maximum permissible ground pressure of agricultural vehicles on Chernozem soils. *Soil Till. Res.* 36, 153-164.
- Mentges, M.I., Reichert, J.M., Rodrigues, M.F., Awe, G.O., Mentges, L.R., 2016. Capacity and intensity soil aeration properties affected by granulometry, moisture, and structure in no-tillage soils. *Geoderma* 263, 47-59.
- Millington, R., Quirk, J.P., 1961. Permeability of porous solids. *Trans. Faraday Soc.* 57(8), 1200-1207.
- Moldrup, P., 2000. Predicting the gas diffusion coefficient in repacked soil: water-induced linear

- reduction model. *Soil Sci. Soc. Am. J.* 64 (5), 1588-1594.
- Moldrup, P., T. Olesen, T. Komatsu, P. Schjønning, D.E. Rolston. 2001. Tortuosity, diffusivity, and permeability in the soil liquid and gaseous phases. *Soil Sci. Soc. Am. J.* 65, 613-623.
- Moldrup, P., Yoshikawa, S., Olesen, T., Komatsu, T., Rolston, D.E., 2003. Air permeability in undisturbed volcanic ash soil: Predictive model test and soil structure finger print. *Soil Sci. Soc. Am. J.* 67, 32-40.
- Mordhorst, A., Zimmermann, I., Peth, S., Horn, R., 2012. Effect of hydraulic and mechanical stresses on cyclic deformation processes of a structured and homogenized silty Luvic Chernozem. *Soil Till. Res.* 125, 3-13.
- Mosaddeghi, M.R., Koolen, A.J., Hajabbasi, M.A., Hemmat, A., Keller, T., 2007. Suitability of pre-compression stress as the real critical stress of unsaturated agricultural soils. *Biosystems Engineering.* 98 (1), 90-101.
- Munkholm, L.J., Schjønning, P., Kay, B.D., 2002. Tensile strength of soil cores in relation to aggregate strength, soil fragmentation and pore characteristics. *Soil Till. Res.* 64, 125-135.
- Naveed, M., Per Schjønning, Keller, T., de Jonge, L. W., Per Moldrup, Lamandé, M., 2016. Quantifying vertical stress transmission and compaction-induced soil structure using sensor mat and X-ray computed tomography. *Soil Till. Res.* 158, 110-122.
- Osunbitan, J.A., Oyedele, D.J., Adekalu, K.O., 2005. Tillage effects on bulk density, hydraulic conductivity and strength of a loamy sands soil in Southwestern Nigeria. *Soil Till. Res.* 82, 57-64.
- Pagliai, M., Marsili, A., Servadio, P., Vignozzi, N., Pellegrini, S., 2003. Changes in some physical properties of a clay soil in Central Italy following the passage of rubber tracked and wheeled tractors of medium power. *Soil Till. Res.* 73 (1-2), 119-129.
- Papendick, R.I., Runkles, J.R., 1965. Transient-state oxygen diffusion in soil: I. The case when rate of oxygen consumption is constant. *Soil Sci.* 100, 251-261.
- Peng, X., Horn, R., Zhang, B., Zhao, Q.G., 2004. Mechanisms of soil vulnerability to compaction of homogenized and recompact Ultisols. *Soil Till. Res.* 76 (2), 125-137.
- Peng, X., Zhang, Z.B., Wang, L.L., Gan, L., 2012. Does soil compaction change soil shrinkage behaviour? *Soil Till. Res.* 125, 89-95.
- Penman, H.L., 1940. Gas and vapour movements in the soil I. The diffusion of vapours through porous solids. *J. Agric. Sci.* 30, 437-462.

- Peth, S., Horn, R., 2006. The mechanical behaviour of structured and homogenized soil under repeated loading. *J. Plant Nutr. Soil Sci.* 169, 401-410.
- Peth, S., Rostek, J., Zink, A., Mordhorst, A., Horn, R., 2010. Soil testing of dynamic deformation processes of arable soils. *Soil Till. Res.* 106 (2), 317-328.
- Pytka, J., 2005. Effects of repeated rolling of agricultural tractors on soil stress and deformation state in sand and loess. *Soil Till. Res.* 82 (1), 77-88.
- Reicosky, D.C., Voorhees, W.B., Radke, J.K., 1981. Unsaturated water flow through a simulated wheel track. *Soil Sci. Soc. Am. J.* 45, 3-8.
- Reinecke, S.A., and B.E. Sleep. 2002. Knudsen diffusion, gas permeability, and water content in an unsaturated porous medium. *Water Resour. Res.* 38, 1280-1294.
- Reszkowska, A., Krümmelbein, J., Gan, L., Peth, S., Horn, R., 2011. Influence of grazing on soil water and gas fluxes of two Inner Mongolian steppe ecosystems. *Soil Till. Res.* 111, 180-189.
- Richard, G., Boizard, H., Roger-Estrade, J., Boiffin, J., Guérif, J., 1999. Field study of soil compaction due to traffic in northern France: pore space and morphological analysis of the compacted zones. *Soil Till. Res.* 51 (1-2), 151-160.
- Richard, G., Cousin, I., Sillon, J.F., Bruand, A., Guérif, J., 2001. Effect of compaction on the porosity of a silty soil: influence on unsaturated hydraulic properties. *Eur. J. Soil Sci.* 52, 49-58.
- Saffih-Hdadi, K., Défossez, P., Richard, G., Cui, Y.-J., Tang, A.-M., Chaplain, V., 2009. A method for predicting soil susceptibility to the compaction of surface layers as a function of water content and bulk density. *Soil Till. Res.* 105 (1), 96-103.
- Schäfer-Landefeld, L., Brandhuber, R., Fenner, S., Koch, H.J., Stockfisch, N., 2004. Effects of agricultural machinery with high axle load on soil properties of normally managed fields. *Soil Till. Res.* 75, 75-86.
- Schäffer, B., Stauber, M., Mueller, T.L., Müller, R., Schulin, R., 2008. Soil and macropores under uniaxial compression. I. Mechanical stability of repacked soil and deformation of different types of macro-pores. *Geoderma* 146, 183-191.
- Schäffer, B., Stauber, M., Müller, M., Schulin, R., 2007. Changes in macro-pore structure of restored soil caused by compaction beneath heavy agricultural machinery: a morphometric study. *Eur. J. Soil Sci.* 58, 1062-1073.
- Schjønning, P., Lamandé, M., Berisso, F.E., Simojoki, A., Alakukku, L., Andreasen, R.R., 2013. Gas

- diffusion, non-Darcy air permeability, and computed tomography images of a clay subsoil affected by compaction. *Soil Sci. Soc. Am. J.* 77, 1977-1990.
- Schjønning, P., Munkholm, L.J., Moldrup, P., Jacobsen, O.H., 2002. Modelling soil pore characteristics from measurements of air exchange: the long-term effects of fertilization and crop rotation. *Eur. J. Soil Sci.* 53 (2), 331-339.
- Schjønning, P., Rasmussen, K.J., 2000. Soil strength and soil pore characteristics for direct drilled and ploughed soils. *Soil Till. Res.* 57, 69-82.
- Semmel, H., 1993. Auswirkungen kontrollierter Bodenbelastungen auf das Druckfortpflanzungsverhalten und physikalisch-mechanische Kenngrößen von Ackerboden. Christian Albrechts University, Kiel, Germany, Schriftenreihe Inst. Pflanzenern. Bodenkd, 26, 183.
- Severiano, E. C., Oliveira, G. C., Dias Junior, M. S., Curi, N., Costa, K. A. P., Carducci, C. E., 2013. Preconsolidation pressure, soil water retention characteristics, and texture of Latosols in the Brazilian Cerrado. *Soil Research*, 51, 193-202.
- Seyfried, M.S., Murdock, M.D., 1997. Use of air permeability to estimate infiltrability of frozen soil. *J. Hydrol.* 202, 97-107.
- Sillon, J.F., Richard, G., Cousin, I., 2003. Tillage and traffic effects on soil hydraulic properties and evaporation. *Geoderma* 116, 29-46.
- Simojoki, A., Jaakkola, A., Alakukku, L., 1991. Effect of compaction on soil air in a pot experiment and in the field. *Soil Till. Res.* 19(2-3), 175-186.
- Słowińska-Jurkiewicz, A., Domżał, H., 1991. The structure of the cultivated horizon of soil compacted by the wheels of agricultural tractors. *Soil Till. Res.* 19, 215-226.
- Soane, B.D., 1990. The role of organic matter in soil compactibility: a review of some practical aspects. *Soil Till. Res.* 16, 179-201.
- Soehne, W., 1958. Fundamentals of pressure distribution and soil compaction under tractor tires. *Agric. Eng.* 39, 276-281.
- Stange, C.F., Horn, R., 2005. Modeling the Soil Water Retention Curve for Conditions of Variable Porosity. *Vadose Zone J.* 4, 602-613.
- Startsev, A.D., McNabb, D.H., 2001. Skidder traffic effects on water retention, pore-size distribution, and van Genuchten parameters of Boreal forest soils. *Soil Sci. Soc. Am. J.* 65, 224-231.

- Sumner, M. E., 1999. Handbook of soil science. Boca Raton, Fla: CRC Press.
- Tang, A.M., Cui, Y., Richard, G., Défossez, P., 2011. A study on the air permeability as affected by compression of three French soils. *Geoderma* 162, 171-181.
- Tanner, C.B., Wengel, R.W., 1957. An air permeameter for field and laboratory use. *Soil Sci. Soc. Am. Proc.*, 21, 663-664.
- Uteau, D., Pagenkemper, S.K., Peth, S., Horn, R., 2013. Root and time dependent soil structure formation and its influence on gas transport in the subsoil. *Soil Till. Res.* 132, 69-76.
- van Asselen, S., Stouthamer, E., van Asch, Th.W.J., 2009. Effects of peat compaction on delta evolution: A review on processes, responses, measuring and modeling. *Earth-Science Reviews.* 92 (1-2), 35-51.
- van den Akker, J.J.H., Hoogland, T., 2011. Comparison of risk assessment methods to determine the subsoil compaction risk of agricultural soils in The Netherlands. *Soil Till. Res.* 114 (2), 146-154.
- van Genuchten, M. T., 1980. A closed-form equation for predicting the hydraulic conductivity of unsaturated soils, *Soil Sci. Soc. Am. J.*, 44, 892-898.
- Vogel, H.J., 1997. Morphological determination of pore connectivity as a function of pore size using serial sections. *Eur. J. Soil Sci.* 48, 365-377.
- Warrick, A.W., 2002. *Soil Physics Companion*. Boca Raton, Fla: CRC Press.
- Werner, D., Werner, B., 2001. Compaction and recovery of soil structure in a silty clay soil (Chernozem): physical, computer tomographic and scanning electron microscopic investigations. *J. Plant Nutr. Soil Sci.* 164, 79-90.
- Wiermann, C., Werner, D., Horn, R., Rostek, J., Werner, B., 2000. Stress/strain processes in a structured unsaturated silty loam Luvisol under different tillage treatment in Germany. *Soil Till. Res.* 53, 117-128.
- Wösten, J.H.M., Van Genuchten, M. Th., 1988. Using texture and other soil properties to predict the unsaturated soil hydraulic function. *Soil Sci. Soc. Am. J.* 52, 1762-1770.
- Zhang, S., Grip, H., Lövdahl, L., 2006. Effect of soil compaction on hydraulic properties of two loess soils in China. *Soil Till. Res.* 90(1-2), 117-125.
- Zink, A., Fleige, H., Horn, R., 2011. Verification of harmful subsoil compaction in loess soils. *Soil Till. Res.* 114, 127-134.

4 OBJECTIVES

Soil compaction is one of the major causes of soil degradation in modern agriculture. Hence, it is very important and necessary to understand how far soil quality is affected by different deformation processes and how far we can explore solutions to alleviate the negative effects resulting from it. Soil deformation is the response of a soil to the relationship of internal soil strength and external stresses. It consists of soil compaction and soil shearing. In order to evaluate the effect of soil compaction on soil deformation, the changes in soil mechanical and hydraulic behaviors should be generally considered. An increase in bulk density coincides with a reduction of pore space and the macroporosity in particular due to compaction. If we consider the shearing effect, the pore continuity and pore anisotropy will change at the identical pore volume due to the rearrangement of soil particles. Hence, soil pore functions are influenced by soil compaction and shearing, which may result in a decrease in gas, water or heat transport. Gas transport parameters are suitable indicators for identifying soil pore characteristics and changes in soil structure, and can be determined without further pretreatment in between. Thus, the effects of soil compaction and soil structural properties (continuous and non-tortuous macropores) on soil aeration are more effectively quantified by intensity properties of soil pore functions. Related stress-induced consequences on soil deformation, pore functions, soil aeration and hydraulic properties in this study were investigated by repacked soils with different soil textures (sand, silt loam, clay loam) and initial matric potentials (-60 and -300 hPa) under static and cyclic loading with different compaction levels. In this study, I focused on three topics as follows:

- 1) The 1st and 2nd papers deal with the influence of mechanical loading on soil pore functions and gas transport depending on soil texture, initial matric potential, and soil structure

Soil pore functions play an important role in some physical processes such as gas transport and water flow. Therefore, it can be used as an indicator for soil structure quality. Soil compaction not only affects the volume of macropores and their size distribution, but also alters their continuity. Although the effect of compaction on capacity parameters (total porosity and air-filled porosity) on soil pore functions has been investigated by many

4 OBJECTIVES

researchers, the experimental data of changes in intensity parameters (pore continuity and tortuosity) after compaction has rarely been documented. Soil aeration is one of the most important factors influencing crop production and microbial activity, because it directly affects respiration processes. In general, stress application leads to a reduction of gas transport accompanied by the deterioration of soil pore functions. Once continuous, non-tortuous macropores exist in soils, the preferential gas flow will take place, which may result in a significant increase in soil aeration. However, related investigations have rarely been reported.

a) With respect to changes in the quantity and quality of air-filled pores and gas transport due to static and cyclic loading (Chapter 5, Publication I: “*Effect of static and cyclic loading including spatial variation caused by vertical holes on changes in soil aeration*”): **it is hypothesized that soil pore functions and gas transport properties are a function of soil texture and initial matric potential during mechanical load applications under a given compaction level. Spatial variation is expected to ameliorate soil physical properties (Hypothesis I).** Hypothesis I was tested on repacked soil cores for a given compaction level (50 kPa). This involved the following research questions:

- How far is the pore function and gas transport parameters influenced by static and cyclic loading?
- What is the impact of different soil texture and initial matric potential on soil physical properties during compaction?
- How far are soil physical properties affected by the change in soil structure (artificially vertical holes)?

b) With respect to changes in soil pore functions and gas transport by mechanical loading with different compaction levels (Chapter 6, Publication II: “*Dynamics of pore functions and gas transport parameters in artificially ameliorated soils due to static and cyclic loading*”): **it is hypothesized that intensity of mechanical loading has a crucial impact on soil pore functions and gas transport. The reduction of soil aeration is related to the deterioration of soil pore functionality after compaction. (Hypothesis II).**

4 OBJECTIVES

Hypothesis II was tested on repacked soil cores with different texture and initial matric potential, which are subjected to different types (static and cyclic) and intensity (50, 100 and 200 kPa) of mechanical loading under laboratory conditions. Therefore, investigations are based on solving the following research questions:

- What is the impact of static and cyclic loading with different compaction levels on soil physical properties?
- Is there a linkage between the capacity and intensity properties of pore functions?
- How far is the gas transport behavior influenced by pore function properties?
- How far can the compacted and deformed soils be ameliorated by artificially prepared vertical holes and are there limits to apply such technique when it is used under in situ conditions and what needs to be considered beforehand??

2) Influence of soil internal strength and external stresses on soil mechanical and hydraulic deformation

Stress application can result in not only mechanical deformation (vertical displacement) and affects soil pore functions and soil aeration, but also hydraulic deformation (pore water pressure), which reflects soil water retention and hydraulic conductivity. Soil deformation depends on soil internal strength and external stresses. If the external stress is smaller than the internal soil strength, elastic deformation will take place. However, if the internal soil strength is exceeded, soil deformation is considered as plastic. Agricultural management practices can significantly affect soil hydraulic properties and processes in space and time. It is essential to quantify and to predict compaction effects on soil properties in order to model their effects on production and the environment. There is a variation in hydraulic conductivity and volumetric water content for different textured soils under different compaction levels. It is reasonable to assume that the coupled effects of the intensity and type of stresses and structure play an important role in pore functions and, as a result, are principle factors influencing hydraulic properties, which can lead to soils becoming either weaker or stronger after compaction.

With respect to consequences on time- and stress-dependent changes in vertical displacement and pore water pressure after compaction (Chapter 7, Publication III: “*Influence*

4 OBJECTIVES

of static and cyclic loading on mechanical and hydraulic properties of soils with different textures and matric potentials”), **it is hypothesized that soils with different texture and initial matric potential are differently susceptible for mechanical load applications. The extent of soil deformation is also a function of external factors such as loading types, loading magnitude and loading time (Hypothesis III).** In order to test Hypothesis III following research questions are investigated:

- What is the impact of compaction levels and types of stress applications (static and cyclic loading) on soil mechanical (vertical displacement), hydraulic properties (soil water retention curve, hydraulic conductivity and pore water pressure) and soil strength (effective stress)?
- How far is the mechanical and hydraulic deformation behavior influenced by soil texture and initial matric potential?
- How far occur time-dependent changes in vertical displacement and pore water pressure during static and cyclic loading?

5 Effect of static and cyclic loading including spatial variation by vertical holes on changes in soil aeration

Xiafei Zhai, Rainer Horn

Published in Soil and Tillage Research (2018). Volume 177: 61-67.

5.1 Abstract

Gas transport properties are important factors influencing soil quality and crop production, as it directly affects respiration processes of plant roots and microorganisms. They depend not only on soil characteristics such as soil texture, matric potential and soil structure, but also on the type of applied stress (i.e. static loading and cyclic loading). Although there are some studies investigating the effects of compaction on soil gas transport properties, experimental data related to spatial variation caused by vertical holes during static loading are scarce. Therefore, the effect of static, following cyclic loading, and the effect of vertical pores during static loading on total porosity, air-filled porosity (ϵ_a), air permeability (K_a) and relative gas diffusivity (D_s/D_o) at matric potentials of -60 hPa and -300 hPa were investigated by using repacked soil samples with three different textures (sand, silt loam, clay loam). Total porosity and air-filled porosity (ϵ_a) after static loading and subsequent cyclic loading were lower than before loading. Compaction caused a reduction in total porosity mainly due to the decrease of macropores, which can be derived from the reduced air-filled porosity after compaction. The same is also true for air permeability (K_a) and relative gas diffusivity (D_s/D_o), except for clay soil at the matric potential of -300 hPa which may be equilibrated by an enhanced soil shrinkage and crack formation. The higher water content and the lower number of macropores of fine-textured soil might be the reason that the silt loam soil at the matric potential of -60 hPa revealed the lowest values of all observed parameters. The effect of artificially drilled continuous and non-tortuous vertical holes in the samples resulted in a slight but insignificant increase in total porosity and air-filled porosity, as they only accounts for 0.2 % of the total bulk soil volume. Because these samples with vertical holes were equilibrated with the major principle stress, they remained rigid during consecutive static loading. Consequently, K_a significantly increased up to more than one order

of magnitude, irrespective of the texture and matric potential. Drilling holes caused D_s/D_o to increase by 0.13-14.89 times especially in the fine-textured soil (silt loam) at less negative matric potential (-60 hPa).

Keywords: Soil compaction; Pore function; Gas transport

5.2 Introduction

The process of soil aeration is an important determinant of soil productivity. In the unsaturated zone, gas is transported either in the gaseous phase or in dissolved form through the liquid phase. Since the rate of gas transport in the air phase is much greater than in the liquid phase, soil aeration is mostly dependent on the volume fraction of air-filled pores (Hillel, 2003). Soil aeration is restricted when the network of air-filled pores is partially or entirely blocked, when the soil is extremely compacted or when it is excessively wet (Hillel, 2003).

Generally, there are two main mechanisms of gas transport in soils: mass flow or advection/convection and molecular diffusion. Air permeability (K_a) is the governing parameter for mass flow induced by air pressure gradients. Concerning the relative gas diffusivity (D_s/D_o , the ratio of apparent gas diffusion in soil, and gas diffusion in air), we consider it as the governing parameter for molecular diffusion induced by concentration gradients (Glinski et al., 2011).

Gas transport is limited by some resistance factors: (i) Soil texture. It is directly related to soil particle size distribution, and results in different patterns of the water retention curve or pore size distribution, pore continuity and tortuosity, thus influencing air permeability and gas diffusion (Mentges et al., 2016; Deepagoda et al., 2011; Neira et al., 2015). According to Glinski and Stepniewski (1985), the values of air permeability in soils are within the range of $0.01-500 \times 10^{-12} \text{ m}^2$. Clay soil has more fine pores with lower pore continuity, which leads to lower air permeability, whereas air permeability in sandy soil is more dependent on macroporosity and less influenced by pore continuity at a given matric potential (Ball et al., 1981; Mentges et al., 2016). Even though the clay soil and sand soil may have an identical water content, air permeability of clay soil is still orders of magnitude smaller than of sand soil (Logsdon et al., 2013). Based on the existing literature, approximate ranges for air

permeability in homogeneous soils of different texture range from clay: $<1 \mu\text{m}^2$; to silt: $1-10 \mu\text{m}^2$; while fine sand: $10-100 \mu\text{m}^2$; coarse sand: $100-1000 \mu\text{m}^2$; gravel: $> 1000 \mu\text{m}^2$ (Logsdon et al., 2013). (ii) Water content. With the increase of water content, the amount of air-filled pores decreases, which is directly related to pore diameter, continuity and tortuosity, thus affecting soil gas transport (Mentges et al., 2016). (iii) Structure. Air permeability strongly depends on soil structure, especially on the continuity of the active (or functional) air-filled pores. Consequently, it is very sensitive to even small structural changes (Logsdon et al., 2013). If gas diffuses in the continuous, non-tortuous and non-constricted pores and these pores are parallel to the concentration gradient, then relative gas diffusivity equals porosity (Gradwell, 1961). However, since non-continuous, tortuous and constricted air-filled pores, influenced by soil texture, water content and soil structure dominate in soils, relative gas diffusivity is generally smaller than air-filled porosity (Ball, 1981).

Soil compaction increases bulk density and decreases porosity, and the macroporosity in particular (Simojoki et al., 2008; Weisskopf et al., 2010), which affects the geometry and continuity of the pore system. Air permeability and relative gas diffusivity are suitable indicators for identifying soil pore characteristics (Moldrup et al., 2003; Iversen et al., 2001), and for evaluating the changes in soil structure (Fish and Koppi, 1994; Moldrup et al., 2001). Thus, the effects of soil compaction on soil aeration are usually quantified by capacity parameters like air-filled porosity, or by more reliable intensity parameters: air permeability, or relative gas diffusivity (Lipiec and Hatano, 2003). In this study, our objective was to evaluate the effect of differences in soil texture (sand, silt loam, clay loam), matric potential (-60 hPa and -300 hPa) and soil structure (artificially prepared as vertical holes) on soil aeration properties, and to investigate the effect of static and consecutive cyclic loading on gas transport.

5.3 Materials and methods

5.3.1 Soil sampling and properties

Disturbed soil samples with different textures were collected from three sites in Germany: (i) The Podsol derived from glacial outwash has sand texture with quite a lot of stones. The experimental agricultural site is located in Schuby ($54^{\circ}52'N$, $9^{\circ}45'E$) where the vegetation is

annual ryegrass (*Lolium multiflorum*). (ii) The Haplic Luvisol derived from loess has silt loam texture. The arable site was established at the experimental station Klein Altendorf (50°37'N, 6°59'E) in Bonn. (iii) The Stagnosol derived from glacial till is located in Fehmarn (54°27'N, 11°16'E) under arable management. The soil has clay loam texture. The basic soil properties are shown in Table 5-1. Particle size distribution was determined by the Pipette method after the destruction of organic matter and removal of carbonate. Soil texture was classified according to USDA classification. pH was determined by the Potentiometric method with soil extractant of 0.01 mol/L CaCl₂ solution. CaCO₃ content was measured by gas volume method. Organic carbon was determined according to Schlichting et al. (1995).

Table 5-1 Basic physical and chemical soil properties of studied soils

Sampling site	Depth (cm)	Particle size distribution (%)			Soil texture	pH (CaCl ₂)	CaCO ₃ (%)	OM (%)
		Sand	Silt	Clay				
		63-2000 μm	2-63 μm	< 2μm				
Schuby	5-20	85.8	10.2	4.0	Sand	5.00	0.07	6.34
Bonn	5-20	10.7	73.1	16.2	Silt loam	7.39	0.21	2.04
Fehmarn	35-55	38.3	25.3	36.4	Clay loam	7.59	13.92	0.72

5.3.2 Sample preparation

The samples were air-dried, sieved through 2 mm and then repacked with an initial dry bulk density of 1.4 g cm⁻³ in 235 cm³ soil cylinders (10 cm in diameter and 3 cm in length). The prepared soil cylinders were saturated and then successively drained to matric potentials of -60 hPa on sandboxes and -300 hPa on ceramic plates. The cylinders of clay loam soil at the matric potential of -60 hPa were not prepared, due to the extremely low air-filled porosity which would result in very low values of air permeability and gas diffusivity.

Shrinkage occurred in both silty and clayey samples from saturation to the matric potential of -300 hPa, resulting in the change of initial bulk density and an enhanced preferential air flow along the gaps developing between the soil matrix and the cylinder wall. Therefore, at the matric potential of -300 hPa the cylinders of silt loam and clay loam soils were prepared by another method. The amount of water of silt loam and clay loam soils at the

matric potential of -300 hPa was added to the air-dried samples by spraying distilled water to achieve the desired water content and samples were kept in plastic bags for 24 h for water content equilibration. Thereafter, the prepared soil samples were repacked into the cylinders.

5.3.3 Compaction experiment

The prepared cylinders were compacted under static loading of 50 kPa. The stress was applied for 4 h, followed by an unloading for 1h. Prior to the loading and thereafter the air permeability and gas diffusivity were determined. Thereafter, these cylinders were compacted under cyclic loading (50 cycles) with a constant external stress of 50 kPa. Each cycle consisted of 30s of loading and 30s of unloading. The same soil functionality measurements (air permeability and gas diffusivity) were carried out. Finally, five vertical holes ($\varnothing = 2$ mm each) were drilled by a straight core with a diameter of 2 mm in each of these pre-stressed cylinders and they were compacted again under static loading of 50 kPa for 4 h, unloaded for 1 h. Thereafter, the same properties were determined. Each treatment included 5 replicated samples.

5.3.4 Measurements of air permeability and gas diffusivity

A steady state method was used to determine air permeability. Under a constant air pressure difference of 0.1 kPa across the soil sample, an steady-state air flux was established. The pressure gradient was measured by air flow meter. The air permeability was calculated by the equation based on Darcy's law (Ball et al., 1981):

$$K_a = \frac{q' L_s \eta}{A_s \Delta p} \quad (1)$$

where K_a is air permeability (m^2), q' is the volumetric flow rate ($m^3 s^{-1}$), η is the air dynamic viscosity (Pa s), Δp is the pneumatic pressure difference (Pa), L_s (m) and A_s (m^2) are the length of the sample and the cross sectional area of the cylindrical sample, respectively.

Gas diffusion coefficient was measured by a double chamber method. The cylinder was installed between two closed chambers, the upper one filled with synthetic air ($20.5 \pm 0.5\%$ O_2 in N_2) and the lower one filled with nitrogen at the beginning. Oxygen sensors in each chamber monitored the change of oxygen concentration. When the equilibrium was reached,

the values of sensors were nearly identical. According to Fick's law, gas diffusion coefficient can be calculated by the following equation (Ball, 1981):

$$D_s = \frac{-\ln(\Delta C / (2 \times C_{eq})) \times V_s \times L_s}{A_t \times t \times 2} \quad (2)$$

where D_s is the apparent soil gas diffusion coefficient ($\text{m}^2 \text{s}^{-1}$), ΔC is the oxygen concentration difference between two chambers (g m^{-3}), C_{eq} is the final oxygen concentration at equilibrium (g m^{-3}), V_s (m^3), L_s (m) and A_s (m^2) are the volume, the length and cross sectional area of the sample, respectively. t is time (s). Relative gas diffusion coefficient (D_s/D_o), being the ratio of gas diffusion coefficient in soil (D_s) to that of the same gas in free air (D_o) taken at the same pressure and temperature (Glinski et al., 2011). The value of D_s/D_o in soil is usually below 1, due to tortuosity and limited connectivity of air-filled pores in soil (Uteau et al., 2013).

An overview of the process of experiments is shown in Fig.5-1. Air permeability and gas diffusion coefficients were measured (i) before loading (B.L.), (ii) after static loading (A.SL.), (iii) after cyclic loading (A.CL.), (iv) after having drilled five vertical holes and before static loading (A.Hs & B.SL.) and (v) after having drilled five vertical holes followed by static loading (A.Hs & A.SL.).

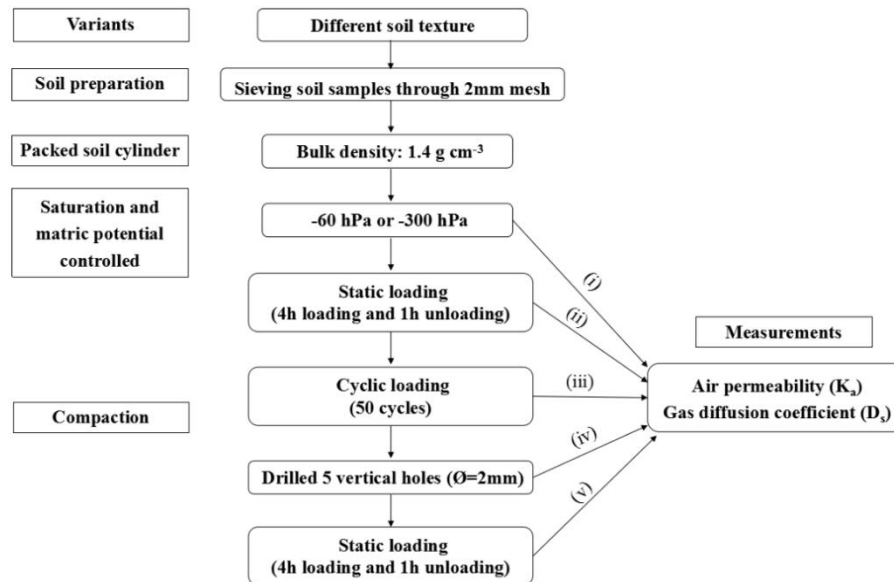


Fig.5-1 Schematic chart of the experiments.

5.3.5 Models for gas transport prediction and pore geometry indexes

As proposed by Ball et al. (1988), K_a and ε_a were regressed by logarithmic transformation of an exponential model:

$$\log K_a = \log M + N \log \varepsilon_a \quad (3)$$

where M and N are empirical constants. K_a is the air permeability (μm^2) and ε_a is the air-filled porosity ($\text{cm}^3 \text{cm}^{-3}$).

The study of Buckingham (1904) found an exponential relationship between D_s/D_o and ε_a :

$$D_s/D_o = A\varepsilon_a^B \quad (4)$$

where A and B are empirical constants. The classical values for predicting models are $A=1$ and $B=2$ (Buckingham, 1904).

D_s/D_o and ε_a may also be related by a straight line (Gradwell, 1961; Ball et al., 1988):

$$D_s/D_o = E\varepsilon_a - F \quad (5)$$

where E and F are empirical constants. The widely known values proposed by Penman (1940) are $E=0.66$ and $F=0$.

Groenevelt et al. (1984) introduced the pore continuity index (C_2) as follows, which was further used by Ball et al. (1988), Blackwell et al. (1990), and Dörner et al. (2012).

$$C_2 = \frac{K_a}{\varepsilon_a} \quad (6)$$

where K_a is the air permeability (μm^2) and ε_a is the air-filled porosity ($\text{cm}^3 \text{cm}^{-3}$).

An index of tortuosity, τ , is defined as the ratio of the average capillary tube length, L , to the porous media (soil sample) length, L_e , which can be calculated by air-filled porosity (ε_a) and relative gas diffusivity (D_s/D_o) (Currie, 1960; Ball, 1981; Hamamoto et al., 2009).

$$\tau = \frac{L}{L_e} = \sqrt{\frac{\varepsilon_a}{D_s/D_o}} \quad (7)$$

5.3.6 Statistical analyses

The mean comparisons were tested with ANOVA followed by the Tukey's HSD test for probability $p < 0.05$. All statistical analyses were undertaken using the SPSS (Statistical Product and Service Solutions) statistics software.

5.4 Results and discussion

5.4.1 Total porosity

The stress application and vertical holes change the total porosity in each treatment (Fig.5-2a). At a given initial bulk density, soil compaction always results in a decrease in total porosity primarily caused by reduction of the coarse pores (Blume et al., 2016; Horn et al., 1995). After static loading, total porosity decreased significantly ($p < 0.05$) for all treatments compared to before loading. Total porosity of silt loam soil at the matric potential of -60 hPa decreased significantly by 14.61 %. However, there was no difference among other treatments where total porosity only decreased by 3.05-5.23 %. These results are expected, because both textural properties and water content affect the soil compressibility (Hillel, 1998).

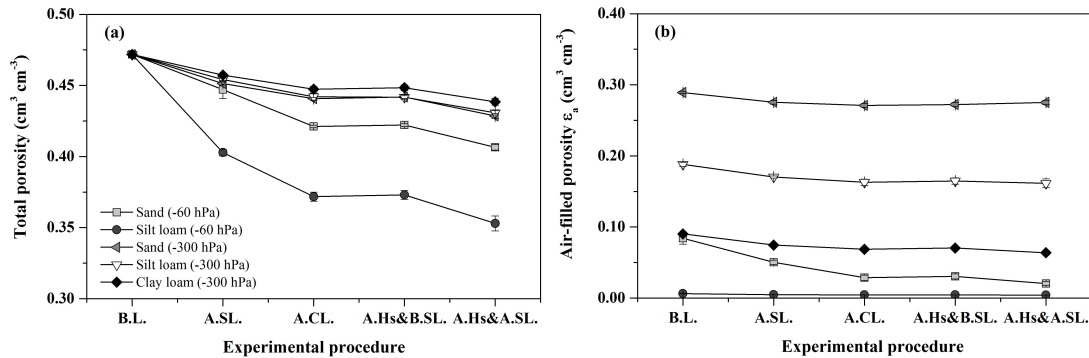


Fig.5-2 Stress application and vertical holes effects on changes of (a) total porosity and (b) air-filled porosity (ϵ_a) in each treatment. X axis: B.L. = before loading; A.S.L. = after static loading; A.C.L. = after cyclic loading; A.Hs&B.SL. = after having drilled holes and before static loading; A.Hs&A.SL. = after having drilled holes and after static loading.

Cyclic loading at the same stress results in a less intense decline of total porosity compared to the effect of static loading by 5.81 %, 7.72 %, 2.36 %, 2.67 % and 2.20 %, respectively for the sand soil (-60 hPa), silt loam soil (-60 hPa), sand soil (-300 hPa), silt loam soil (-300 hPa), clay loam soil (-300 hPa). These findings are in agreement with those of Peth et al. (2010), who found that for the first loading with a load of 6.5 Mg in the plowed topsoil, total porosity decreased by 10.6 %, while for the subsequent loading, it only decreased by additional 2.8 %.

By implementing five vertical holes, total porosity became a bit higher. However, there

was no significant difference compared to before having drilled holes, perhaps because the volume of holes (0.40 cm^3) only accounts for 0.2 % of the total volume. After compaction, there was a significant decrease in total porosity for all treatments. However, after static loading with an identical applied stress, the actual extent of reduction in total porosity after having drilled holes was less than before. Previous static and cyclic loading before drilling resulted in an increase in soil strength, which might contribute to the soil becoming less susceptible to compaction after having drilled these five vertical holes.

5.4.2 Air-filled porosity

The results of stress application and vertical hole effects on changes of air-filled porosity are shown in Fig.5-2 (b). For a given initial total porosity, the lower volumetric water content, the higher was the air-filled porosity. Before loading, ϵ_a of sand soil (-300 hPa) was the highest and of silt loam soil (-60 hPa) was the lowest which was almost near to 0. It was attributed to soil textural properties and initial matric potential. The finer the texture and the higher the matric potential, the smaller was air filled porosity.

After static loading, ϵ_a decreased significantly ($p < 0.05$) for all treatments compared to before loading. After cyclic loading, ϵ_a remained nearly constant, but there was a significant difference among all treatments. The higher water content and the lower number of macropores of fine-textured soil might be the reason that the silt loam soil at the matric potential of -60 hPa had the lowest value of air-filled porosity.

Although ϵ_a did not change significantly after having drilled vertical holes, pore diameter was altered obviously which could affect soil aeration. Before having drilled vertical holes, ϵ_a of sand soil (-60 hPa), silt loam soil (-60 hPa), sand soil (-300 hPa), silt loam soil (-300 hPa), clay loam soil (-300 hPa) before the procedure had a significantly reduction by 39.99 %, 24.64 %, 4.76 %, 9.41 % and 17.35 %, respectively after static loading compared to before loading. However, there was no difference for all treatments between before and after static loading after having drilled these five vertical holes. Compared to before loading, ϵ_a of sand soil (-60 hPa), silt loam soil (-60 hPa), silt loam soil (-300 hPa), clay loam soil (-300 hPa) after having drilled vertical holes and after static loading had a decrease by 32.70 %, 8.30 %, 1.86 % and 9.59 %, respectively and only a small increase in the sand soil (-300 hPa). The

theoretical expectation that drilling vertical holes in a compacted soil results in an additional strain was not verified because these new pores were already equilibrated with the major vertical stress.

5.4.3 Air permeability

Fig.5-3 (a) shows the effect of stress application and of vertical holes on changes in air permeability. K_a was strongly correlated with ϵ_a . Before loading, K_a of sand soil (-300 hPa) was the highest and silt soil (-60 hPa) was the lowest.

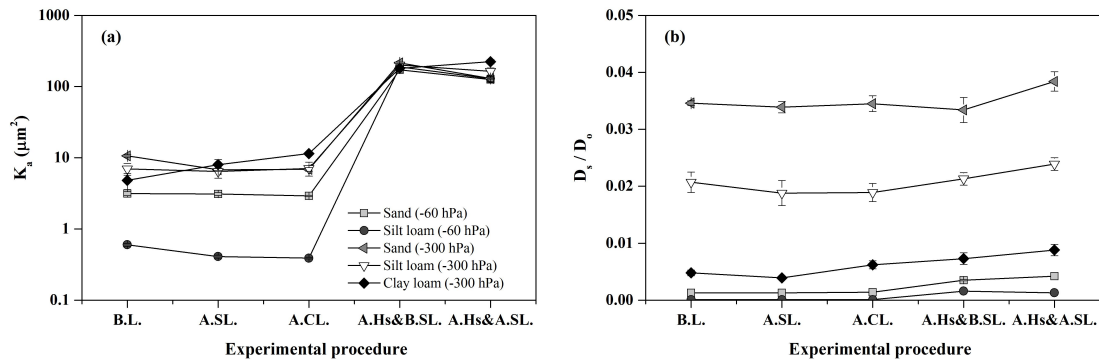


Fig.5-3 Stress application and vertical holes effects on changes of (a) air permeability (K_a) and (b) relative gas diffusivity (D_s/D_0) in each treatment. X axis: B.L. = before loading; A.SL. = after static loading; A.CL. = after cyclic loading; A.Hs&B.SL. = after having drilled holes and before static loading; A.Hs&A.SL. = after having drilled holes and after static loading.

Compared to before loading, compaction led to a little decrease in K_a after static loading and after cyclic loading, except in the clay loam soil (-300 hPa). Soil shrinkage occurred due to the reduction in water content after compaction, which resulted in a gap forming between soil sample and the inner wall of cylinder. Therefore, K_a of clay loam soil (-300 hPa) increased after compaction.

Although there were significant differences of ϵ_a among all treatments (sand soil (-300 hPa) > silt loam soil (-300 hPa) > clay loam soil (-300 hPa) > sand soil (-60 hPa) > silt loam soil (-60 hPa)) after static loading and after cyclic loading, there was no difference among treatments at similar matric potential (-60 hPa or -300 hPa). It implied that K_a is controlled not only by the quantity of air-filled pores, but also by the quality of air-filled pores. The latter term is related to pore size distribution and continuity which depends on bulk density, water

5 EFFECT OF STATIC AND CYCLIC LOADING INCLUDING SPATIAL VARIATION BY VERTICAL HOLES
ON CHANGES IN SOIL AERATION

content, organic matter and soil texture (Ball, 1981; Glinski et al., 2011; Mentges et al., 2016; Groenevelt et al., 1984; Lipiec and Hatano, 2003). Similarly, K_a was measured by Sánchez-Giróna et al. (1998), on repacked soil with textures ranging from sandy-loam to clay at different gravimetric water content (5, 10, 15, 20 and 25%). The results showed that under the compression stress of 50 kPa, the average air permeability was almost constant below 20 % water content but further decreased as the water content was raised to 25 %.

Table 5-2 Arithmetic Means and standard deviation of pore continuity (C_2) and tortuosity (τ) indexes for all treatments at each procedure.

Treatments	C_2 ($\mu\text{m}^2 \times 100$)					τ				
	B.L.	A.SL.	A.CL.	A.Hs &	A.Hs &	B.L.	A.SL.	A.CL.	A.Hs &	A.Hs &
				B.SL.	A.SL.				B.SL.	A.SL.
Sand soil	0.39 ±	0.63 ±	1.10 ±	63.46 ±	64.12 ±	7.87 ±	6.23 ±	4.39 ±	2.93 ±	2.18 ±
(-60 hPa)	0.04 b	0.07 bc	0.16 b	15.14 b	8.25 b	0.27 a	0.27 a	0.25 b	0.15 a	0.14 bc
Silt loam soil	0.97 ±	0.88 ±	0.87 ±	426.14 ±	317.84 ±	7.89 ±	6.85 ±	6.66 ±	1.67 ±	1.77 ±
(-60 hPa)	0.04 a	0.05 ab	0.04 b	14.48 a	27.82 a	0.11 a	0.10 a	0.09 a	0.01 b	0.03 c
Sand soil	0.37 ±	0.25 ±	0.25 ±	7.91 ±	4.71 ±	2.89 ±	2.86 ±	2.81 ±	2.87 ±	2.69 ±
(-300 hPa)	0.01 b	0.01 c	0.01 c	0.24 c	0.11 c	0.01 c	0.04 c	0.04 c	0.09 a	0.07 b
Silt loam soil	0.37 ±	0.37 ±	0.43 ±	12.24 ±	10.31 ±	3.04 ±	3.07 ±	2.97 ±	2.79 ±	2.60 ±
(-300 hPa)	0.07 b	0.07 c	0.09 c	0.41 c	1.46 bc	0.10 c	0.17 c	0.14 c	0.10 a	0.05 ab
Clay loam soil	0.52 ±	1.07 ±	1.69 ±	25.96 ±	35.86 ±	4.39 ±	4.39 ±	3.40 ±	3.17 ±	2.75 ±
(-300 hPa)	0.12 b	0.18 a	0.13 a	2.68 bc	3.94 bc	0.17 b	0.16 b	0.22 c	0.20 a	0.19 a

Note that Different letters behind the standard deviation indicate differences among treatments at each procedure by Tukey's HSD test (* $P < 0.05$).

According to Poiseuille's law, air permeability depends on the fourth power of pore

radius (Ball, 1981). Vertical holes increased not only pore continuity (shown in Table 5-2), but also average pore diameter. After having drilled vertical holes, K_a significantly increased up to more than one order of magnitude. Although ε_a of silt loam soil (-60 hPa) was significantly lower than other treatments, pore continuity index (C_2) was significantly higher than other treatments (Table 5-2), which resulted in no difference in K_a among all treatments. It implied that K_a depends not only on air-filled porosity, but also on pore continuity. After compaction, K_a of sand soil (-60 hPa), silt loam soil (-60 hPa), sand soil (-300 hPa), silt loam soil (-300 hPa) was significantly reduced by 27.02 %, 31.50 %, 39.77 % and 18.60 % respectively, except for the clay loam soil (-300 hPa) which may be related to soil shrinkage. The reduction in K_a after compaction might reasonably be attributable to the reduced values of air-filled porosity, and on the other hand, to the reduction of pore continuity.

5.4.4 Relative diffusion coefficient

Fig.5-3 (b) shows the effect of stress application and of vertical holes on changes in relative gas diffusivity. Before loading, D_s/D_o of sand soil (-300 hPa) was the highest and of silt (-60 hPa) was the lowest. This may suggest that the decrease in D_s/D_o might be attributed to the reduction of air-filled porosity. Similar observations were reported in Wickramarachchi et al. (2011) and Kuncoro et al. (2014).

After static loading and after cyclic loading, there was a slight reduction in D_s/D_o , except for clay loam soil (-300 hPa) which may be related to soil shrinkage. Ball and Ritchie (1999) measured gas diffusion coefficient by using undisturbed soil with texture between loam and sandy loam from 0-25 cm. The results showed that relative gas diffusivity decreased after heavy compaction using a laden tractor (up to 4.2 Mg).

After having drilled vertical holes, D_s/D_o of sand soil (-60 hPa), silt loam soil (-60 hPa), silt loam soil (-300 hPa) and clay loam soil (-300 hPa) increased by 1.40, 14.89, 0.13, 0.18 times, except for sand soil (-300 hPa). This indicated that for fine-textured soil at less negative matric potential (-60 hPa), these drilled vertical holes can effectively ameliorate soil gas diffusion, whereas for soils at more negative matric potential (-300 hPa), the influence of having drilled vertical holes on gas diffusion was smaller. Although air-filled porosity decreased for all treatments at the matric potential of -300 hPa after compaction, pore

tortuosity (Table 5-2) also decreased which may be the reason that there was no difference in D_s/D_o . Relative gas diffusion coefficient D_s/D_o in silt soil at the matric potential of -60 hPa decreased significantly ($p < 0.05$), which may be due to the reduction of air-filled porosity and the increase of pore tortuosity (Table 5-2) caused by partly blockage and distortion of vertical holes. It implied that D_s/D_o depended not only on air-filled porosity but also pore tortuosity.

5.5 Models for gas transport prediction

A positive linear log-log relationship between ϵ_a and K_a in all samples was found before having drilled vertical holes (Fig.5-4a). This is in agreement with Ball et al. (1988), Dörner and Horn (2006) and Berisso et al. (2013). However, a poor correlation between ϵ_a and K_a in all samples after having drilled vertical holes is shown in Fig.5-4b. The reason might be that although ϵ_a did not change significantly after having drilled vertical holes, the present of a few large continuous holes just let the participation of smaller pores in the total air flow become negligible which caused K_a was at a much larger magnitude after having drilled vertical holes than before. Therefore, these results underline the fact, the value of air permeability is controlled by both the amount of air-filled pores and its configuration.

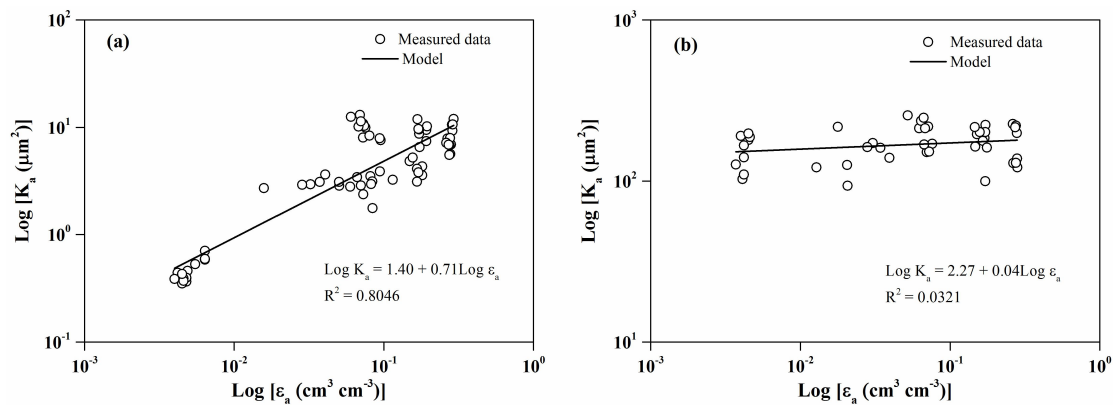


Fig.5-4 Relationship between air-filled porosity (ϵ_a) and air permeability (K_a) before having drilled vertical holes (a) and after having drilled vertical holes (b). The open symbols represent measured data for all samples. The solid lines represent the linear regression for all data.

Both positive linear and exponential relationships between ϵ_a and D_s/D_o are shown,

which appears to be satisfactory for all samples before (Fig.5-5a) and after (Fig.5-5b) having drilled vertical holes. This suggests that the decrease in D_s/D_o is reasonably attributable to the decrease in ϵ_a . Gradwell (1961) reported that relative gas diffusivity equals porosity in pores which are continuous, non-tortuous and non-constricted. In our study, the porosity of vertical holes is 0.002. The value of D_s/D_o of the silt loam soil (-60 hPa) is lower than 0.002, whereas D_s/D_o of other treatments is higher than 0.002. It implies that gas diffusion of silt loam soil at a matric potential of -60 hPa only took place in the vertical holes, and the pore diameter may alert due to soil shrinkage and compaction resulting in the overestimation of the porosity of vertical holes. Gas diffusion of other treatments took place in both the vertical holes and other well connected pores.

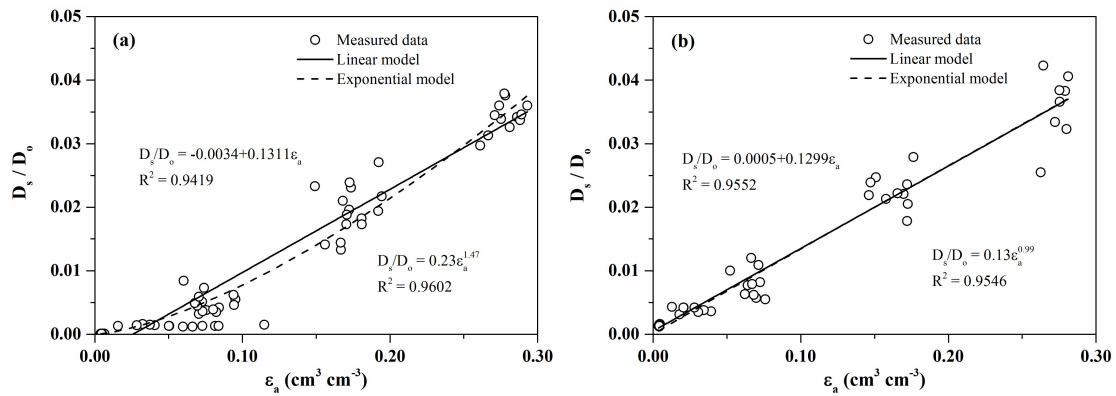


Fig.5-5 Relationship between air-filled porosity (ϵ_a) and relative gas diffusivity (D_s/D_o) before having drilled vertical holes (a) and after having drilled vertical holes (b). The open symbols represent the measured data for all samples. The solid and dashed lines represent the linear and exponential regression for all data, respectively.

Air permeability is more dependent than gas diffusion on the radius, length and continuity of the largest pores in the sample and it is less dependent on total air-filled porosity (Ball, 1981). Since air permeability depends on the fourth power of pore radius and gas diffusion on the square of pore radius, the vertical holes contributes much less to the magnitude of D_s/D_o than to the magnitude of K_a .

5.6 Conclusion

- 1) Static loading and following cyclic loading significantly affect total porosity and

air-filled porosity of the studied soils. Due to the decrease in air-filled porosity, air permeability and relative gas diffusivity also decreased after compaction, except for clay soil at the matric potential of -300 hPa, which may be related to soil shrinkage and crack formation.

2) Vertical and continuous holes within the soil prevent further stress induced strain processes which results in no significant differences in total porosity and air-filled porosity between before and after drilling holes. Since vertical holes increased not only pore continuity, but also pore diameter, both K_a and D_s/D_o significantly increased compared to before having drilled holes, except for sand soil (-300 hPa).

3) The relationship of between K_a and ϵ_a in all samples can be fitted to the positive linear log-log model, except for after having drilled vertical holes. The linear and exponential models in this study explain well the processes and correlations for all samples before and after having drilled vertical holes to predict the relationship between D_s/D_o and ϵ_a .

5.7 Acknowledgement

This study was funded by the China Scholarship Council (CSC) for Xiafei Zhai.

5.8 References

- Ball, B.C., O'Sullivan, M. F., Hunter, R., 1988. Gas diffusion, fluid flow and derived pore continuity indices in relation to vehicle traffic and tillage. *J. Soil Sci.* 39, 327-339.
- Ball, B.C., 1981. Pore characteristics of soils from two cultivation experiments as shown by gas diffusivities and permeabilities and air-filled porosities. *J. Soil Sci.* 32, 483-498.
- Ball, B.C., Harris, W., Burford, J.R., 1981. A laboratory method to measure gas diffusion and flow in soil and other porous materials. *J. Soil Sci.* 32, 323-333.
- Ball, B.C., Ritchie, R.M., 1999. Soil and residue management effects on arable cropping conditions and nitrous oxide fluxes under controlled traffic in Scotland: 1. Soil and crop responses. *Soil Till. Res.* 52(3-4), 177-189.
- Berisso, F.E., Schjønning, P., Keller, T., Lamandé, M., Simojoki, A., Iversen, B.V., Alakukku, L., Forkman, J., 2013. Gas transport and subsoil pore characteristics: Anisotropy and long-term effects of compaction. *Geoderma* 195-196, 184-191.

5 EFFECT OF STATIC AND CYCLIC LOADING INCLUDING SPATIAL VARIATION BY VERTICAL HOLES
ON CHANGES IN SOIL AERATION

- Blackwell, P.S., Ringrose-Voase, A.F., Jayawardane, N.S., Olsson, K.A., McKenzie, D.C., Mason, W.K.,
1990. The use of air-filled porosity and intrinsic permeability to characterize macropore structure
and saturated hydraulic conductivity of clay soils. *J. Soil Sci.* 41, 215-228.
- Blume, H.P., Brümmer, G.W., Fleige, H., Horn, R., Kandeler, E., Kögel-Knabner, I., Kretzschmar, R.,
Stahr, K., Wilke, B.M., 2016. *Scheffer/Schachtschabel Soil Science*. Springer.
- Buckingham, E., 1904. *Contributions to our Knowledge of the Aeration of Soils*. U.S. Dept. Of
Agriculture, Bureau of Soils.
- Currie, J.A., 1960. Gaseous diffusion in porous media: Part II. Dry granular materials. *Br. J. Appl. Phys.*
11, 318-324.
- Deepagoda, T.K.K.C., Moldrup, P., Schjønning, P., De Jonge, L.W., Kawamoto, K., Komatsu, T., 2011.
Density-corrected models for gas diffusivity and air permeability in unsaturated soil. *Vadose Zone
J.* 10, 226-238.
- Dörner, J., Dec, D., Feest, E., Vasquez, N., Diaz, M., 2012. Dynamics of soil structure and pore
functions of a volcanic ash soil under tillage. *Soil Till. Res.* 125, 52-60.
- Dörner, J., Horn, R., 2006. Anisotropy of pore functions in structured Stagnic Luvisols in the
Weichselian moraine region in N Germany. *J. Plant Nutr. Soil Sci.* 169 (2), 213-220.
- Fish, A.N., Koppi, A.J., 1994. The use of a simple field air permeameter as a rapid indicator of
functional soil pore space. *Geoderma* 63, 255-264.
- Glinski, J., Horabik, J., Lipiec, J., 2011. *Encyclopedia of agrophysics*. Springer.
- Glinski, J., Stepniewski, W., 1985. *Soil Aeration and Its Role for Plants*. Boca Raton: CRC Press.
- Gradwell, M.W., 1961. A laboratory study of the diffusion of oxygen through pasture topsoils. *N. Z. J.
Agric. Res.* 4, 250-270.
- Groenevelt, P.H., Kay, B.D., Grant, C.D., 1984. Physical assessment of soil with respect to rooting
potential. *Geoderma* 34, 101-114.
- Hamamoto, S., Moldrup, P., Kawamoto, K., Komatsu, T., 2009. Effect of Particle Size and Soil
Compaction on Gas Transport Parameters in Variably Saturated, Sandy Soils. *Vadose Zone J.* 8(4),
986-995.
- Hillel, D., 1998. *Environmental Soil Physics*. Academic Press, California, CA.
- Hillel, D., 2003. *Introduction to Environmental Soil Physics*. Academic Press. California, CA.
- Horn, R., Domżał, H., Słowińska-Jurkiewicz, A., van Ouwerkerk, C., 1995. Soil compaction processes

5 EFFECT OF STATIC AND CYCLIC LOADING INCLUDING SPATIAL VARIATION BY VERTICAL HOLES
ON CHANGES IN SOIL AERATION

- and their effects on the structure of arable soils and the environment. *Soil Till. Res.* 35 (1-2), 23-36.
- Iversen, B.V., Moldrup, P., Schjønning, P., Loll, P., 2001. Air and water permeability in differently textured soils at two measurement scales. *Soil Sci.* 166(10), 643-659.
- Kuncoro, P.H., Koga, K., Satta, N., Muto, Y., 2014. A study on the effect of compaction on transport properties of soil gas and water I: Relative gas diffusivity, air permeability, and saturated hydraulic conductivity. *Soil Till. Res.* 143, 172-179.
- Lipiec, J., Hatano, R., 2003. Quantification of compaction effects on soil physical properties and crop growth. *Geoderma* 116 (1-2), 107-136.
- Logsdon, S., Berli, M., Horn, R., 2013. *Advances in Agricultural Systems Modeling 3. Quantifying and Modeling Soil Structure Dynamics.* SSSA.
- Mentges, M.I., Reichert, J.M., Rodrigues, M.F., Awe, G.O., Mentges, L.R., 2016. Capacity and intensity soil aeration properties affected by granulometry, moisture, and structure in no-tillage soils. *Geoderma* 263, 47-59.
- Moldrup, P., T. Olesen, T. Komatsu, P. Schjønning, and D.E. Rolston. 2001. Tortuosity, diffusivity, and permeability in the soil liquid and gaseous phases. *Soil Sci. Soc. Am. J.* 65, 613-623.
- Moldrup, P., Yoshikawa, S., Olesen, T., Komatsu, T., Rolston, D.E., 2003. Air permeability in undisturbed volcanic ash soil: Predictive model test and soil structure finger print. *Soil Sci. Soc. Am. J.* 67, 32-40.
- Neira, J., Ortiz, M., Morales, L., Acevedo, E., 2015. Oxygen diffusion in soils: Understanding the factors and processes needed for modeling. *Chilean J. Agric. Res.* 75, 35-44.
- Penman, H. L. 1940. Gas and vapour movements in the soil: I. The diffusion of vapours through porous solids. *J. Agric. Sci.* 30, 437-462.
- Peth, S., Rostek, J., Zink, A., Mordhorst, A., Horn, R., 2010. Soil testing of dynamic deformation processes of arable soils. *Soil Till. Res.* 106 (2), 317-328.
- Sánchez-Giróna, V., Andreub, E., Hernanza, J.L., 1998. Response of five types of soil to simulated compaction in the form of confined uniaxial compression tests. *Soil Till. Res.* 48, 37-55.
- Schlichting, E., Blume, H.P., Stahr, K., 1995. *Bodenkundliches Praktikum.* Blackwell Wissenschafts-Verlag, Berlin.
- Simojoki, A., Fazekas-Becker, O., Horn, R., 2008. Macro- and micro-scale gaseous diffusion in a

5 EFFECT OF STATIC AND CYCLIC LOADING INCLUDING SPATIAL VARIATION BY VERTICAL HOLES
ON CHANGES IN SOIL AERATION

- Stagnic Luvisol as affected by compaction and reduced tillage. *Agric. Food Sci.* 17, 252-264.
- Uteau, D., Pagenkemper, S.K., Peth, S., Horn, R., 2013. Root and time dependent soil structure formation and its influence on gas transport in the subsoil. *Soil Till. Res.* 132, 69-76.
- Weisskopf, P., Reiser, R., Rek, J., Oberholzer, H.-R., 2010. Effect of different compaction impacts and varying subsequent management practices on soil structure, air regime and microbiological parameters. *Soil Till. Res.* 111, 65-74.
- Wickramarachchi, P., Kawamoto, K., Hamamoto, S., Nagamori, M., Moldrup, P., Komatsu, T., 2011. Effects of dry bulk density and particle size fraction on gas transport parameters in variably saturated landfill cover soil. *Waste Manage.* 31(12), 2464-2472.

6 Dynamics of pore functions and gas transport parameters in artificially ameliorated soils due to static and cyclic loading

Xiafei Zhai, Rainer Horn

Published in *Geoderma* (2019). Volume 337: 300-310.

6.1 Abstract

Soil compaction is one of the main threats to sustain soil quality in modern agriculture. To improve our understanding concerning the interaction between soil physical properties and stress-strain on pore functions and soil aeration, measurements were performed with three different textures (sand, silt loam, clay loam), two matric potentials (-60 and -300 hPa), three compaction levels (50, 100 and 200 kPa) and two loading types (static and cyclic loading). Soil compaction led to a reduction in air-filled porosity ϵ_a , air permeability K_a , and relative gas diffusivity D_s/D_o . The differences in K_a and D_s/D_o among the various treatments depend on the remaining air-filled porosity, pore continuity and pore tortuosity. The water blockage effect on K_a and D_s/D_o with lower ϵ_a also should be considered sometimes after compaction. The question how far the compacted and deformed soils can be ameliorated was tested in the same set of samples by artificially prepared vertical holes. Due to this procedure of vertically arranged continuous and non-tortuous holes in the samples, the values of K_a even significantly increased up to more than one order of magnitude, and the values of D_s/D_o also increased obviously, even though the volume of air-filled pores only increased slightly. This situation was mainly attributable to the significant increase in pore continuity and a decrease in pore tortuosity. We also found that there were minor differences on K_a but distinct differences on D_s/D_o among all treatments after having drilled vertical holes.

Keywords: Soil compaction; pore functions; soil aeration; vertical holes

6.2 Introduction

Globally, soil compaction is one of most harmful processes to threaten soil quality. About 33 million ha of arable land in Europe and 68 million ha worldwide are seriously degraded by soil compaction (Peth et al., 2010). It can be caused naturally due to

freezing-thawing (Defosseze and Richard, 2002), swelling-shrinkage (Pagliai et al., 2003) and internal forces by clay migration or organic acids, or glacial processes (Hartge and Horn, 2016). Furthermore, soil deformation can be induced by external forces such as animal trampling (Hamza and Anderson, 2005; Krümmelbein et al., 2006), farm machinery traffic (Horn et al., 1995; Wiermann et al., 2000) and shear processes which even enhance the soil deformation processes. Among these factors, non site adjusted use of machinery has been recognized as the most common reason of soil compaction in agriculture especially if shearing and hydraulic processes are included (Saffih-Hdadi et al., 2009; Kuncoro et al., 2014). To meet the demands of modern agriculture, the weight of machinery has increased in recent decades (Berisso et al., 2012), which further enhances the unpredictability of crop yields, soil functions, environmental and climate change processes (Horn, 2015).

The sensitivity of soils for compaction depends on internal properties like texture and structure, amount and composition of organic matter, actual and former minimum matric potential, chemical properties, and biological processes. External factors like intensity, number of wheeling events and kind of loading (static/dynamic) alter the soil functions as well as the resilience of the soils mostly irreversibly if external stresses applied exceed the internal soil strength (Horn, 1981; Alakukku, 1996; Peng et al., 2004; Peth et al., 2010; Barik et al., 2014; Głąb, 2014; Horn et al., 1995).

Static loading leads to an increase in soil bulk density (Schäffer et al., 2008; Kim et al., 2010), primarily reducing large pores, and it also alters pore morphology and continuity (Servadio et al., 2001; Richard et al., 2001; Munkholm et al., 2002; Chen et al., 2014; Riggert et al., 2015). Consequently, soil aeration and gas fluxes are reduced or retarded which not only affects plant growth but it also alters the production and emission of greenhouse gases (Hamza and Anderson, 2005; Kim et al., 2010; Głąb, 2014; Glinski et al., 2011). In contrast to static loading, dynamic processes can create both a shear induced deterioration of the pore arrangement and continuity as well as it will if puddling is included under wet soil conditions also completely homogenize the formerly existing soil structure up to the complete loss of all strength. Dynamic i.e. repeated loading also results in cumulative effects which can be defined as time dependent strain effects (Wiermann et al. 2000; Alakukku et al., 2003). The first loading event causes the most probably soil deformation by a significant volume loss and

a change in soil functions which can be detected down to deeper depth (Hamza and Anderson, 2005; Berisso et al., 2012, Horn, 1981; Horn et al., 1995; Hartge and Horn, 2016).

In recent studies, some contradictory conclusions related to the effect of compaction on gas transport parameters have been reported. Naveed et al. (2016) observed that air permeability was reduced by 55-80% for topsoils (5-25 cm depth) and by 10-20% for subsoils (25-35 cm depth) under 620 kPa stress and this reduction was associated with lower total porosity and macroporosity and Chen et al. (2014) found that air permeability in 0-12 cm soil depth was decreased with the level of compaction and this reduction was related to the increase of pore tortuosity and the decrease of pore continuity. In the work of Ball and Ritchie (1999), relative gas diffusivity on undisturbed soil with texture between loam and sandy loam from 0-25 cm decreased after heavy compaction using a laden tractor (up to 4.2 Mg). On the contrary, Kuncoro et al. (2014) observed that air permeability in soil mixed with rice straw was lower than in the control soil at compaction levels of 150 and 225 kPa, even though its air content was a bit higher. They proposed that the presence of soil organic matter was likely to block soil pores and might also facilitate the formation of bottle-necks by water menisci, which results in lower air permeability in soils mixed with organic matter than in the control soil for a given air content. Fujikawa and Miyazaki (2005) reported that soil compaction led to an increase in D_s/D_0 at the same air-filled porosity, probably due to lower volumetric water content. Lower water blockage effects resulted in the increase in active air-filled pore space for gas diffusion.

To investigate whether differences in K_a are only attributed to differences in air-filled porosity or whether they should be attributed partly to geometrical aspects of the air-filled pore space, such as pore size distribution, tortuosity and continuity. Groenevelt et al. (1984) introduced two pore continuity indexes (C_2 and C_3), which were further verified by Ball et al. (1988), Blackwell et al. (1990), and Dörner et al. (2012). They proposed that soils with similar values of C_2 , have similar pore size distributions and pore continuities whereas soils with similar values of C_3 , have similar pore size distributions only, so that differences between C_2 , and C_3 can be related to differences in pore continuity independent of pore size distribution. For gas diffusion, Currie et al., (1960) proposed that D_s/D_0 was affected not only by porosity, but also by pore tortuosity. This info was also confirmed by Ball, 1981; Moldrup

et al., 2001 and Hamamoto et al., 2009. Zhai and Horn (2018) determined soil aeration properties at the compaction level of 50 kPa as a function of texture (sand, silt loam, clay loam), matric potential (-60 hPa and -300 hPa) and soil structure (vertical holes). However, the effects of compaction levels and kinds of stress applications on pore functions and gas transport are mostly unknown although it is obvious that the effect of vertical biopores on gas exchange in soils should improve the gas exchange more effective than at random pores due to the better stress attenuation of vertical systems (for more details also see Hartge and Horn, 2016). Therefore, the objective of the experiments was to investigate:

- i) effects of static and cyclic loading with different compaction levels (50, 100 and 200 kPa) on pore properties like air-filled porosity, pore continuity, pore tortuosity and gas transport parameters (air permeability and relative gas diffusivity),
- ii) effects of the quantity and quality of air-filled pores on the changes in K_a and D_s/D_o ,
- iii) impact of vertical holes on the above mentioned functions.

6.3 Material and methods

6.3.1 Soil sampling and properties

Table 6-1 Basic physical and chemical properties of studied arable soils

Sampling site	Depth (cm)	Particle size distribution (%)			Soil texture	pH (CaCl ₂)	CaCO ₃ (%)	OM (%)
		Sand	Silt	Clay				
		63-2000 μm	2-63 μm	< 2 μm				
Schuby	5-20	85.82	10.18	4.00	Sand	5.00	0.07	6.34
Bonn	5-20	10.68	73.10	16.21	Silt loam	7.39	0.21	2.04
Fehmarn	35-55	38.33	25.32	36.35	Clay loam	7.59	13.92	0.72

Disturbed soil samples of with different textures were collected from three sites in Germany: (i) the sandy material of a Podsol derived from glacial outwash was collected at the

experimental agricultural site located in Schuby (54°52'N, 9°45'E) where the vegetation is annual ryegrass (*Lolium multiflorum*). (ii) The silt loam substrate of a Haplic Luvisol derived from loess was collected at the experimental station Klein Altendorf (50°37'N, 6°59'E) in Bonn with the land use of cropland. (iii) The clayey material of a Stagnosol derived from glacial till is located in Fehmarn (54°27'N, 11°16'E) where the land use is cropland. The basic soil properties are shown in Table 6-1.

6.3.2 Sample preparation

The samples were air-dried, sieved through 2 mm and then repacked in 235 cm³ soil cylinders (10 cm wide and 3 cm long) with an initial dry bulk density of 1.4 g/cm³. The soil cylinders were saturated and then successively drained to matric potentials of -60 hPa on sandboxes and -300 hPa on ceramic plates. The cylinders of clay loam soil at the matric potential of -60 hPa were not prepared, due to the extremely low air-filled porosity which would result in very small values of air permeability and gas diffusivity (close to zero).

In both silty and clayey samples occur obviously shrinkage from saturation to the matric potential of -300 hPa, resulting in the change of initial bulk density and an enhanced preferential airflow through the cracks within the soil sample. Therefore, the cylinders of silt loam and clay loam soil at the matric potential of -300 hPa were prepared as follows: the corresponding water contents of silt loam and clay loam soil at the matric potential of -300 hPa were tested. The air-dried samples were wetted by spraying distilled water to achieve the desired water content and kept in plastic bags for 24 h, to achieve a homogeneous distribution of water in the samples. Thereafter, the prepared soil samples were repacked into the cylinders.

6.3.3 Compaction experiments

The prepared cylinders were compacted under static load of 50, 100 and 200 kPa, respectively. The stress was applied for 4 h, followed by an unloading for 1h. Prior to the loading and thereafter the air permeability and gas diffusivity were determined. Then, all cylinders were compacted under cyclic load (50 cycles) with an identical external stress of 50, 100 and 200 kPa. Each cycle consisted of 30s loading and 30s unloading. The same soil

functionality measurements were carried out as before. Five vertical holes ($\varnothing = 2$ mm each) were drilled in each cylinder (The position of vertical holes on the cross-section of the soil core is shown in Fig.6-1.). Finally, they were compacted under static load of 50, 100 and 200 kPa for 4 h and unload for 1 h. Before and thereafter the same properties were determined. Each treatment included 5 replicated samples.

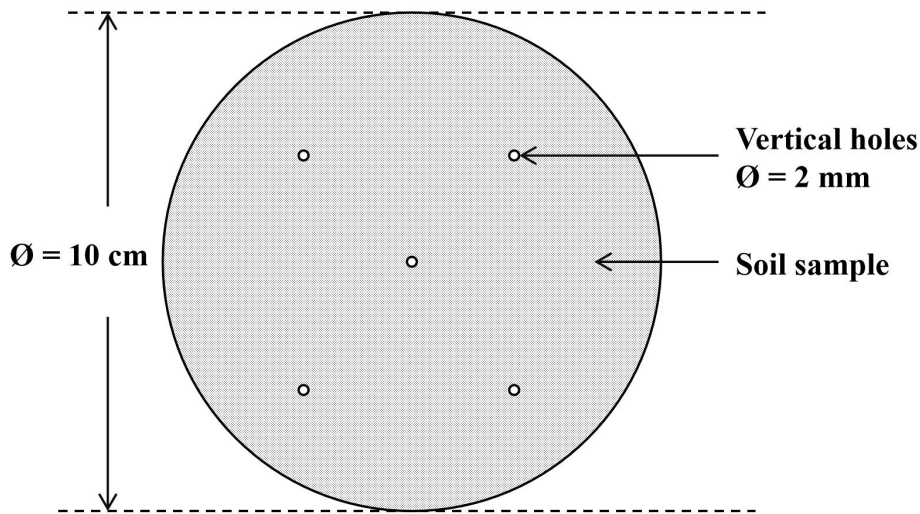


Fig.6-1 Schematic diagram of the position of vertical holes on the cross-section of soil core.

6.3.4 Measurements of gas transport and pore functions

A steady state method was used to determine air permeability. An air flux with the low air pressure of 0.1 kPa was applied constantly and the gas volume per time measured by air flow meter. The air permeability was calculated by

$$K_a = \frac{q' L_s \eta}{A_s \Delta p} \quad (1)$$

where K_a is air permeability (m^2), q' is the volumetric flow rate ($m^3 s^{-1}$), η is the air dynamic viscosity (Pa s), Δp is the pneumatic pressure difference (Pa), L_s (m) and A_s (m^2) are the length of the sample and surface area of the sample, respectively (Ball et al., 1981).

Gas diffusion coefficient was measured by a double chamber method. The cylinder was installed between two closed chambers, the upper one filled with synthetic air ($20.5 \pm 0.5\%$ O_2 in N_2) and the lower one filled with nitrogen at the beginning. Oxygen sensors in each

chamber monitored the change of oxygen concentration. The equilibrium was reached when the values of sensors were nearly identical. According to the Fick's law, gas diffusion coefficient can be calculated by

$$D_s = \frac{-\ln(\Delta C / (2 \times C_{eq})) \times V_s \times L_s}{A_t \times t \times 2} \quad (2)$$

where D_s is the soil gas diffusion coefficient ($\text{m}^2 \text{s}^{-1}$), ΔC is the oxygen concentration difference between two chambers (g m^{-3}), C_{eq} is the final oxygen concentration at equilibrium (g m^{-3}), V_s (m^3), L_s (m) and A_s (m^2) are the volume, the length and surface area of the sample, respectively. t is time (s) (Ball, 1981). The relative gas diffusion coefficient (D_s/D_o) is defined as the ratio of gas diffusion coefficient in soil (D_s) to that of the same gas in the free air (D_o) taken at the same pressure and temperature (Glinski et al., 2011). The value of D_s/D_o in soil is usually below 1, due to tortuosity and limited connectivity of air-filled pores in soils (Uteau et al., 2013).

The pore continuity index (C_2) describes the relationship between air permeability (K_a) and air-filled porosity (ϵ_a), which can be calculated by

$$C_2 = \frac{K_a}{\epsilon_a} \quad (3)$$

An index of tortuosity, τ , is defined as the ratio of the average capillary tube length, L , to the porous media (soil sample) length, L_e , which can be calculated by air-filled porosity and relative gas diffusivity (Currie et al., 1960).

$$\tau = \frac{L}{L_e} = \sqrt{\frac{\epsilon_a}{D_s/D_o}} \quad (4)$$

6.3.5 Statistical analyses

The mean comparisons were tested by ANOVA followed by Tukey's HSD test for probability $*P < 0.05$. All statistical analyses were undertaken using the SPSS statistics software.

6.4 Results

6.4.1 The effect of type and magnitude of loading on pore functions and gas transport

We document the effect of type and magnitude of loading on pore functions and gas transport for sand soil at the matric potential of -60 hPa and clay loam soil at the matric potential of -300 hPa as representatives. This is arguable because the tendencies of the results are always similar, apart from the intensity due to the different textures for a given matric potential which will be mentioned and summed up finally.

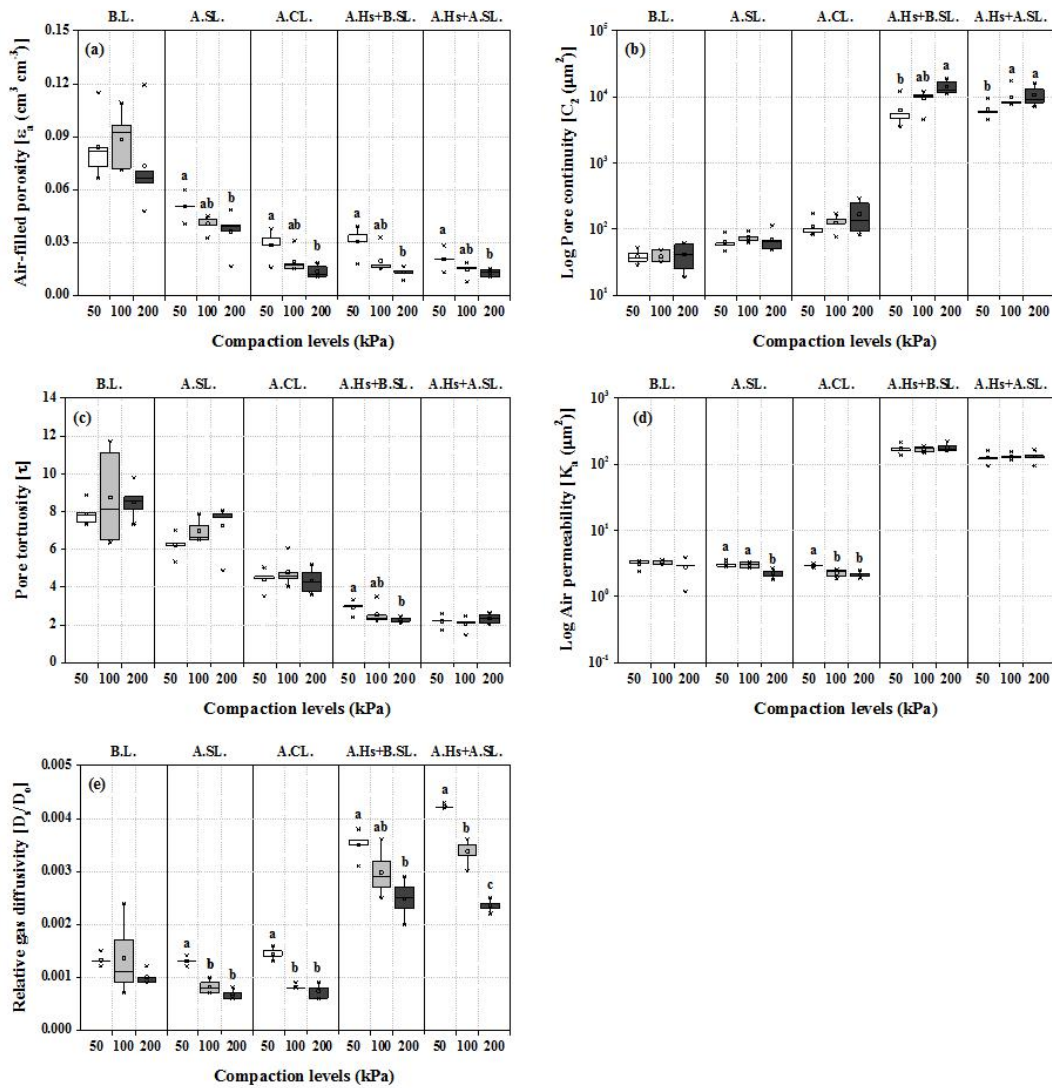


Fig.6-2 Effects of stress application and vertical holes at three different levels (50, 100 and 200 kPa) for sand soil at the matric potential of -60 hPa on changes of (a) air-filled porosity; (b) pore continuity; (c) pore tortuosity; (d) air permeability and (e) relative gas diffusivity. X axis: B.L. = before loading; A.SL. = after static loading; A.CL. = after cyclic loading, A.Hs + B.SL. = after having drilled holes and before static loading; A.Hs + A.SL. = after having drilled holes and after static loading. Letters indicate significant differences on compaction levels (*P < 0.05).

Fig.6-2 shows the results of stress applications and vertical holes on changes of pore function properties (ϵ_a , C_2 and τ) and gas transport parameters (K_a and D_s/D_o) under three compaction levels for sand soil at the matric potential of -60 hPa. After static loading, air-filled porosity (ϵ_a) generally decreased compared to before loading. The extent of reduction increased as the level of compaction increased, with a significant difference between 50 and 200 kPa. Compared to before loading, C_2 increased and τ decreased for sand soil at the matric potential of -60 hPa under all compaction levels after static loading. However, there were no differences in both C_2 and τ under the different compaction levels. Static loading decreased both air permeability (K_a) and relative gas diffusivity (D_s/D_o) under all compaction levels. With increasing vertical stresses, the values of K_a and D_s/D_o decreased but the extent of reduction of K_a and D_s/D_o increased with a significant difference between 50 and 200 kPa.

After cyclic loading, there was the same trend in ϵ_a as after static loading. Values of ϵ_a decreased and the extent of reduction increased with increasing the level of compaction. However, under the same treatment, the extent of reduction in ϵ_a after cyclic loading was higher than after static loading at the matric potential of -60 hPa. Cyclic loading resulted in the further increase in C_2 and decrease in τ , but minor differences in both C_2 and τ between different compaction levels were found. Compared to after static loading, both K_a and D_s/D_o decreased slightly after cyclic loading. The negative relationships between the gas transport parameters (K_a and D_s/D_o) and the applied stresses were found with the difference being significant between 50 and 200 kPa.

The samples with the drilled vertical holes showed ϵ_a values being only slightly higher compared to before, but C_2 , K_a and D_s/D_o increased drastically and τ decreased obviously under all compaction levels. As the applied stresses increased, ϵ_a , τ and D_s/D_o decreased, and C_2 increased significantly, but there were no compaction effects on K_a . After static loading, both ϵ_a and K_a decreased. With increasing the compaction levels, the extent of reduction in ϵ_a decreased significantly, but there was a minor difference in K_a under the different compaction levels. The increase in C_2 and D_s/D_o and the decrease in τ were observed under lower compaction levels (50 and 100 kPa), and there was the opposite trend in C_2 , D_s/D_o and τ under

higher compaction levels (200 kPa).

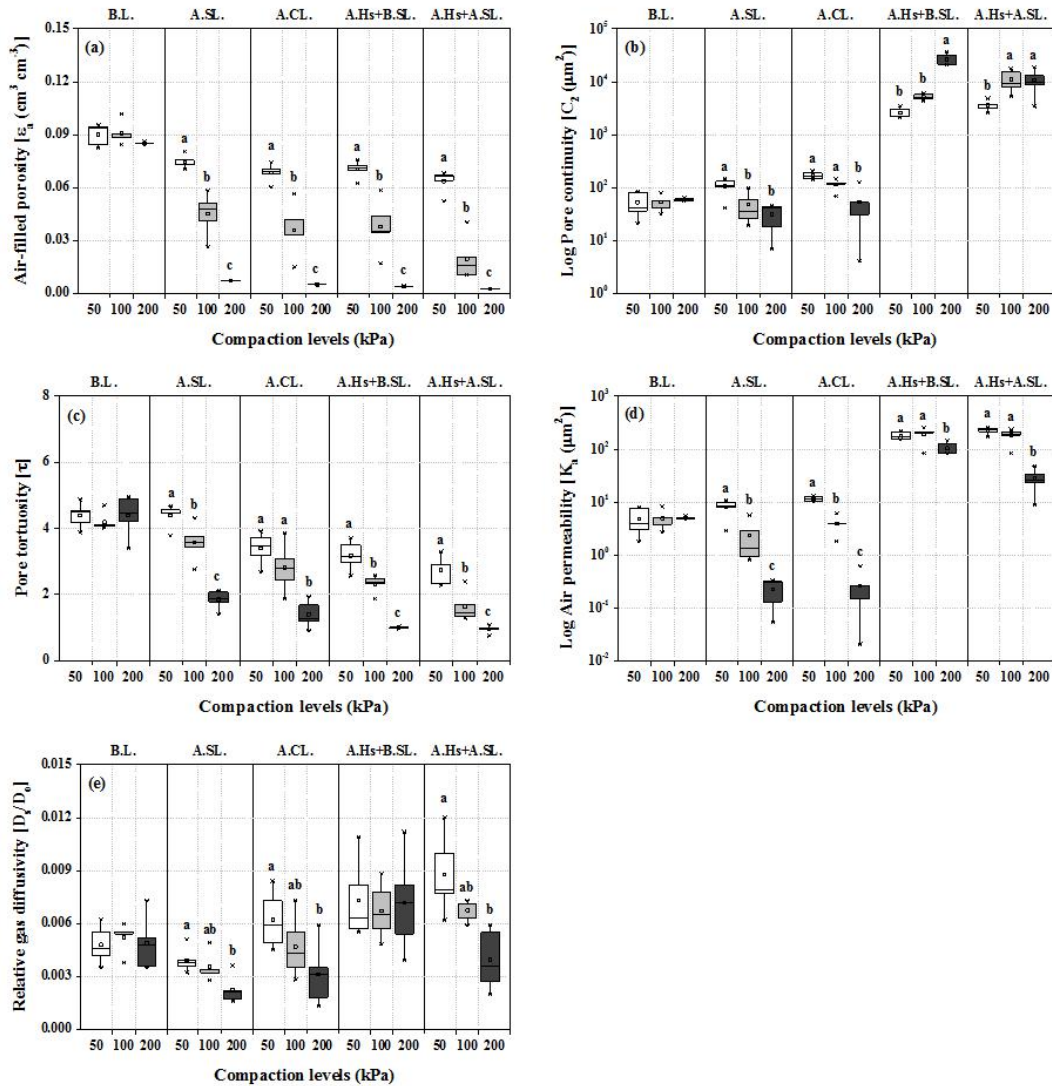


Fig.6-3 Effects of stress application and vertical holes at three different levels (50, 100 and 200 kPa) for clay loam soil at the matric potential of -300 hPa on changes of (a) air-filled porosity; (b) pore continuity; (c) pore tortuosity; (d) air permeability and (e) relative gas diffusivity. X axis: B.L. = before loading; A.S.L. = after static loading; A.C.L. = after cyclic loading, A.Hs + B.S.L. = after having drilled holes and before static loading; A.Hs + A.S.L. = after having drilled holes and after static loading. Letters indicate significant differences on compaction levels (*P < 0.05).

Fig.6-3 shows the results of stress applications and vertical holes on changes of pore function properties (ϵ_a , C_2 and τ) and gas transport parameters (K_a and D_s/D_0) for clay loam soil at the matric potential of -300 hPa. Static loading resulted in the reduction of ϵ_a , τ and

D_s/D_o . Compared to before loading, C_2 and K_a increased under 50 kPa, but decreased under 100 and 200 kPa. Furthermore, significant negative effects of compaction levels on all parameters (ϵ_a , C_2 , τ , K_a and D_s/D_o) were found. After cyclic loading, the decrease in ϵ_a and τ but the increase in C_2 , K_a and D_s/D_o were observed. As the compaction levels increased, all parameters decreased with the difference being significant between 50 and 200 kPa. Vertical holes had almost no change in ϵ_a . However, C_2 , K_a and D_s/D_o increased drastically and τ decreased after having drilled vertical holes. Static loading led to the reduction of ϵ_a and τ for all compaction levels. Other parameters (C_2 , K_a and D_s/D_o) increased under 50 kPa, but the opposite trend occurred under 200 kPa. With increasing level of compaction, C_2 increased and other parameters (ϵ_a , τ , K_a and D_s/D_o) decreased with a significant difference between 50 and 200 kPa.

6.4.2 The relationship between pore functions and gas transport under various stress applications

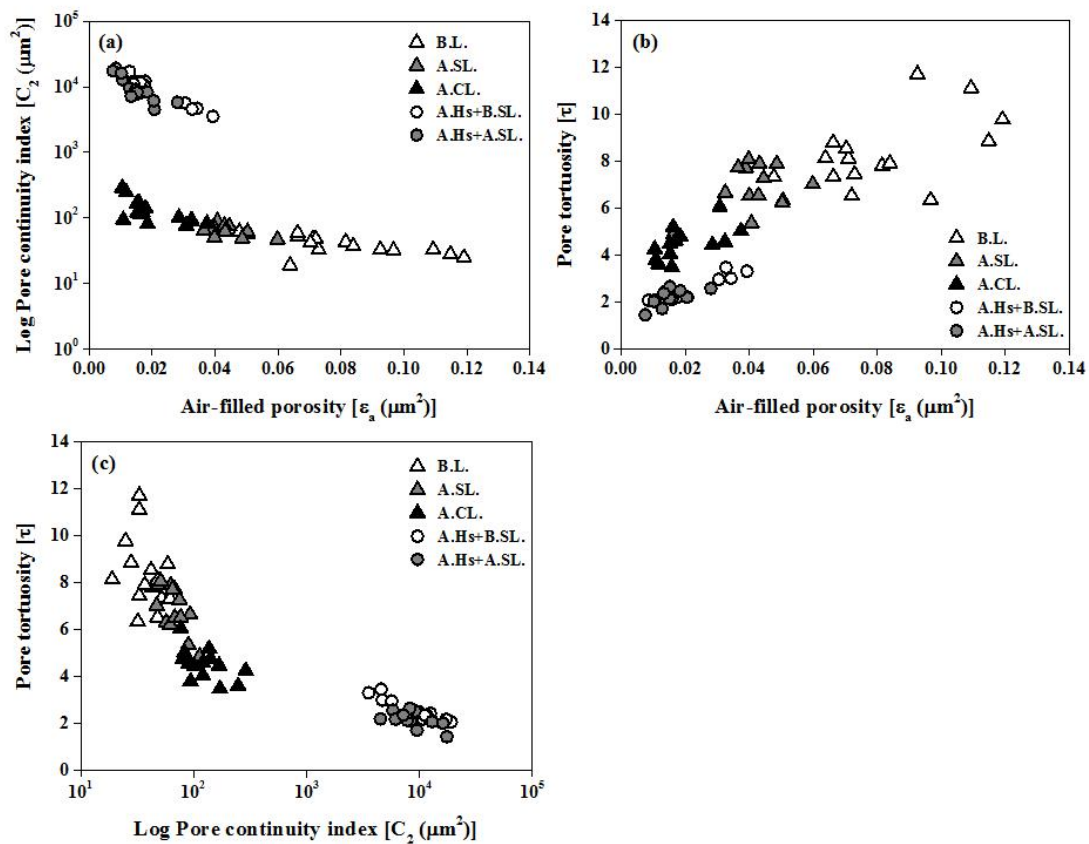


Fig.6-4 The relationships among air-filled porosity, pore continuity or pore tortuosity for all

the measured data in sand soil at the matric potential of -60 hPa.

The relationships between air-filled porosity, pore continuity or pore tortuosity for the sand soil at the matric potential of -60 hPa and all compaction levels are shown in Fig.6-4. For a given texture and matric potential, C_2 decreased and τ increased with increasing values of ϵ_a (Fig.6-4a and 6-4b). The negative relationship between C_2 and τ is documented in Fig.4c. A positive correlation between ϵ_a and gas transport parameters (K_a and D_s/D_0) was shown before having drilled vertical holes for all compaction levels (Fig.6-5a and 6-5c). However, no clear regularity was observed after having drilled vertical holes. We found values of K_a increased with increasing C_2 and values of D_s/D_0 increased with decreasing τ in Fig.6-5b and Fig.6-5d, respectively.

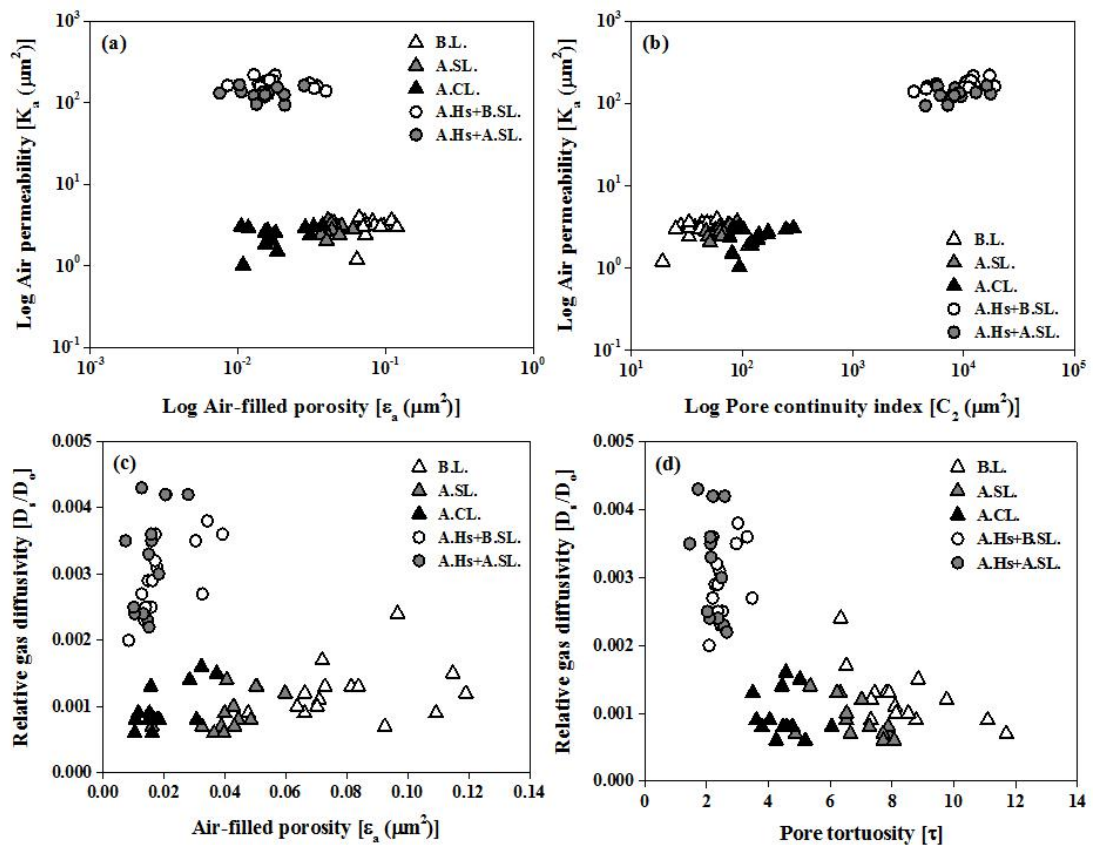


Fig.6-5 Gas transport parameters (air permeability and relative gas diffusivity) as a function of pore functions properties (air-filled porosity, pore continuity and pore tortuosity) for all the measured data in sand soil at the matric potential of -60 hPa.

6.4.3 The effect of artificial vertical pores on pore functions and gas transport for a given stress application

For a given treatment, the relationships among pore functions and gas transport for all treatments after cyclic loading (data not shown) were in the same trend with that after static loading apart from the intensity. Therefore, in this part, we only compared the effect of soil structure on pore functions and gas transport after static loading with and without vertical holes.

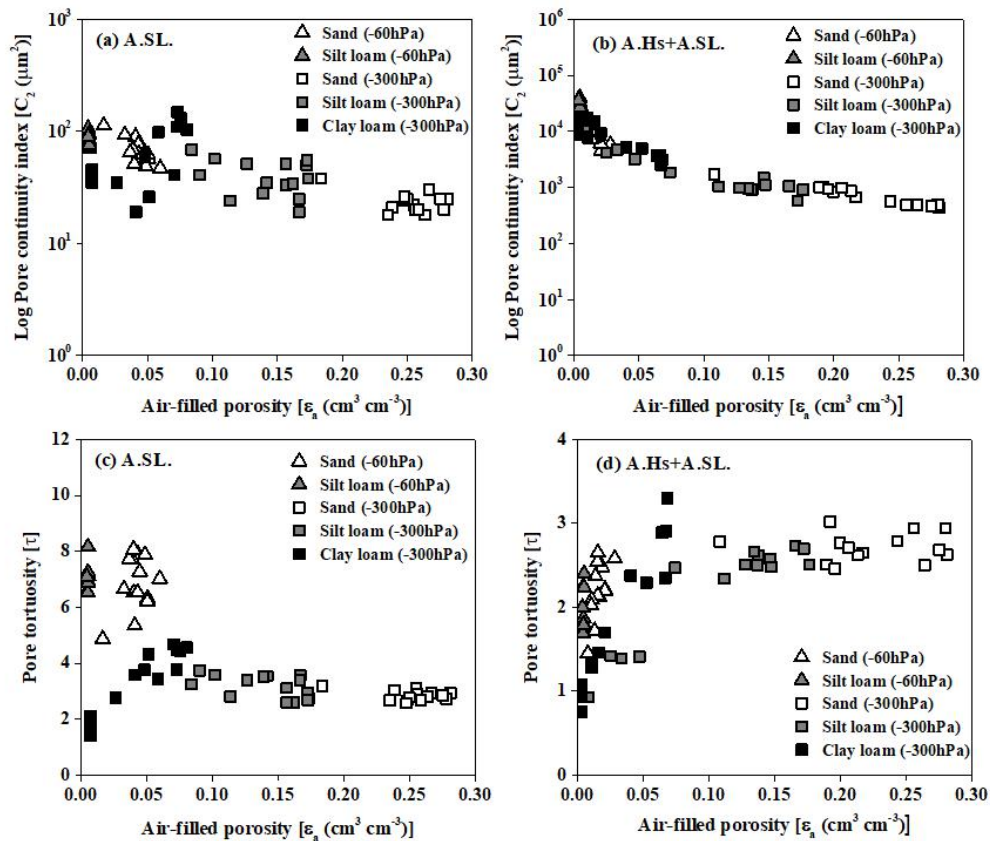


Fig.6-6 Pore continuity and pore tortuosity as a function of air-filled porosity for all treatments under all compaction levels after static loading before and after having drilled vertical holes.

C_2 and τ as a function of ϵ_a for all treatments and compaction levels after static loading before and after having drilled vertical holes are presented in Fig.6-6. The lower the matric potential and the coarser the texture, the higher were the values of ϵ_a . Regardless of vertical holes effects, C_2 decreased as the values of ϵ_a increased after static loading (Fig.6-6a and

6-6b). Before having drilled vertical holes, the negative relationship between ϵ_a and τ was observed (Fig.6-6c), while the opposite trend between ϵ_a and τ was found after having drilled vertical holes (Fig.6-6d).

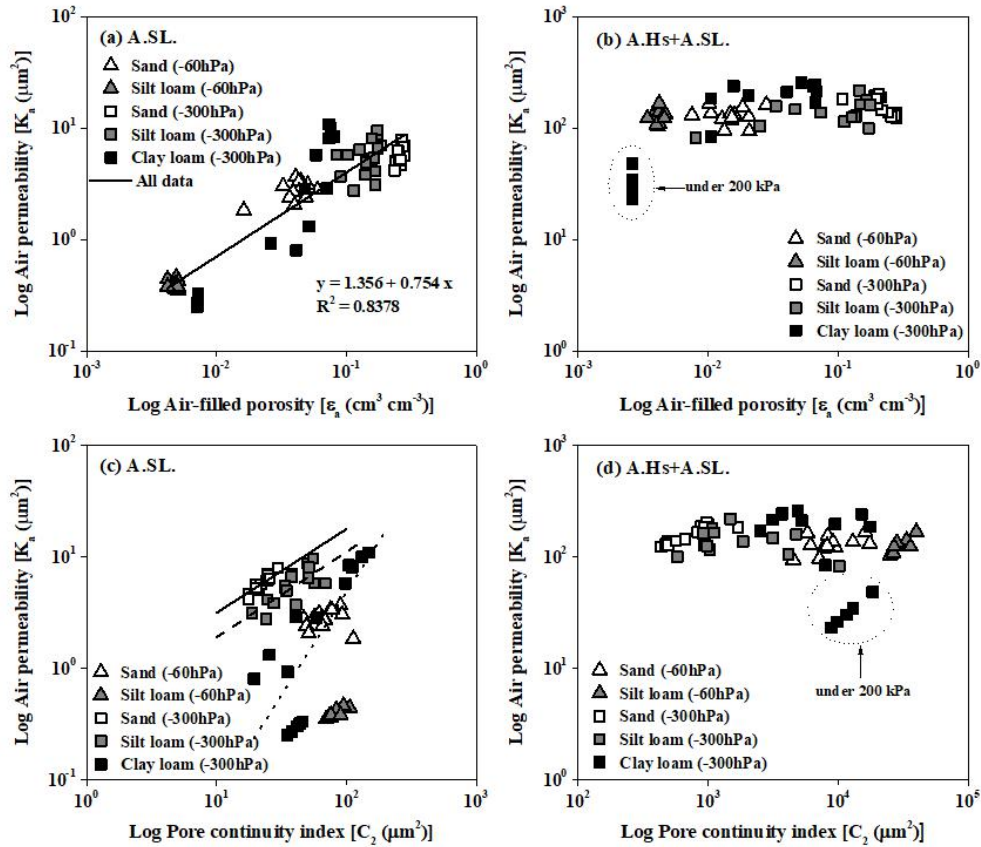


Fig.6-7 Air permeability as a function of air-filled porosity and pore continuity for all treatments under all compaction levels after static loading before and after having drilled vertical holes. The solid line represents the linear regression for all data in Fig.6-7a. The linear regressions for sand (solid line), silt loam (dash line) and clay loam (dot line) soil at -300 hPa matric potential are shown in Fig.6-7c, respectively.

Air permeability (K_a) as a function of the parameters (ϵ_a and C_2) for all treatments and compaction levels after static loading before and after having drilled vertical holes are presented in Fig.6-7. There was a positive linear log-log relationship between ϵ_a and K_a for all data before having drilled vertical holes (Fig.6-7a). For a given treatment, especially at the matric potential of -300 hPa, the positive log-log correlation between C_2 and K_a was also observed (Fig.6-7c). After having drilled vertical holes, there were distinct differences in both

ϵ_a and C_2 , but values of K_a were almost the same for all treatments, except for clay loam soil at the matric potential of -300 hPa and being stressed with 200 kPa (Fig.6-7b and 6-7d).

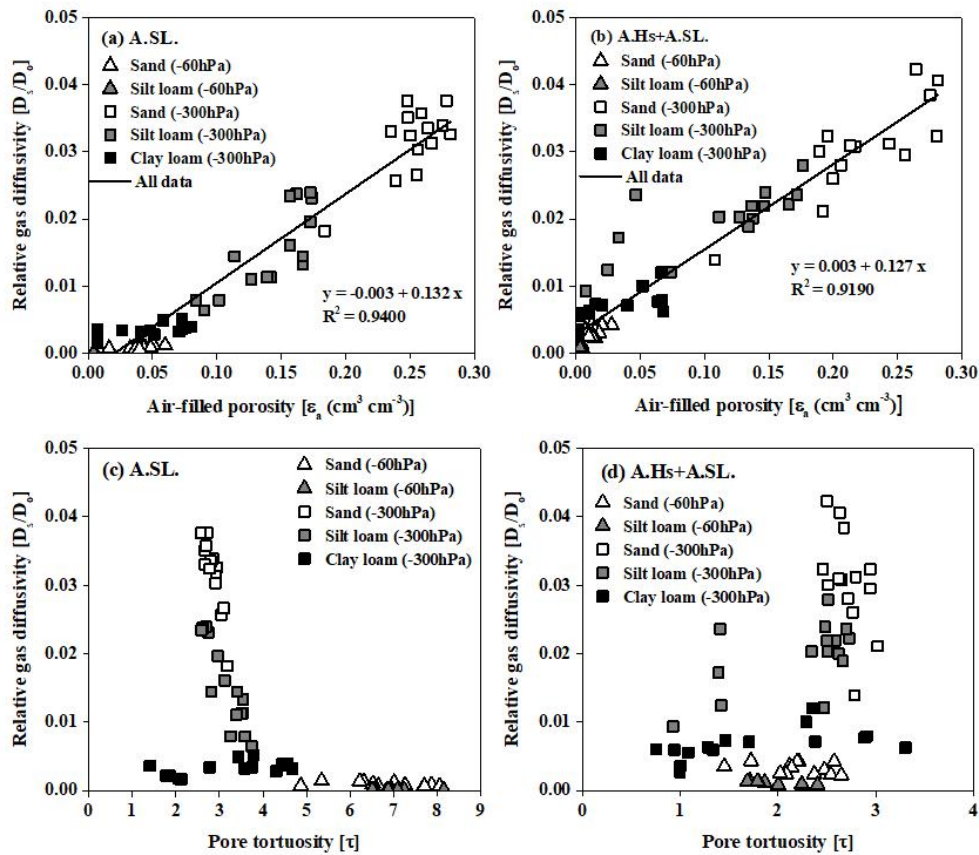


Fig.6-8 Relative gas diffusivity as a function of air-filled porosity and pore tortuosity for all treatments under all compaction levels after static loading before and after having drilled vertical holes. The solid line represents the linear regression for all data in Fig.6-8a and 6-8b.

Relative gas diffusivity effects (D_s/D_0) are presented in Fig.6-8. Regardless of vertical holes effects, D_s/D_0 increased as the values of ϵ_a increased with a linear relationship after static loading (Fig.6-8a and 6-8b). Before having drilled vertical holes, the correlation between τ and D_s/D_0 was negative (Fig.6-8c). However, the differences in the values of D_s/D_0 were found drastically, but the values of τ were similar for all treatments after having drilled vertical holes (Fig.6-8d).

Before having drilled vertical holes, a positive correlation between K_a and D_s/D_0 after static loading was detected (Fig.6-9a). On the other hand, there were minor differences in K_a but distinct differences in D_s/D_0 for all treatments after having drilled vertical holes

(Fig.6-9b).

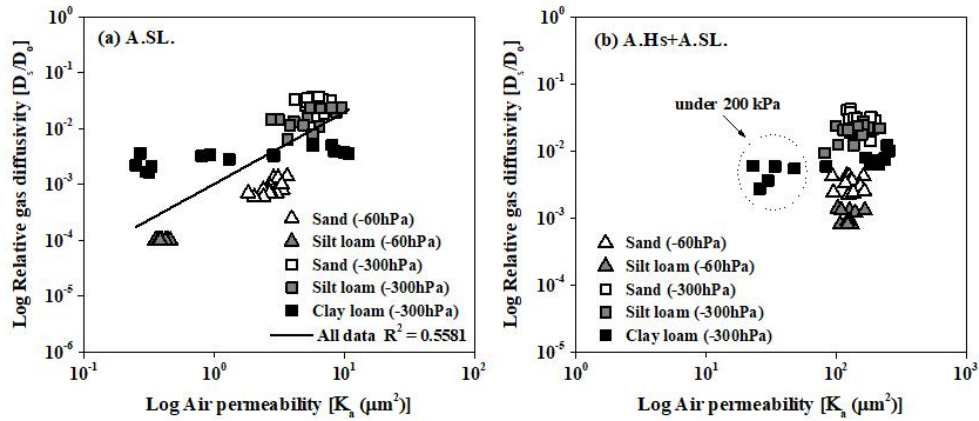


Fig.6-9 Air permeability as a function of relative gas diffusivity for all treatments under all compaction levels after static loading before and after having drilled vertical holes. The solid line represents the linear regression for all data in Fig.6-9a.

6.5 Discussion

6.5.1 The effect of static loading on pore functions and gas transport

If we only consider the effect of static stress application on capacity values, we can see that regardless of texture and matric potential, static loading resulted in an increase in bulk density and a decrease in soil porosity, especially air-filled porosity. According to the capillary rise theory, the values of ϵ_a at the matric potential of -60 and -300 hPa represent the volume of air-filled pores with equivalent pore diameter more than 50 and 10 μm , respectively (Terzaghi et al., 1996; Kuncoro et al., 2014). A capacity parameter like air-filled porosity is defined as a general status which is calculated by the volume relationship, ignoring the internal structure and functions, while an intensity parameter reflects the dynamic reactions or processes of pore functions over time and space such as pore continuity and tortuosity (Horn and Kutilek, 2009; Mentges et al, 2016). Thus, the observed decrease in ϵ_a resembles the reduction of macroporosity, but as this also affects the intensity properties we need to have a closer look on their changes on air permeability or gas diffusion.

One possibility which is often discussed is the approach of Groenevelt et al. (1984) and

Ball et al. (1988) considering the C_2 values and their changes due to various treatments. The pore continuity index (C_2) is defined as the ratio of air permeability (K_a) to air-filled porosity (ϵ_a), which depends on bulk density, water content, organic matter and soil texture (Moldrup et al., 2003; Deepagoda et al., 2011; Kuncoro et al., 2014). The values of C_2 are mostly used as an indicator for similar pore size distributions and pore continuities (Groenevelt et al., 1984; Uteau et al., 2013). At the matric potential of -60 hPa, values of C_2 decreased for the finer-textured soils (data not shown) after static loading and the coinciding reduction of the volume of air-filled pores while the values of C_2 increased for the coarser-textured soils (Fig.6-2b) because higher initial water content and lower water holding capacity for sand soil facilitated the reduction of soil water content after static loading. These processes caused more continuous pores than an increase in C_2 . However, the negative effect of static loading on pore continuity at the matric potential of -300 hPa (Fig.6-3b), was probably related to the reduction of the volume of air-filled pores. Ball et al. (1988) found that at -60 hPa matric potential, pore continuity index (C_2) decreased in direct drilled clay loam soil after one pass of an unladen tractor applied. Munkholm et al. (2002) observed that at the matric potential of -30 and -100 hPa, C_2 decreased significantly after compaction with a 6-8 t tractor, which indicated a relatively poorer continuity of macropores in the compacted soil. Pore tortuosity (τ) reflects the relationship between the length of average gas transport path and the length of soil sample. At a given soil sample length, the more tortuous gas pathways, the higher values of τ were. After static loading, the reduction of water blockage effect coincided with a decrease in τ .

There is a relationship of interaction between pore functions and gas transport. Gas transport parameters are good indicators for identifying soil pore characteristics (Granovsky and McCoy, 1997; Moldrup et al., 2003; Iversen et al., 2001), and soil pore functions in turn affects significantly soil aeration (Schjønning et al., 2002; Deepagoda et al., 2011; Mentges et al., 2016).

On one hand, gas transport properties depend on the capacity values of soil pore functions (i.e. the quantity of air-filled pores ϵ_a). For treatments without artificially vertical holes, air-filled porosity is the main determinant factor affecting gas transport, which results

in the identical variation trends of K_a and D_s/D_o over the same soil air content range. The values of K_a and D_s/D_o were proportional to the values of ϵ_a for all treatments. As ϵ_a decreased after static loading, lower K_a and D_s/D_o values were observed (Fig.6-7a and 6-8a). Berisso et al. (2013) found that at three different matric potential and at four different depths, there was a strong positive linear log-log relationship between K_a and ϵ_a in the control and compacted blocks. This result was also supported by Ball et al. (1988), Dörner and Horn (2006) and Schjønning et al. (2002). Kuncoro et al. (2014) noticed that the observed decrease in D_s/D_o was reasonably attributed to the reduced values of ϵ_a after compaction. Similar observations were reported in Deepagoda et al. (2011), Hamamoto et al. (2009) and Moldrup et al. (2000).

Besides the volume of macropores, gas transport properties are also controlled by the intensity values (i.e. the quality of air-filled pores). For most of treatments, values of K_a decreased as values of C_2 decreased after static loading. Lower C_2 values indicate that there are less active air-filled pores in soils, which results in restricted air flow. However, this general statement is not completely true. For coarser-textured soil at less negative matric potential, values of C_2 therefore increased after static loading which was not accompanied by higher values of K_a . This situation was mainly attributable to the reduced values of ϵ_a . Mentges et al. (2016) found that compared to clayey soils, K_a in sandy soils is mostly ascribable to the volume of macropores, but less correlated with pore continuity. This was in agreement with our findings.

Theoretically, lower τ values indicate the existence of less tortuous pathways for gas transport, thus favoring higher D_s/D_o values. Therefore, for a given stress application, the negative relationship between D_s/D_o and τ was observed after static loading for all treatments that is, the D_s/D_o values were higher with lower τ values (Fig.6-8c). Papendick and Runkles (1965) observed that at the same ϵ_a , values of D_s/D_o in wet media were lower than in dry media, due to the increased tortuosity for gas transport. However, for a given treatment, we found that a lower τ value was not always accompanied by a higher D_s/D_o value. For example, for clay loam soil at the -300 hPa matric potential, the values of D_s/D_o decreased, even though the lower values of τ was observed after static loading. This might be because the extent of the reduction of ϵ_a was higher than the reduction of τ , indicating that the number of active air-filled pores increased, but the volume of these pores was smaller after static loading,

leading to a decrease in D_s/D_o .

6.5.2 The effect of cyclic loading on pore functions and gas transport

The highest irreversible changes in soil volume and soil structure occur during the first loading event, when a significant deformation occurs (Hakansson, 1994; Lipiec et al., 1992; Mordhorst et al., 2012; Pytka, 2005) while further cyclic loading due to such former soil strength increase was less pronounced. This is also confirmed by our results. Although the volume of macropores decreased after the further cyclic loading (Fig6-.2 and 6-3), the quality of air-filled pores was improved (i.e. an increase in C_2 and a decrease in τ), because the further reduction of soil water content caused less bottle-necks formed by water mensci in the pore system after the further cyclic loading. For most of treatments, a combined effect of air-filled pores (as a capacity indicator) and pore continuity/tortuosity (as an intensity indicator) balanced gas transport properties. This result was confirmed by the findings of Uteau et al. (2013). Therefore, there was a minor effect of the further cyclic loading on values of K_a and D_s/D_o .

6.5.3 The effect of loading intensity on pore functions and gas transport

After static loading or the further cyclic loading, the effect of loading intensity on pore functions and gas transport depends on soil texture and matric potential. In sandy soils, values of ϵ_a decreased with increasing compaction levels at both matric potentials with a significant difference between 50 and 200 kPa. It was expected and also confirmed by Kuncoro et al. (2014). They noticed that at the matric potential of -100 hPa, the air content decreased with increasing the level of compaction in the remoulded sandy loam volcanic ash soil. However, the effect of compaction levels on the intensity parameters of pore functions was less pronounced. Therefore, the observed decrease in values of K_a and D_s/D_o with increasing stresses was reasonably attributable to the decrease in the volume of macropores for the coarser-textured soils.

In case of the finer-textured soils, however, matric potential plays an important role in the effect of compaction levels on pore functions and gas transport. At the matric potential of -60 hPa (data not shown), values of ϵ_a have been already very low before loading due to

higher volumetric water content resulting from greater water retention. Therefore, there was no further intense decrease of these values during relatively short term compaction, finally resulting in a minor difference in gas transport parameters between 50 and 100 kPa, while the squeezing out of the material at 200 kPa stress in the silt loam soil prevented us from further descriptions. At a lower matric potential (-300 hPa), the volume of air-filled pores increased which resulted in a higher sensitivity to soil compaction, especially in more clayey soils. As the compaction levels increased, not only the capacity but also the intensity parameters of pore functions declined, resulting in restricted gas transport. Our results were confirmed by Tang et al. (2011) who investigated both remoulded and undisturbed soils with three kinds of textures (sandy loam, silty clay loam and clay) at different water contents under seven vertical stresses ranging from 30 kPa to 800 kPa, and found that there were a strong negative correlation between air permeability and the applied vertical stresses on sandy loam and silty clay loam soils, while no unique correlation was observed on clay soil. Linear log-log relationship between air permeability and the vertical stress was also observed by Mosaddeghi et al. (2007) for repacked soils with different textures and four matric potential values under three compaction levels.

6.5.4 The effect of soil structure (artificial vertical pores) on pore functions and gas transport

Irrespective of only a slightly higher air-filled porosity, the ability of soil pore functions were improved significantly by these 5 vertical holes as also proofed by the threshold values of K_a proposed in Reszkowska et al. (2011). It corresponds to different classes (very low-low-medium-high-very high). Based on these limits, pore continuity index (C_2) varied from very low and low to very high for all treatments with vertical holes before static loading. The existence of five continuous, non-tortuous and non-constricted holes resulted in the reduction of τ by 2.77-75.38 %, particularly for treatments at wet condition (-60hPa). After static loading with vertical holes, a negative correlation between ε_a and C_2 , and a positive relationship between ε_a and τ were observed for all treatments (Fig.6-6b and 6-6d). This can be explained that the value of τ greater than 1 means that gas transport can happen in both the vertical holes and other connected air-filled pores. The more other pores except for vertical

holes (the higher value of ϵ_a) exist, the more possible for the presence of the non-continuous and tortuous pathways it has, resulting in a decrease in C_2 and an increase in τ .

It is obvious that pore functions can be obviously ameliorated by artificially vertical holes and then soil aeration is improved. For a given treatment (Fig.6-2 and 6-3), even though only a slight increase in ϵ_a occurred after having drilled vertical holes, K_a significantly increased up to more than one order of magnitude, which was strongly correlated with the significant increase in the pore continuity compared to without vertical holes. Mentges et al. (2016) found that C_2 was directly proportional to K_a for four different textured soils (from sandy loam to clay). The findings of Kuncoro et al., (2014) that higher ϵ_a can not result in a higher K_a value for soil mixed with rice straw at compaction levels of 150 and 225 kPa, can be explained by the blockage effect of organic matter on K_a which again proves that the pore continuity and its maintenance are of major importance. Moldrup et al. (2001) found that an increase in K_a with decreasing soil air content for repacked sand and loamy sand soil, due to the preferential gas flow effect by the larger and more continuous pores at low soil air content also confirmed our findings.

Soil structure (artificially vertical holes) also affects gas diffusion. Gradwell (1961) found that wormholes (4 mm in diameter) may be mainly responsible for gas diffusion in the region of lower airspace less than 5%, while gas diffusion through the soil mass other than through the wormholes can be negligible for airspace above 5%. For a given treatment, the higher values of D_s/D_o with vertical holes were attributed to the decrease in the pore tortuosity compared to without holes. This can be confirmed by Deepagoda et al. (2011). They observed that at the same air-filled porosity, less water-induced tortuosity resulted in increasing gas diffusivity.

Gas transport parameters are good indicators for evaluating the changes in soil structure (Fish and Koppi, 1994; Moldrup et al., 2001; Moldrup et al., 2003). After static loading with vertical holes, minor differences in K_a but distinct differences in D_s/D_o were observed among different treatments (Fig.6-9b), because values of K_a was more closely related to soil structure (pore size distribution, pore radius, and particularly the continuity of the largest air-filled pores) than the values of D_s/D_o . Similar observations were reported in Wickramarachchi et al. (2011) and Moldrup et al. (2003). On the other hand, the preferential gas flow through

macropore networks was rather dominant for gas advection. Therefore, artificially vertical pores reduced the differences in K_a among the different treatments, even if values of D_s/D_o were still affected by the total air-filled porosity.

6.6 Conclusion

1) Investigations of studied soils showed that gas transport parameters are a function of soil texture, matric potential, soil structure (artificially prepared as vertical holes), and type and intensity of compaction. Due to the decrease in air-filled porosity after static and cyclic loading, air permeability and relative gas diffusivity also decreased.

2) The effect of soil compaction was not always negative. Even though air-filled porosity was reduced after compaction, K_a and D_s/D_o can increase, if water is drained off, which led to the increase in active air-filled pore space for gas transport. Hence, the differences in air permeability and relative gas diffusivity among different treatments and stress applications were attributed to changes in air-filled porosity as well as in pore continuity and tortuosity.

3) Gas transport is controlled by soil structure. Having drilled vertical holes can increase pore continuity and decrease pore tortuosity, which results in the significant increase in air permeability and relative gas diffusivity. The effect of preferential macropores on values of K_a is more pronounced than those of D_s/D_o .

4) Therefore, artificially vertical holes eliminated the differences in values of K_a among treatments, but the obvious differences in values of D_s/D_o still existed. Regardless of vertical holes, static loading will lead to a decline of soil quality. For a given stress application (static loading), the extend of this reduction was lower for treatments after than before having drilled vertical holes, because previous static loading and the further cyclic loading made an increase in soil strength, thus the loading support capacity of soils increased.

6.7 Acknowledgement

This study was supported by the State Scholarship Fund from the China Scholarship Council (CSC) for Xiafei Zhai (No.201406300027).

6.8 References

Alakukku, L., 1996. Persistence of soil compaction due to high axle load traffic: I. Short-term effects

6 DYNAMICS OF PORE FUNCTIONS AND GAS TRANSPORT PARAMETERS IN ARTIFICIALLY
AMELIORATED SOILS DUE TO STATIC AND CYCLIC LOADING

- on the properties of clay and organic soils. *Soil Till. Res.* 37, 211-222.
- Alakukku, L., Weisskopf, P., Chamen, W.C.T., Tijink, F.G.J., van der Linden, J.P., Pires, S., Sommer, C., Spoor, G., 2003. Prevention strategies for field traffic-induced subsoil compaction: a review: part 1. Machine/soil interactions. *Soil Till. Res.* 73, 145-160.
- Ball, B.C., 1981. Pore characteristics of soils from two cultivation experiments as shown by gas diffusivities and permeabilities and air-filled porosities. *J. Soil Sci.* 32, 483-498.
- Ball, B.C., Harris, W., Burford, J.R., 1981. A laboratory method to measure gas diffusion and flow in soil and other porous materials. *J. Soil Sci.* 32, 323-333.
- Ball, B.C., O'Sullivan, M. F., Hunter, R., 1988. Gas diffusion, fluid flow and derived pore continuity indices in relation to vehicle traffic and tillage. *J. Soil Sci.* 39, 327-339.
- Ball, B.C., Ritchie, R.M., 1999. Soil and residue management effects on arable cropping conditions and nitrous oxide fluxes under controlled traffic in Scotland: 1. Soil and crop responses. *Soil Till. Res.* 52(3-4), 177-189.
- Barik, K., Aksakal, E.L., Islam, K.R., Sari, S., Angin, I., 2014. Spatial variability in soil compaction properties associated with field traffic operations. *CATENA* 120, 122-133.
- Berisso, F.E., Schjønning, P., Keller, T., Lamandé, M., Simojoki, A., Iversen, B.V., Alakukku, L., Forkman, J., 2013. Gas transport and subsoil pore characteristics: Anisotropy and long-term effects of compaction. *Geoderma* 195-196, 184-191.
- Berisso, F.E., Schjønning, P., Keller, T., Lamandé, M., Etana, A., de Jonge, L.W., Iversen, B.V., Arvidsson, J., Forkman, J., 2012. Persistent effects of subsoil compaction on pore size distribution and gas transport in a loamy soil. *Soil Tillage Res.* 122(3-4), 42-51.
- Blackwell, P.S., Ringrose-Voase, A.F., Jayawardane, N.S., Olsson, K.A., McKenzie, D.C., Mason, W.K., 1990. The use of air-filled porosity and intrinsic permeability to characterize macropore structure and saturated hydraulic conductivity of clay soils. *J. Soil Sci.* 41, 215-228.
- Chen, G., Weil, R.R., Hill, R.L., 2014. Effects of compaction and cover crops on soil least limiting water range and air permeability. *Soil Tillage Res.* 136, 61-69.
- Currie, J.A., 1960. Gaseous diffusion in porous media: Part II. Dry granular materials. *Br. J. Appl. Phys.* 11, 318-324.
- Deepagoda, T.K.K.C., Moldrup, P., Schjønning, P., De Jonge, L.W., Kawamoto, K., Komatsu, T., 2011. Density-corrected models for gas diffusivity and air permeability in unsaturated soil. *Vadose Zone*

J. 10, 226-238.

Defosse, P., Richard, G., 2002. Models of soil compaction due to traffic and their evaluation. *Soil Tillage Res.* 67 (1), 41-64.

Dörner, J., Dec, D., Feest, E., Vasquez, N., Diaz, M., 2012. Dynamics of soil structure and pore functions of a volcanic ash soil under tillage. *Soil Till. Res.* 125, 52-60.

Dörner, J., Horn, R., 2006. Anisotropy of pore functions in structured Stagnic Luvisols in the Weichselian moraine region in N Germany. *J. Plant Nutr. Soil Sci.* 169 (2), 213-220.

Fish, A.N., Koppi, A.J., 1994. The use of a simple field air permeameter as a rapid indicator of functional soil pore space. *Geoderma* 63, 255-264.

Fujikawa, T., Miyazaki, T., 2005. Effects of bulk density on the gas diffusion coefficient in repacked and undisturbed soils. *Soil Sci.* 170, 892-901.

Głąb, T., 2014. Effect of soil compaction and N fertilization on soil pore characteristics and physical quality of sandy loam soil under red clover/grass sward. *Soil Till. Res.* 144, 8-19.

Glinski, J., Horabik, J., Lipiec, J., 2011. *Encyclopedia of agrophysics.* Springer.

Gradwell, M.W., 1961. A laboratory study of the diffusion of oxygen through pasture topsoils. *N. Z. J. Agric. Res.* 4, 250-270.

Granovsky, A.V., McCoy, E.L., 1997. Air flow measurements to describe field variation in porosity and permeability of soil macropores. *Soil Sci. Soc. Am. J.* 61, 1569-1576.

Groenevelt, P.H., KAY, B.D., Grant, C.D., 1984. Physical assessment of soil with respect to rooting potential. *Geoderma* 34, 101-114.

Hakansson, I., 1994. Subsoil compaction by high axle load traffic. *Soil Till. Res.* 29, 105–306 (special issue).

Hamamoto, S., Moldrup, P., Kawamoto, K., Komatsu, T., 2009. Effect of Particle Size and Soil Compaction on Gas Transport Parameters in Variably Saturated, Sandy Soils. *Vadose Zone J.* 8(4), 986-995.

Hamza, M.A., Anderson, W.K., 2005. Soil compaction in cropping systems: A review of the nature, causes and possible solutions. *Soil Tillage Res.* 82 (2), 121-145.

Hartge, K.H., Horn, R., 2016. *Essential Soil Physics, An introduction to soil processes, functions, structure and mechanics.* Schweizerbart Science Publishers.

Horn, R., 1981. Eine Methode zur Ermittlung der Druckbelastung von Böden anhand von

- Drucksetzungsversuchen. Zeitschrift für Kulturtechnik und Flurbereinigung 22, 20-26.
- Horn, R., 2015. Soil Compaction and consequences of soil deformation on changes in soil functions. 28-33, in S.Nortcliff (ed): Task Force: Soil matters- Solutions under Foot. Catena Publ. Geocology Essays. ISBN: 978-3-923381-63-0.
- Horn, R., Domal, H., Sowińska-Jurkiewicz, A., van Ouwerkerk, C., 1995. Soil compaction processes and their effects on the structure of arable soils and the environment. Soil Tillage Res. 35 , 23-36.
- Horn, R., Kutilek, M., 2009. The intensity-capacity concept-How far is it possible to predict intensity values with capacity parameters. Soil Tillage Res. 103, 1-3.
- Iversen, B.V., Moldrup, P., Schjønning, P., Loll, P., 2001. Air and water permeability in differently textured soils at two measurement scales. Soil Sci. 166(10), 643-659.
- Kim, H., Anderson, S.H., Motavalli, P.P., Gantzer, C.J., 2010. Compaction effects on soil macropore geometry and related parameters for an arable field. Geoderma 160, 244-251.
- Krümmelbein, J., Wang, Z., Zhao, Y., Peth, S., Horn, R., 2006. Influence of various grazing intensities on soil stability, soil structure and water balance of grassland soils in Inner Mongolia, P.R. China. CATENA 38, 93-101.
- Kuncoro, P.H., Koga, K., Satta, N., Muto, Y., 2014. A study on the effect of compaction on transport properties of soil gas and water I: Relative gas diffusivity, air permeability, and saturated hydraulic conductivity. Soil Tillage Res. 143, 172-179.
- Lipiec, J., Szustak, S., Tarkiewicz, S., 1992. Soil compaction: responses of soil physical properties and crop growth. Zeszyty Problemowe Postępowania w Nauk Rolniczych 398, 113–117.
- Mentges, M.I., Reichert, J.M., Rodrigues, M.F., Awe, G.O., Mentges, L.R., 2016. Capacity and intensity soil aeration properties affected by granulometry, moisture, and structure in no-tillage soils. Geoderma 263, 47-59.
- Moldrup, P., Olesen, T., Komatsu, T., Schjønning, P., Rolston, D.E., 2001. Tortuosity, diffusivity, and permeability in the soil liquid and gaseous phases. Soil Sci. Soc. Am. J. 65, 613-623.
- Moldrup, P., Olesen, T., Schjønning, P., Yamaguchi, T., Rolston, D.E., 2000. Predicting the gas diffusion coefficient in undisturbed soil from soil water characteristics. Soil Sci. Soc. Am. J. 64, 1588-1594.
- Moldrup, P., Yoshikawa, S., Olesen, T., Komatsu, T., Rolston, D.E., 2003. Air permeability in undisturbed volcanic ash soil: Predictive model test and soil structure finger print. Soil Sci. Soc.

6 DYNAMICS OF PORE FUNCTIONS AND GAS TRANSPORT PARAMETERS IN ARTIFICIALLY
AMELIORATED SOILS DUE TO STATIC AND CYCLIC LOADING

- Am. J. 67, 32–40.
- Mordhorst, A., Zimmermann, I., Peth, S., Horn, R., 2012. Effect of hydraulic and mechanical stresses on cyclic deformation processes of a structured and homogenized silty Luvisol Chernozem. *Soil Tillage Res.* 125, 3-13.
- Mosaddeghi, M.R., Koolen, A.J., Hajabbasi, M.A., Hemmat, A., Keller, T., 2007. Suitability of pre-compression stress as the real critical stress of unsaturated agricultural soils. *Biosyst. Eng.* 98(1), 90-101.
- Munkholm, L.J., Schjønning, P., Kay, B.D., 2002. Tensile strength of soil cores in relation to aggregate strength, soil fragmentation and pore characteristics. *Soil Tillage Res.* 64, 125-135.
- Naveed, M., Schjønning, P., Keller, T., de Jonge, L.W., Moldrup, P., Lamandé, M., 2016. Quantifying vertical stress transmission and compaction-induced soil structure using sensor mat and X-ray computed tomography. *Soil Tillage Res.* 158, 110-122.
- Pagliari, M., Marsili, A., Servadio, P., Vignozzi, N., Pellegrini, S., 2003. Changes in some physical properties of a clay soil in Central Italy following the passage of rubber tracked and wheeled tractors of medium power. *Soil Tillage Res.* 73 (1-2), 119-129.
- Papendick, R.L., Runkles, J.R., 1965. Transient-state oxygen diffusion in soil: I. The case where rate of oxygen consumption is constant. *Soil Sci.* 100, 251-261.
- Peng, X.H., Horn, R., Zhang, B., Zhao, Q.G., 2004. Mechanisms of soil vulnerability to compaction of homogenized and recompacted Ultisols. *Soil Tillage Res.* 76 (2), 125-137.
- Peth, S., Rostek, J., Zink, A., Mordhorst, A., Horn, R., 2010. Soil testing of dynamic deformation processes of arable soils. *Soil Till. Res.* 106 (2), 317-328.
- Pytko, J., 2005. Effects of repeated rolling of agricultural tractors on soil stress and deformation state in sand and loess. *Soil Tillage Res.* 82 (1), 77-88.
- Reszkowska, A., Krümmelbein, J., Gan, L., Peth, S., Horn, R., 2011. Influence of grazing on soil water and gas fluxes of two Inner Mongolian steppe ecosystems. *Soil Till. Res.* 111, 180-189.
- Richard, G., Cousin, I., Sillon, J.F., Bruand, A., Guérif, J., 2001. Effect of compaction on the porosity of a silty soil: influence on unsaturated hydraulic properties. *Eur. J. Soil Sci.* 52, 49-58.
- Riggert, R., Fleige, F., Kietz, B., Gaertig, T., Horn, R., 2015. Stress Distribution under Forestry Machinery and Consequences for Soil Stability. *Soil Sci. Soc. Am. J.* 80, 38-47.
- Saffih-Hdadi, K., Défossez, P., Richard, G., Cui, Y.-J., Tang, A.-M., Chaplain, V., 2009. A method for

6 DYNAMICS OF PORE FUNCTIONS AND GAS TRANSPORT PARAMETERS IN ARTIFICIALLY
AMELIORATED SOILS DUE TO STATIC AND CYCLIC LOADING

- predicting soil susceptibility to the compaction of surface layers as a function of water content and bulk density. *Soil Tillage Res.* 105 (1), 96-103.
- Schäffer, B., Stauber, M., Mueller, T.L., Muller, R., Schulin, R., 2008. Soil and macropores under uniaxial compression. I. Mechanical stability of repacked soil and deformation of different types of macro-pores. *Geoderma* 146, 183-191.
- Schjønning, P., Munkholm, L.J., Moldrup, P., Jacobsen, O.H., 2002. Modelling soil pore characteristics from measurements of air exchange: the long-term effects of fertilization and crop rotation. *Eur. J. Soil Sci.* 53 (2), 331-339.
- Servadio, P., Marsili, A., Pagliai, M., Pellegrini, S., Vignozzi, N., 2001. Effects on some clay soil qualities following the passage of rubber-tracked and wheeled tractors in central Italy. *Soil Till. Res.* 61, 143-155.
- Tang, A.M., Cui, Y., Richard, G., Défossez, P., 2011. A study on the air permeability as affected by compression of three French soils. *Geoderma* 162, 171-181.
- Terzaghi, K., Peck, R.B., Mesri, G., 1996. *Soil mechanics in engineering practice* (3rd edition). John Wiley and Sons, New York, NY.
- Uteau, D., Pagenkemper, S.K., Peth, S., Horn, R., 2013. Root and time dependent soil structure formation and its influence on gas transport in the subsoil. *Soil Till. Res.* 132, 69-76.
- Wickramarachchi, P., Kawamoto, K., Hamamoto, S., Nagamori, M., Moldrup, P., Komatsu, T., 2011. Effects of dry bulk density and particle size fraction on gas transport parameters in variably saturated landfill cover soil. *Waste Manage.* 31, 2464-2472.
- Wiermann, C., Werner, D., Horn, R., Rostek, J., Werner, B., 2000. Stress/strain processes in a structured unsaturated silty loam Luvisol under different tillage treatments in Germany. *Soil Tillage Res.* 53 (2), 117-128.
- Zhai, X., Horn, R., 2018. Effect of static and cyclic loading including spatial variation caused by vertical holes on changes in soil aeration. *Soil Tillage Res.* 177, 61-67.

7 Influence of static and cyclic loading on mechanical and hydraulic properties of soils with different textures and matric potentials

Xiafei Zhai, Rainer Horn

Revision for Soil Science Society of America Journal

7.1 Abstract

Soil deformation is the response of a soil to an applied stress, which occurs if the external soil stress applied exceeds the internal soil strength. Either mechanical, hydraulic, chemical or biological processes on various scales and intensities can alone or as coupled processes cause soil deformation. In order to quantify the effect of mechanical and hydraulic stresses on changes in soil functions, vertical displacement and pore water pressure were detected on repacked soils with three different textures (sand, silt loam and clay loam) at two matric potential values (-60 and -300 hPa). Two types of loading (static and cyclic loading) and three compaction levels (50, 100 and 200 kPa) were analyzed. In the case of static loading, the time-dependent vertical displacement curves for all treatments under all compaction levels are similar in shape but different in scale. However, different situations of time-dependent changes in pore water pressure were found due to different internal soil strength (soil texture and initial matric potential). After static loading, the extent of vertical displacement and the change in pore water pressure increased with increasing applied vertical stresses. Under the same type of loading (static), there was a similar trend in soil deformation between before and after having drilled vertical holes. In the case of cyclic loading, vertical displacement increased during loading but an elastic rebound of vertical displacement was observed during unloading. Cyclic loading resulted in an increase in pore water pressure during loading and a decrease during unloading due to change in pore continuity and the shape of water menisci in each cycle. The frequency of loading also plays an important role in soil deformation, e.g. soil deformation increased with increasing number of cycles. After each stress application, the saturated hydraulic conductivity decreased with increasing compaction levels, while the unsaturated hydraulic conductivity relatively increased except for silt loam

soils predried at -60 hPa. When the vertical displacement increased, the extent of water flux also increased due to higher hydraulic gradients which resulted in the more pronounced changes in pore water pressure in most cases. Due to the occurrence of the dissipation of excess water for treatments at -60 hPa during static loading, the change in pore water pressure increased firstly and then decreased with increasing vertical displacement. The alternation of soil strength under compaction is reflected by the effective stress, which depends on the change in pore water pressure and degree of saturation. In our experiment, we found that as the stress application advanced, the effective stress decreased (i.e. soils became more sensitive against external stress) for treatments of -60 hPa matric potential, and increased (i.e. soils became more stable to compaction) for treatments of -300 hPa matric potential for a given compaction level.

Keywords: Static loading; Cyclic loading; Vertical displacement; Pore water pressure; Hydraulic conductivity

7.2 Introduction

In modern agriculture, soil deformation is a major problem, mainly caused by stress-strain and shear processes induced by farm machines or the trampling of farm animals. Soil deformation due to grazing mostly affects primarily the topsoil (Krümmelbein et al., 2006; Drewry and Paton, 2005; Martinez and Zinck, 2004; Greenwood and McKenzie, 2001; Hamza and Anderson, 2005), while soil deformation due to heavy traffic can affect deeper depths. The stress distribution depends on soil internal strength which is influenced by soil structure, soil texture, organic matter content and its water status, bulk density, contact area and ground contact pressures, etc. (Krümmelbein et al., 2008; Lebert and Horn, 1991; Horn and Fleige, 2003).

If the internal soil strength is exceeded by external stresses, soil deformation is considered as plastic, i.e. irreversible and permanent while at stresses smaller than the internal soil strength, soils react with elastic deformation, and the majority of soil deformation is recoverable when the external stresses are removed (Keller et al., 2013; Peth et al., 2010; Destain et al., 2016). However, during cyclic loading, a slight plastic deformation may also take place even if the precompression stress is still not exceeded because the shear-induced

changes in pore continuity weakens the interactions between mineral particles and pore water gets more fluid during stress application and stress release (Peth and Horn, 2006; Larson and Gupta, 1980; Krümmelbein et al., 2008). Therefore, soil deformation is also affected by soil external factors, which depend on the magnitude, duration, numbers/frequency, type and the speed of loading (Krümmelbein et al., 2008; Horn and Fleige, 2003; Hartge and Horn, 2016; Richard et al., 1999; Naveed et al., 2016).

Arable soils are loaded or wheeled by various agricultural machinery, resulting in an increase in irreversible deformation in the last decades due to the increase in mass of machines as well as in the frequency of wheeling (Peth and Horn, 2006; Zapf, 1997; Krümmelbein et al., 2008). The verification of the expected changes concerning the ability of soils to resist the application of external stress to recover from deformation as well as the extent of strain processes are mostly quantified by static compression tests (Gubiani et al., 2018), whereas the effect of cyclic loading has rarely been analyzed in detail (Krümmelbein et al., 2008). Furthermore, the determination of the stress induced changes in pore water pressure in combination with the interaction of stress types was mostly undefined (Simmel, 1993; Nissen, 1999; Horn et al., 2019). Thus, these interactions between the kind, intensity and frequency of loading affect not only the pore size distribution but also the soil functions. In combination with the altered water saturation and hydraulic strength also change the various pore functions like hydraulic conductivity, air permeability (Dörner et al., 2012; Mentges et al., 2016; Mordhorst et al., 2012; Peth et al., 2010; Peth and Horn, 2006), water transport (Dörner et al., 2010; Dörner et al., 2012; Krümmelbein et al., 2008) and swelling intensity (Peng et al., 2004).

The extent of how far stress application results in an increase in bulk density and the alteration of pore size distribution, shape, continuity and tortuosity of soil pores depends apart from the internal soil strength also on the possible changes with time. Baumgarten and Horn (2013), based on the data of Nissen (1999), analyzed the time dependent strain processes in structured soils and showed that the less aggregated soils and the higher the applied static stresses were, the more pronounced were the changes in pore water pressure values up to very positive ones. They also found that pore water pressure can remain for a longer time while positive if the change in hydraulic conductivity caused by strain was reduced drastically and

thus resulted in a time dependent dynamic delay in the drainage off the excess soil water. This process is often defined as aquaplaning, well known on streets but in total seldom analyzed in soils. This is especially true if in addition various types of loading as well as different stresses are applied, which may have an intense interaction with the hydraulic conductivity characteristics and soil strength (Horton et al., 1994; Green et al., 2003; Richard et al., 2001; Dexter, 2004; Reicosky et al., 1981).

Under field conditions, arable soils are cultivated by multiple wheeling passes of machinery regularly, and dynamic processes can result in the rearrangement of soil particles and a shear-induced deterioration of pores, hence cyclic loading should be considered in fact. Thus, cyclic loading tests in the laboratory can be a tool to evaluate the effect of long-term field operations with specific soil properties (i.e. bulk density, texture, water content, structure) and traffic conditions (i.e. magnitude and duration of loading) on soil quality. Peth and Horn (2006) defined cyclic loading as the application of a constant load with the same duration of loading and unloading for each cycle throughout the test.

The hydraulic properties and especially the hydraulic or pneumatic functions like conductivity, permeability and diffusion depend on the actual stresses applied in relation to the internal soil strength. Therefore, accurate determination and prediction of soil water retention curve (WRC) under stress conditions plays an important role in the interpretation of the mechanical and hydraulic behavior of unsaturated soils. While a drastic reduction of saturated hydraulic conductivity with increasing compaction has been reported in many studies (Alaoui et al., 2011; Birlle et al., 2008; Reicosky et al., 1981), the experimental data relating to the effect of soil compaction on unsaturated flow are quite scarce (Richard et al., 2001; Alaoui et al., 2011; Assouline, 2006).

The preferential loss of larger pores results in the reduction of cross-sectional area of pores for water flow. Furthermore, the increased tortuosity with increasing bulk density are dynamic processes, which depend on the internal strain, i.e. particle movements and their rearrangement, but the extent is regulated by the drainage off the excess soil water (Assouline, 2006; Horn et al., 2000; Baumgartl et al., 1995; Gräsle et al., 1995; Fredlund und Rahadjo, 1993; Hartge and Horn, 2016).

In order to evaluate additional potential risks for irreversible soil deformation, it is

necessary to quantify the mechanical stability of soils and consequences for pore water pressure in combination with the changing hydraulic conductivity and pore continuity (Larson and Gupta, 1980; Peng et al., 2004). These changes in soil properties and functionality can result either in a decrease or an increase in pore water pressure during stress application, and both the direction and the intensity depend on the hydraulic conductivity (Krümmelbein et al., 2008), air-filled porosity, and pore continuity (Larson and Gupta, 1980). Within the recompression range, stresses cause only minor changes in pore water pressure, while the great changes can be expected in the virgin compression range. The overall effect of pore water pressure on soil strength can be quantified by the effective stress equation for both saturated and unsaturated soils (Bishop, 1959). When the soil is loaded under undrained conditions, an increase in pore water pressure is expected, and consequently the soil gets weaker after compaction, while the opposite can occur if coarser air-filled pores are compressed and a further rearrangement of the available water results in even more negative matric potential values (Hartge and Horn, 2016). If formerly air-filled pores become water-filled due to further compaction, the increase in matric potential finally results in positive pore water pressure values which pretend a higher internal soil strength because of the incompressibility of water, although the time dependency and the altered accessibility of mineral surfaces including swelling processes should be classified as highly relevant, because they govern the whole strain process. The uncertainty furthermore increases if the effect of various forms of stress application like cyclic loading is considered because stress-dependent changes in pore water pressure under cyclic loading leads to a rearrangement of particles and changes in voids, which prevent a rapid water drainage. Consequently, cyclic loading not only weakens soil structure due to serious deformation, but may also pump under in situ conditions additional soil water from deeper depth. Irrespective of which process dominates, soil structure will deteriorate due to swelling in combination with a kind of kneading and finally results in a completely homogenized particle arrangement (like puddling) (Horn, 2003; Pietola et al., 2005; Krümmelbein et al., 2008; Reszkowska et al., 2011).

Soil deformation induced changes in soil functions are therefore the result of the interactions between mechanical and hydraulic processes. Hence, both processes are always interlinked and are essential to assess and to predict soil deformation on the process basis, to

reflect modifications in soil structure and stability, and to estimate related changes in soil functions such as aeration, hydraulic or thermal fluxes. However, limited information is available on this topic area (Green et al., 2003; Stange and Horn, 2005; Horn et al., 2019). Additionally, the time dependency of stress application must be considered (Peth et al., 2010), because most soil mechanical and hydraulic properties change dynamically with time (Alaoui et al., 2011; Horn, 2004; Horn et al., 2003; Horn and Smucker, 2005). Therefore, in this study, our objectives were the following:

(1) how far affects the type of loading (static and cyclic) under three compaction levels in sandy, silt loam and clay loam soil samples, predried to different matric potentials (-60 hPa and -300 hPa), and soil structure (artificially prepared as vertical holes)

i) soil water retention curve (van Genuchten parameters α and n) and volumetric water content;

ii) mechanical properties (vertical displacement);

iii) hydraulic properties (pore water pressure, saturated and unsaturated hydraulic conductivity);

iv) soil strength (effective stress).

(2) how far occur time-dependent changes in vertical displacement, pore water pressure and hydraulic conductivity during static and cyclic loading, and

(3) how far can we define the relationships among vertical displacement, changes in pore water pressure and water flux during each stress application.

7.3 Material and methods

7.3.1 Soil sampling and properties

Disturbed soil samples with different textures (sand, silt loam and clay loam) were collected from three sites (Schuby, Bonn and Fehmarn) in Germany, respectively. More detailed information on site and soil properties is given in Zhai and Horn (2018).

7.3.2 Sample preparation

The samples were air-dried, sieved through 2 mm and then repacked with an initial dry bulk density of 1.4 g cm^{-3} in 235 cm^3 soil cylinders (10 cm wide and 3 cm long). The prepared

soil cylinders were saturated and then successively drained to matric potentials of -60 hPa on sandboxes and -300 hPa on ceramic plates.

In both silty and clayey soil samples occur obviously shrinkage from saturation to the matric potential of -300 hPa, resulting in the change of initial bulk density. Therefore, the cylinders of silt loam and clay loam soil at the matric potential of -300 hPa were prepared differently. Firstly, water content of silt loam and clay loam soil at the matric potential of -300 hPa were tested and the air-dried soils were wetted by spraying distilled water to achieve the desired water content. The samples were kept in the plastic bags for 24 h for water homogenization. Finally, the prepared soil samples were repacked into the cylinders.

7.3.3 Compaction experiment

The prepared cylinders were compacted for 4 h under static loads of 50, 100 and 200 kPa, respectively, followed by an unload for 1h. Thereafter, all cylinders were compacted under cyclic loading (50 cycles) with a constant external stress of 50, 100 and 200 kPa, respectively. Each cycle consisted of 30s of loading and 30s of unloading. In order to analyze the effect of additional vertical pores on soil functions at given stresses and type of loading, all samples were perforated with five vertical holes ($\varnothing = 2$ mm each), and thereafter compacted again under static loads of 50, 100 and 200 kPa for 4 h. Each treatment included 5 replicated samples.

7.3.4 Measurements of mechanical and hydraulic properties

Soil vertical displacement and the change in pore water pressure during loading and unloading were measured with potentiometric displacement sensors at the top of soil samples, and microtensiometers inserted into the bottom of soil samples, respectively. The detail measurement processes were described by Peth et al. (2010). Due to high water content in the silt loam soil (-60 hPa), soil material was squeezed out of the cylinders at about 200 kPa, therefore related measurements could not be made.

7.3.5 Models of hydraulic properties and pore functions

7.3.5.1 Water retention curve

Among various empirical equations, one of the most frequently used form was proposed by van Genuchten (1980). Hence, in this study, the experimental data for each treatment and each stress application was fitted to the van Genuchten equation using an optimization program RETC (U.S. Salinity Laboratory, USDA, ARS).

$$\theta(h) = (\theta_s - \theta_r) \left[1 + (\alpha h)^n \right]^{-m} + \theta_r$$

where θ_s and θ_r are the saturated and residual water content ($\text{cm}^3 \text{ cm}^{-3}$), respectively. In general, θ_s is assumed to be equal or close to soil total porosity. h is matric suction (the negative value of matric potential) (hPa). α , n and m are empirical fitting parameters which affect the shape of soil water retention curve (WRC).

Another widely used model for WRC is expressed as

$$S_e(h) = \frac{1}{\left[1 + (\alpha h)^n \right]^m}$$

where $S_e(h)$ is the effective saturation at matric suction h . Suction is the negative of the matric potential. It is sometimes used to eliminate the need for negative numbers in unsaturated soils.

7.3.5.2 Hydraulic conductivity

Unsaturated hydraulic conductivity measurements are often carried out according to Plagge et al. (1990) and give direct data of changes in water content and matric potential with time, which are the basis for direct calculations. However, often an indirect calculation procedure is preferred because of time-consuming and extensive variability using field and laboratory methods (van Genuchten, 1980; Stange and Horn, 2005). Within our research program, we decided to choose the indirect method to predict the saturated and unsaturated hydraulic conductivity.

The Kozeny-Carman model was proposed by Kozeny (1927), and modified by Carman (1938, 1956) for predicting the saturated hydraulic conductivity. The model is expressed as

$$K_s = (g / \mu) (1 / C_{K-C}) (1 / S_o^2) \left[e^3 / (1 + e) \right]$$

where K_s is saturated hydraulic conductivity (cm s^{-1}), g is unit weight of permanent, μ is viscosity of permanent, C_{K-C} is Kozeny-Carman empirical coefficient (usually taken as 5), S_o

is specific surface area per unit volume of particles (cm^{-1}), and e is void ratio ($\text{cm}^3 \text{ cm}^{-3}$).

When the permanent is water at 20°C , $g/\mu = 9.93 \times 10^4 \text{ 1/cm s}$.

The van Genuchten equation is frequently combined with a Mualem theory to predict unsaturated hydraulic conductivity (van Genuchten, 1980).

$$K(h) = K_s \frac{\left\{ 1 - (\alpha h)^{n-1} \left[1 + (\alpha h)^n \right]^{-m} \right\}^2}{\left[1 + (\alpha h)^n \right]^{m/2}}$$

where $K(h)$ (cm s^{-1}) is unsaturated hydraulic conductivity at matric suction h . α , n and m are empirical fitting parameters of soil water retention curve (WRC).

7.3.5.3 Water flux

The water flow in porous medium can be described by Darcy's law which depends on the hydraulic gradient and the hydraulic conductivity.

$$q = -K \frac{\Delta h}{\Delta x}$$

where q is the hydraulic flux (cm s^{-1}), K is the hydraulic conductivity (cm s^{-1}), Δh is the difference in matric suction between after and before loading, and Δx is vertical displacement after loading.

7.3.5.4 Effective stress

In saturated soils, the effective stress σ' is defined as the difference between the total stress, σ , and the pore water pressure, u_w .

$$\sigma' = \sigma - u_w$$

In unsaturated soils, the most widely used relationship for the effective stress, σ' , is expressed as (Bishop, 1959):

$$\sigma' = (\sigma - u_a) + \chi(u_a - u_w)$$

where σ' is the effective stress, σ is the normal stress, u_a and u_w is the pore air and water pressure, respectively, and χ is the factor which depends on the degree of saturation (for completely dry soils, $\chi = 0$; while for fully saturated soils, $\chi = 1$).

7.3.6 Statistical analyses

All statistical analyses were undertaken using the Excel statistics software (Microsoft

7 INFLUENCE OF STATIC AND CYCLIC LOADING ON MECHANICAL AND HYDRAULIC PROPERTIES OF SOILS WITH DIFFERENT TEXTURES AND MATRIC POTENTIALS

Corporation, USA), and all figures were made by Origin 9.1 graphing software (OriginLab Corporation, USA).

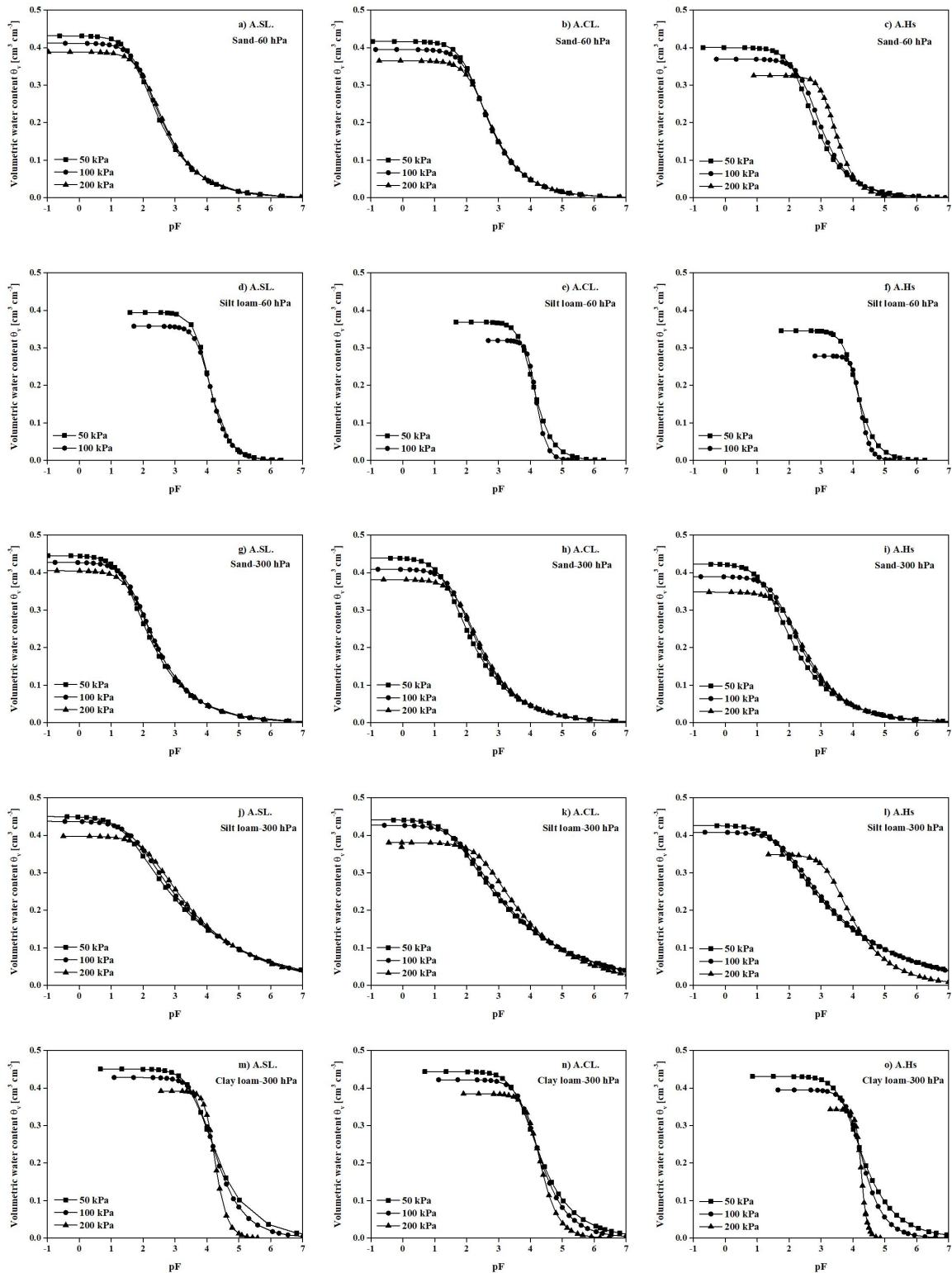


Fig.7-1 The effect of compaction levels (50, 100 and 200 kPa) on soil water retention curve (volumetric water content as a function of matric suction) for five different treatments (sand

soil (-60 hPa), silt loam soil (-60 hPa), sand soil (-300 hPa), silt loam soil (-300 hPa), clay loam soil (-300 hPa)) after static loading (A.SL.), cyclic loading (A.CL.) and static loading with vertical holes (A.Hs).

7.4 Results

7.4.1 Water retention curve

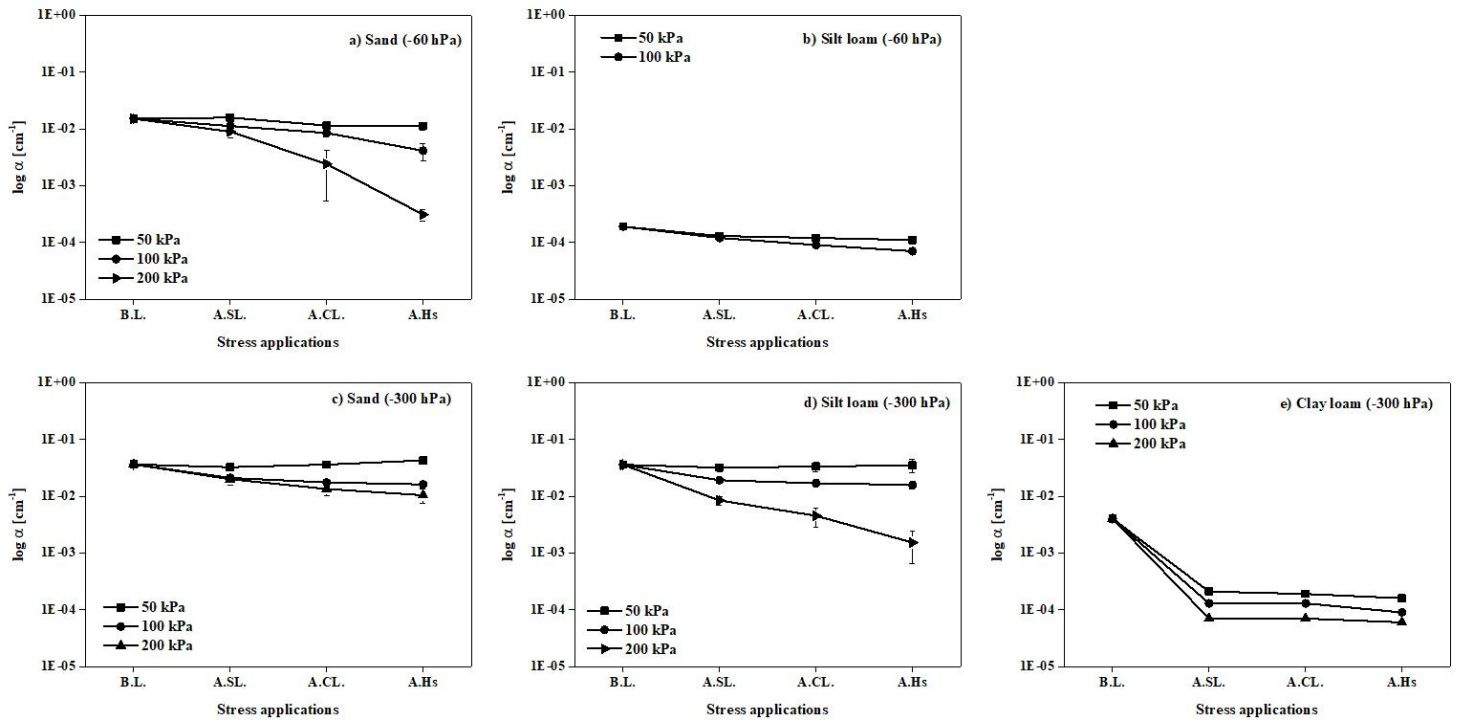


Fig.7-2 The effect of compaction levels (50, 100 and 200 kPa) on van Genuchten parameter α for (a) sand soil (-60 hPa), (b) silt loam soil (-60 hPa), (c) sand soil (-300 hPa), (d) silt loam soil (-300 hPa) and (e) clay loam soil (-300 hPa) before loading (B.L.) and after static loading (A.SL.), cyclic loading (A.CL.) and static loading with vertical holes (A.Hs).

The effect of compaction on soil water retention curve patterns for all treatments and after each stress application shows that the saturated water content decreased with increasing compaction levels (Fig.7-1). The applied stresses increased the air-entry matric potential to higher pF values and the slopes of the water retention curves got steeper, as can be derived

7 INFLUENCE OF STATIC AND CYCLIC LOADING ON MECHANICAL AND HYDRAULIC PROPERTIES OF SOILS WITH DIFFERENT TEXTURES AND MATRIC POTENTIALS

from decreasing α values of the van Genuchten equation (Fig.7-2). Furthermore, n increased with increasing compaction levels (Fig.7-3). For a given compaction level, the α value decreased during the consecutive sequence of treatments (Fig.7-2). The value of n was almost stable for all treatments under the compaction level smaller than 50 kPa, but the value of n increased when 200 kPa stress was applied, except for the sand soil at the matric potential of -300 hPa, as the stress applications advanced (Fig.7-3).

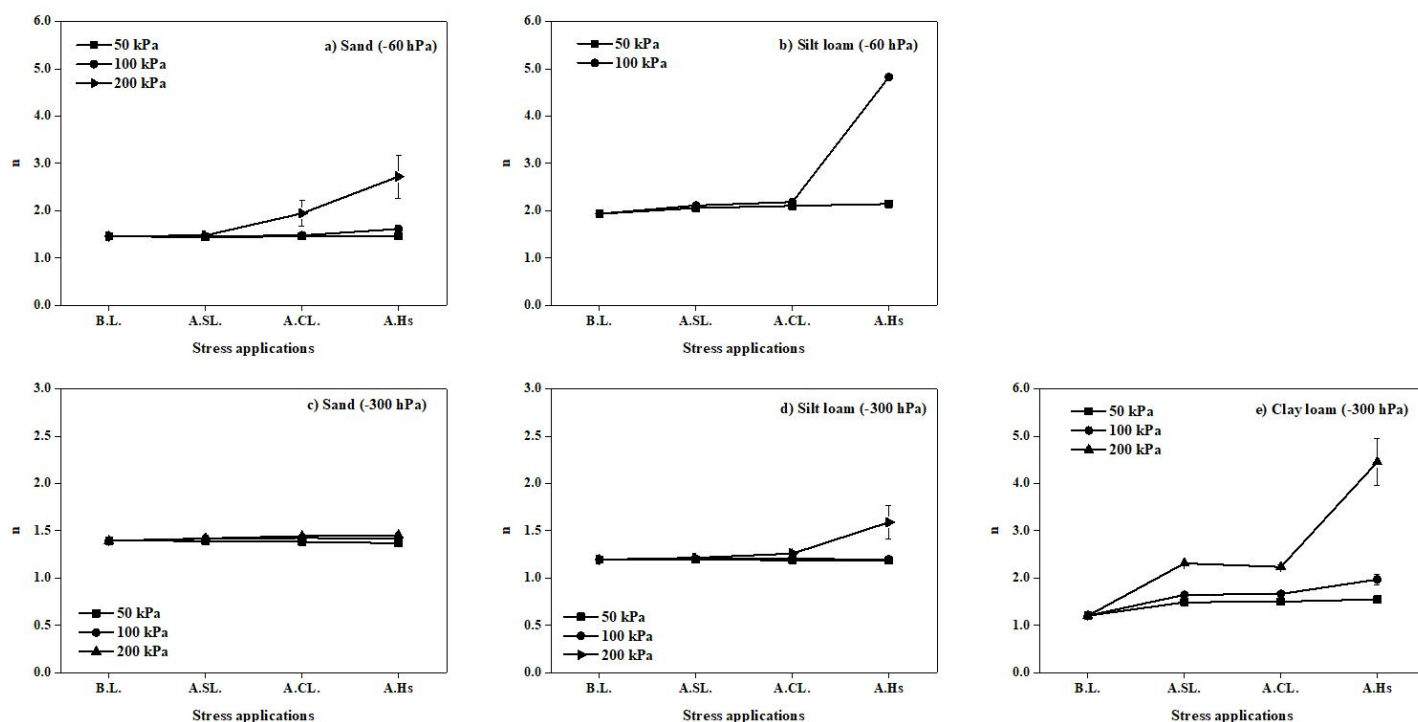


Fig.7-3 The effect of compaction levels (50, 100 and 200 kPa) on van Genuchten parameter n for (a) sand soil (-60 hPa), (b) silt loam soil (-60 hPa), (c) sand soil (-300 hPa), (d) silt loam soil (-300 hPa) and (e) clay loam soil (-300 hPa) before loading (B.L.) and after static loading (A.S.L.), cyclic loading (A.C.L.) and static loading with vertical holes (A.Hs).

The results of type and magnitude of loading on changes of volumetric water content θ_w for all treatments before and after each stress application (static loading, cyclic loading, static loading with vertical holes) are shown in Fig.7-4. The effect of compaction levels on volumetric water content after compaction depends on the initial matric potential. For treatments at the matric potential of -60 hPa, volumetric water content decreased with increasing stresses. However, the opposite trend was found for treatments at the matric

potential of -300 hPa after each stress application, especially for the finer-textured soils. For a given compaction level, during the consecutive sequence of treatments, volumetric water content decreased for treatments at -60 hPa matric potential, while it either remained constant or increased slightly for different textured treatments at -300 hPa matric potential.

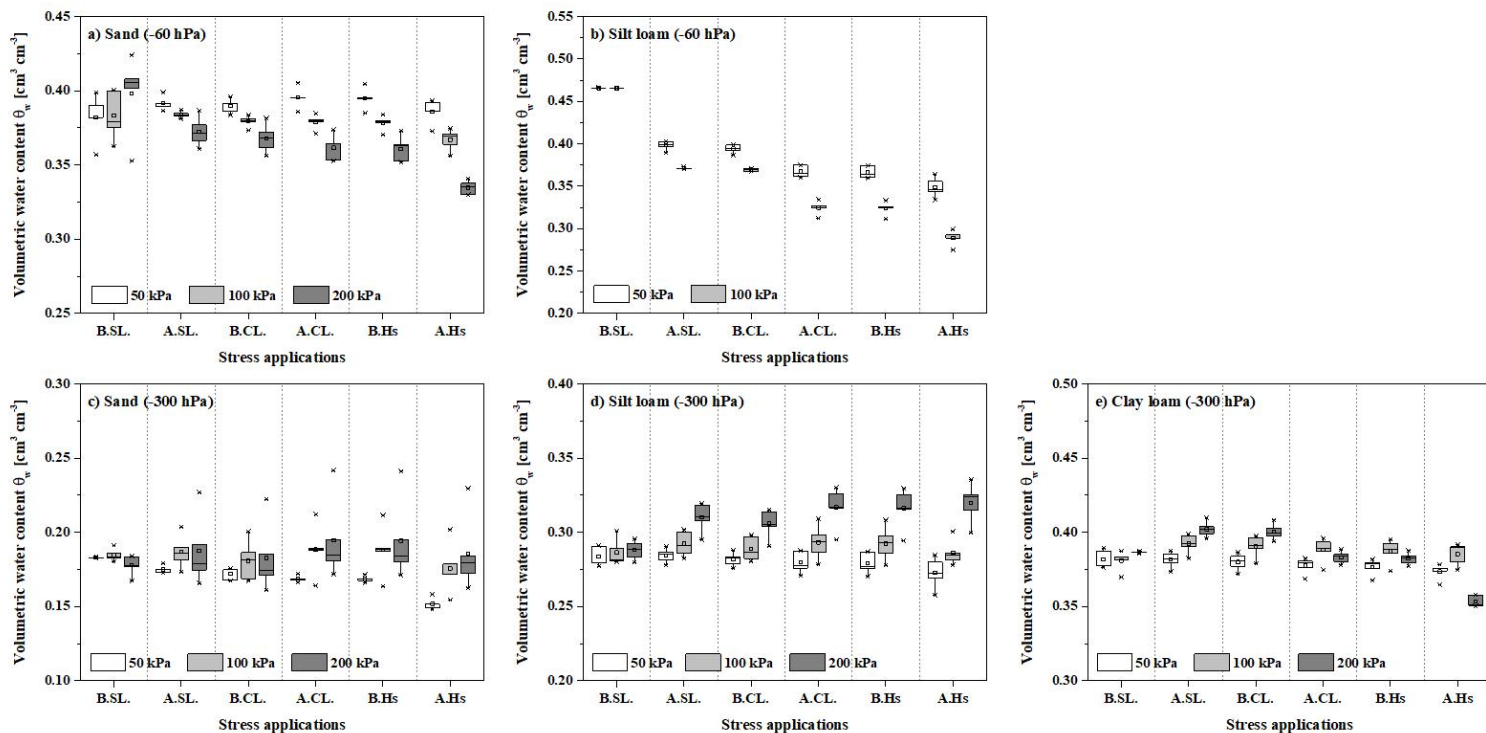


Fig.7-4 The effect of compaction levels (50, 100 and 200 kPa) on volumetric water content θ_w for (a) sand soil (-60 hPa), (b) silt loam soil (-60 hPa), (c) sand soil (-300 hPa), (d) silt loam soil (-300 hPa) and (e) clay loam soil (-300 hPa) before (B.S.L.) and after (A.S.L.) static loading, before (B.C.L.) and after (A.C.L.) cyclic loading, before (B.Hs) and after (A.Hs) static loading with vertical holes.

7.4.2 Time- and stress-dependent change in mechanical properties (vertical displacement) for each treatment after each stress application

The changes in vertical displacement for all treatments during each stress application documents are shown in Fig.7-5. During static loading, an intensive vertical displacement was observed in the beginning of stress application, while it tended to be a constantly slight decline with increasing loading time. Soil deformation recovered partly when the external

7 INFLUENCE OF STATIC AND CYCLIC LOADING ON MECHANICAL AND HYDRAULIC PROPERTIES OF SOILS WITH DIFFERENT TEXTURES AND MATRIC POTENTIALS

stresses were removed. After static loading, the extent of vertical displacement increased significantly with increasing stress formerly applied.

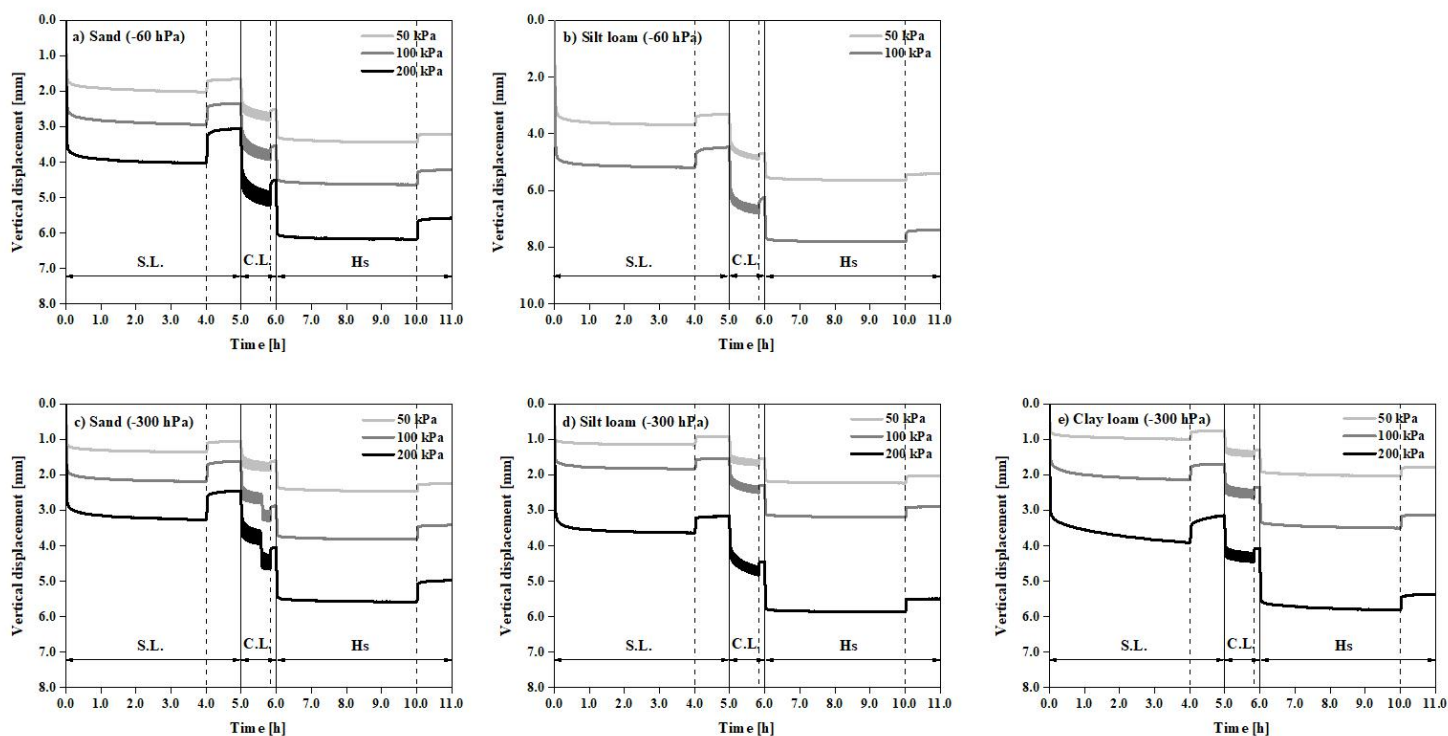


Fig.7-5 Time- and stress-dependent change in vertical displacement for (a) sand soil (-60 hPa), (b) silt loam soil (-60 hPa), (c) sand soil (-300 hPa), (d) silt loam soil (-300 hPa) and (e) clay loam soil (-300 hPa) during static loading (S.L.), cyclic loading (C.L.) and static loading with vertical holes (Hs). Vertical solid and dotted lines distinguish different type of stress application and loading and unloading process for a given stress application, respectively.

During the following cyclic loading, only the first loading event caused a significant increase in vertical displacement and faded off with only slight changes as the number of cycles increased for most of treatments. Noticeably, a special time-dependent vertical displacement curve was found for the sand soil at the matric potential of -300 hPa (Fig.7-5c). There was a slight increase in vertical displacement during the first 36 cycles at 100 kPa, and then shifted to a pronounced increase in the 37th cycle event and returned to a slight increase with the subsequent cycles. This situation was also observed at 200 kPa and the shifted point occurred in the 35th cycle event. After cyclic loading, there was a similar trend in vertical displacement as after static loading (e.g. the higher the load, the higher was the vertical

displacement), but the extent of vertical displacement decreased compared to static loading.

The more in detail about the effect of cyclic loading on changes in vertical displacement is shown in Fig.7-6a. During cyclic loading, the vertical displacement increased during loading events and decreased during unloading events in each cycle event. We also found that the differences in vertical displacement between loading and unloading events increased with increasing applied stresses.

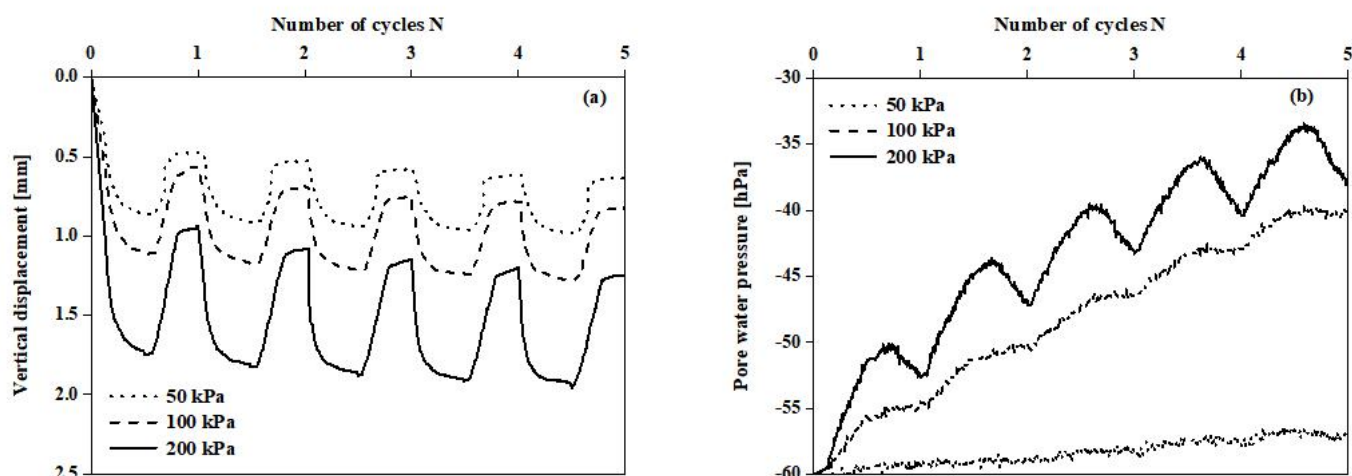


Fig.7-6 Vertical displacement (a) and pore water pressure (b) as a function of the first 5 cycles under three compaction levels (50, 100 and 200 kPa) for sand soil at the matric potential of -60 hPa.

With the same type of loading (static), a similar trend of the time-dependent vertical displacement curve was obtained after having drilled vertical holes in the samples compared to before, but the extent of additional vertical displacement decreased.

Under the same compaction level, different mechanical deformation behavior among treatments was found due to the distinct differences in soil internal strength which was controlled by soil texture and initial matric potential. For all stress applications, with a given soil texture, the vertical displacement was more pronounced for treatments at higher matric potential (-60 hPa) than at more negative matric potential (-300 hPa). At a given matric potential, various patterns were observed. At the matric potential of -60 hPa, the vertical displacement was always greater for finer-textured than for coarser-textured soils. However,

the opposite trend was found at the matric potential of -300 hPa, i.e. the finer-textured soils were less sensitive to stress application, except for the clay loam samples.

7.4.3 Time- and stress-dependent change in hydraulic properties for each treatment after each stress application

7.4.3.1 Pore water pressure

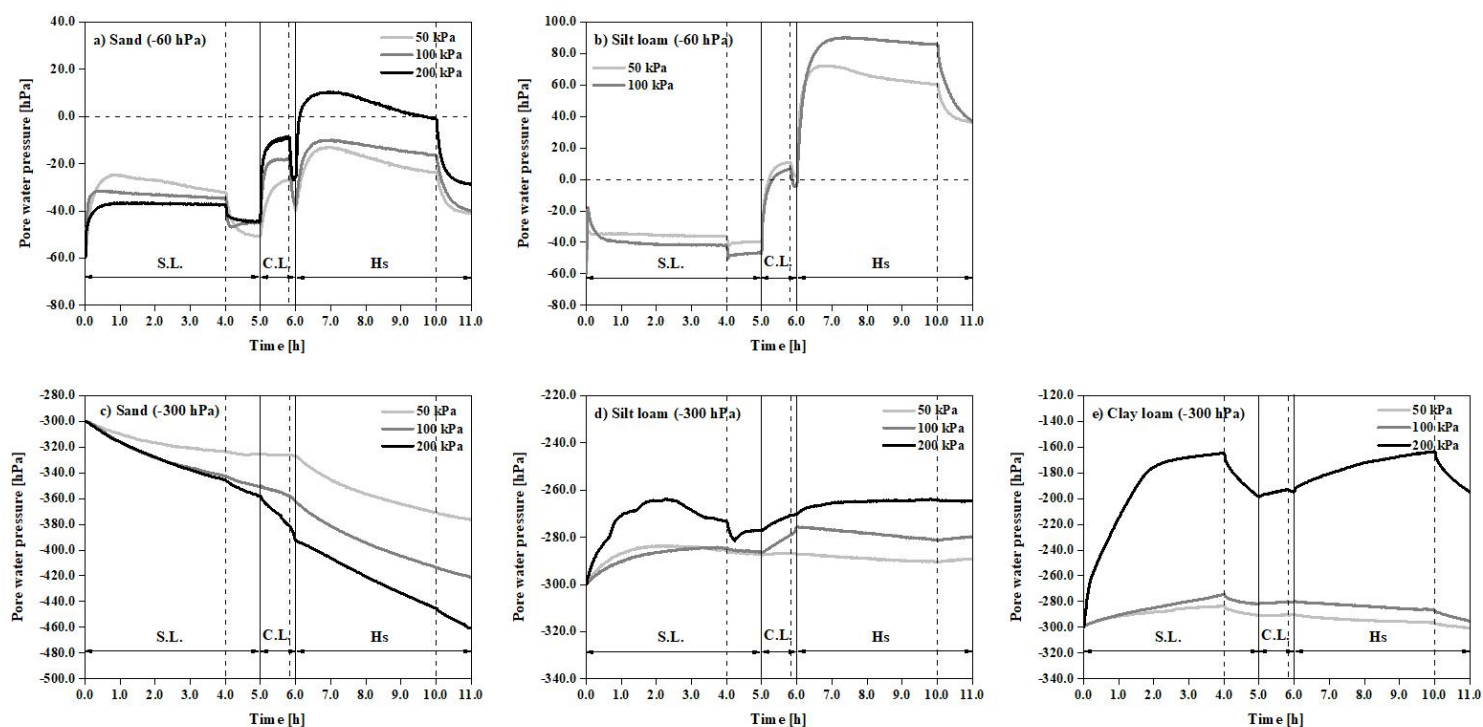


Fig.7-7 Time- and stress-dependent change in pore water pressure for (a) sand soil (-60 hPa), (b) silt loam soil (-60 hPa), (c) sand soil (-300 hPa), (d) silt loam soil (-300 hPa) and (e) clay loam soil (-300 hPa) during static loading (S.L.), cyclic loading (C.L.) and static loading with vertical holes (Hs). Vertical solid and dotted lines distinguish different type of stress application and loading and unloading process for a given stress application, respectively.

Time- and stress-dependent changes in pore water pressure for treatments with different soil texture and matric potential during each compaction process are presented in Fig.7-7. For treatment at higher initial matric potential (-60 hPa), the extent of changes in pore water pressure decreased with increasing the compaction levels after static loading, but increased

after the subsequent stress applications (cyclic loading and static loading with vertical holes). For treatments at more negative initial matric potential (-300 hPa), greater changes in pore water pressure were observed under higher compaction levels for each stress application.

At -60 hPa matric potential, static loading resulted in an increase in pore water pressure, but the process of time-dependent change in pore water pressure was different for treatments with different textures. For coarser-textured (sand) soils (Fig.7-7a), an initially fast increase in pore water pressure declined slightly with increasing loading time. For finer-textured (silt loam) soils (Fig.7-7b), a remarkable increase in pore water pressure was observed in the beginning of static loading. As the time of loading increased, this peak was followed by a fast decrease and remained thereafter constant. In case of -300 hPa matric potential, different situations of time-dependent changes in pore water pressure were observed for different textured soils during static loading. In coarser-textured (sand) soils (Fig.7-7c), the pore water pressure decreased continuously with increasing loading time. However, the opposite trend was found for finer-textured (silt loam and clay loam) soils (Fig.7-7d and 7-7e), and static loading resulted in a constant pore water pressure increase during compaction.

Subsequent cyclic loading resulted in increasing pore water pressure values during loading and decreasing ones during unloading (Fig.7-6b). As the level of compaction increased, this effect became more pronounced and pore water pressure tended to a greater amplitude during a single loading or unloading event. In the case of treatments at the matric potential of -60 hPa (Fig.7-7a and 7-7b), pore water pressure increased with the number of cycles. Furthermore, at the matric potential of -300 hPa, a minor change in pore water pressure was found with time if stressed with 50 kPa. Under higher compaction levels (100 and 200 kPa), two opposite trends of time-dependent pore water pressure were observed, which were related to different soil texture. For coarser-textured (sand) soils, the pore water pressure decreased while for finer-textured (silt loam and clay loam) soils, pore water pressure increased slightly with the number of loading cycles.

During static loading, the time dependent change in pore water pressure curves for a given treatment between before and after having drilled holes are similar in shape but different in scale (Fig.7-7). For silt loam soil (-60 hPa) with vertical holes, there was a fast and remarkable increase in pore water pressure and then a minor change in pore water

pressure with increasing loading time compared to without holes. Positive pore water pressure was also detected for silt loam soil (-60 hPa) during static loading after having drilled vertical holes.

7.4.3.2 Hydraulic conductivity

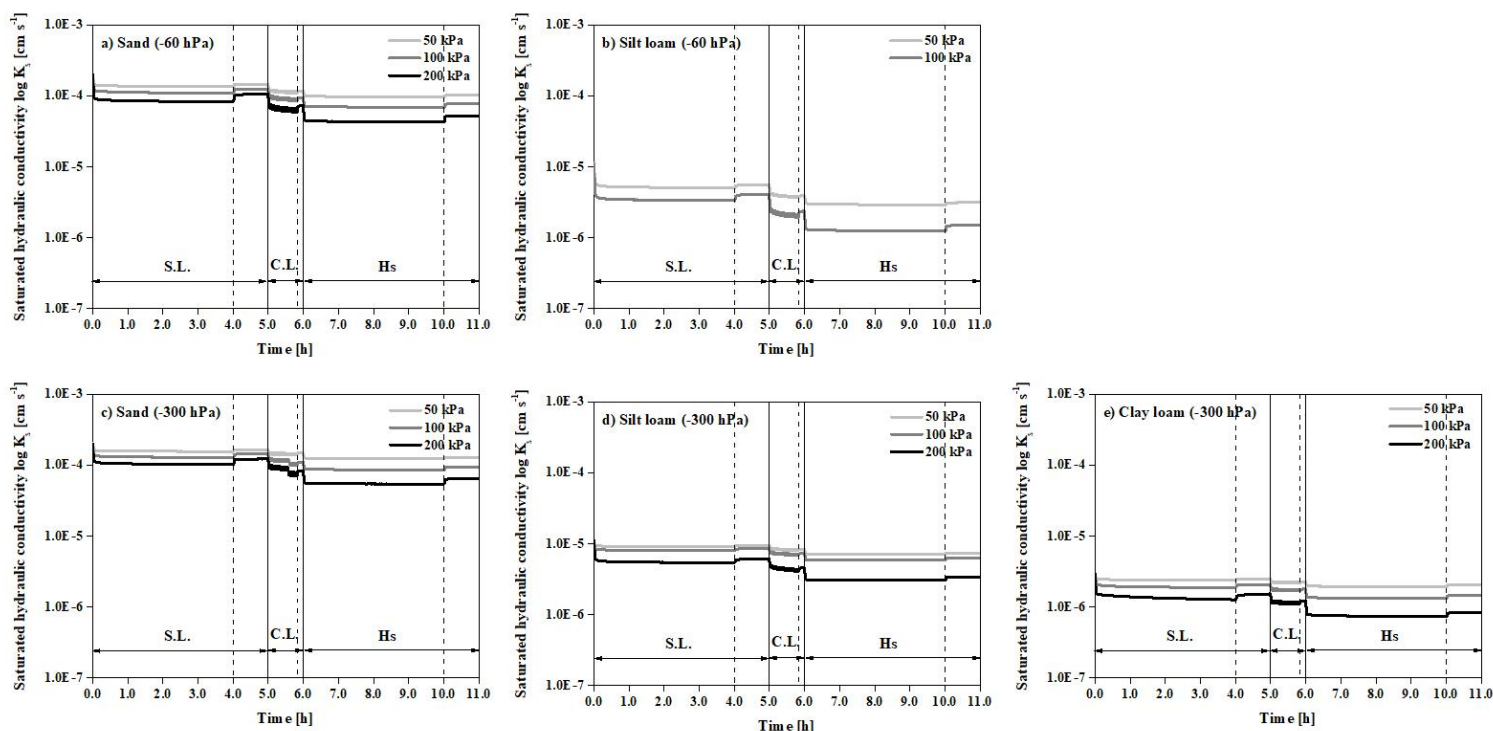


Fig.7-8 Time- and stress-dependent change in saturated hydraulic conductivity K_s for (a) sand soil (-60 hPa), (b) silt loam soil (-60 hPa), (c) sand soil (-300 hPa), (d) silt loam soil (-300 hPa) and (e) clay loam soil (-300 hPa) during static loading (S.L.), cyclic loading (C.L.) and static loading with vertical holes (Hs). Vertical solid and dotted lines distinguish different type of stress application and loading and unloading process for a given stress application, respectively.

The calculated time- and stress-dependent changes in saturated (K_s) and unsaturated (K) hydraulic conductivity for treatments with different soil textures and matric potential pretreatments (Fig.7-8 and Fig.7-9). The time-dependent saturated hydraulic conductivity curves (based on the Kozeny model) for a given treatment are similar in shape during each

7 INFLUENCE OF STATIC AND CYCLIC LOADING ON MECHANICAL AND HYDRAULIC PROPERTIES OF SOILS WITH DIFFERENT TEXTURES AND MATRIC POTENTIALS

stress application. During loading, the value of K_s decreased drastically in the beginning of stress application, followed by a slight decline with loading time. The value of K_s increased when the external stresses were removed but did not reach the original values again.

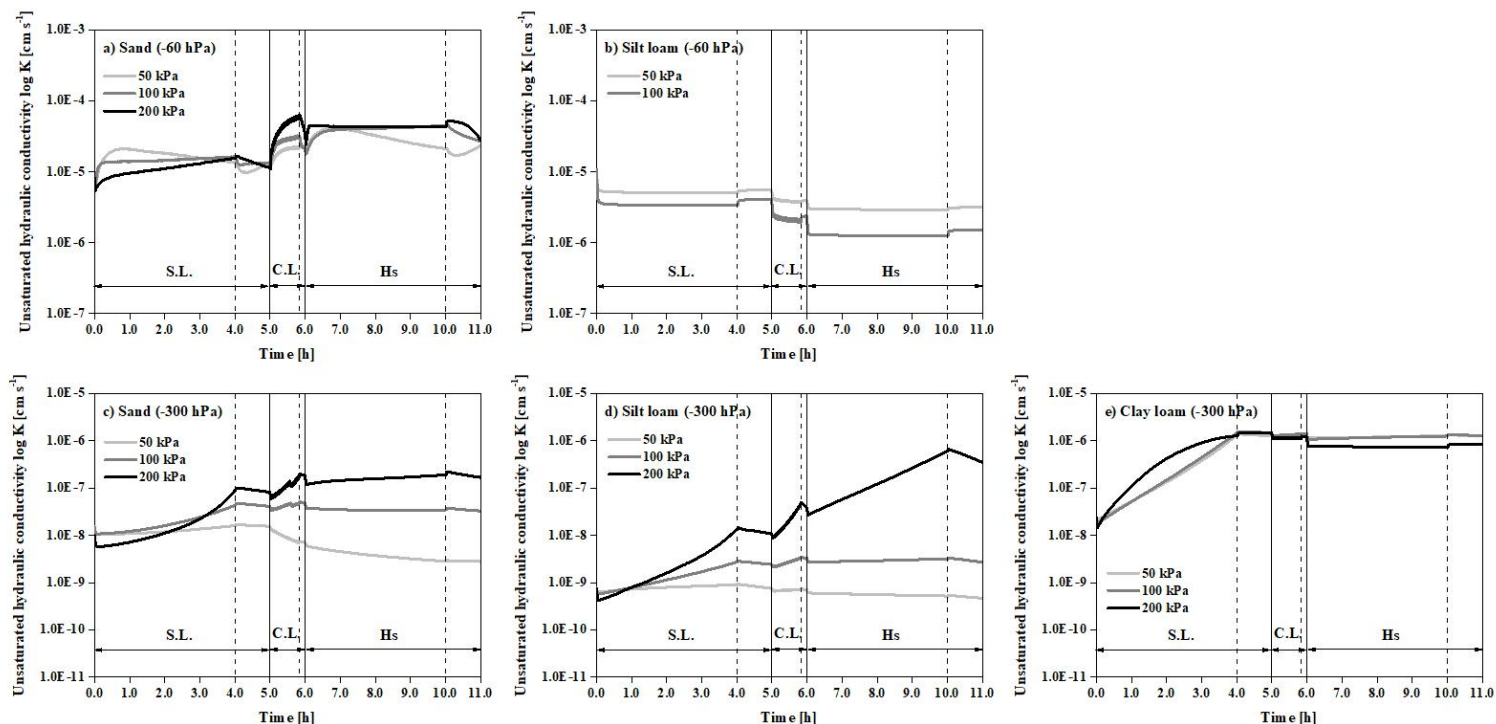


Fig.7-9 Time- and stress-dependent change in unsaturated hydraulic conductivity K for (a) sand soil (-60 hPa), (b) silt loam soil (-60 hPa), (c) sand soil (-300 hPa), (d) silt loam soil (-300 hPa) and (e) clay loam soil (-300 hPa) during static loading (S.L.), cyclic loading (C.L.) and static loading with vertical holes (Hs). Vertical solid and dotted lines distinguish different type of stress application and loading and unloading process for a given stress application, respectively.

Three different trends (decrease, increase or even stable with time) could be detected for the unsaturated hydraulic conductivity curves calculated for various treatments with different texture and initial matric potential. For silt loam soils at -60 hPa matric potential, the time- and stress-dependent unsaturated hydraulic conductivity curves were identical to those of the saturated ones. For clay loam soils at -300 hPa matric potential, the value of K increased with loading time during static loading but minor changes in K were found during cyclic loading and static loading with vertical holes. There were minor differences in the value of K for all

compaction levels after each stress application. For sand soils (-60 and -300 hPa) and silt loam soils (-300 hPa), the value of K increased with increasing loading time during each stress application. After loading, the value of K increased with increasing stress application.

7.4.4 The relationships between mechanical and hydraulic deformation for a given treatment

The relationships between vertical displacement and change in pore water pressure or water flux are shown in Fig.7-10 and Fig.7-11, respectively. For treatments at -60 hPa matric potential, the change in pore water pressure increased firstly and then decreased with increasing vertical displacement during static loading regardless of vertical holes. During cyclic loading, the pore water pressure constantly increased with an increase in vertical displacement. For treatments at -300 hPa matric potential, for all stress applications, the change in pore water pressure remained stable firstly and then increased quickly with increasing vertical displacement (Fig.7-10). The higher the vertical displacement, the higher was the water flux for all treatments during each stress application (Fig.7-11).

7 INFLUENCE OF STATIC AND CYCLIC LOADING ON MECHANICAL AND HYDRAULIC PROPERTIES OF SOILS WITH DIFFERENT TEXTURES AND MATRIC POTENTIALS

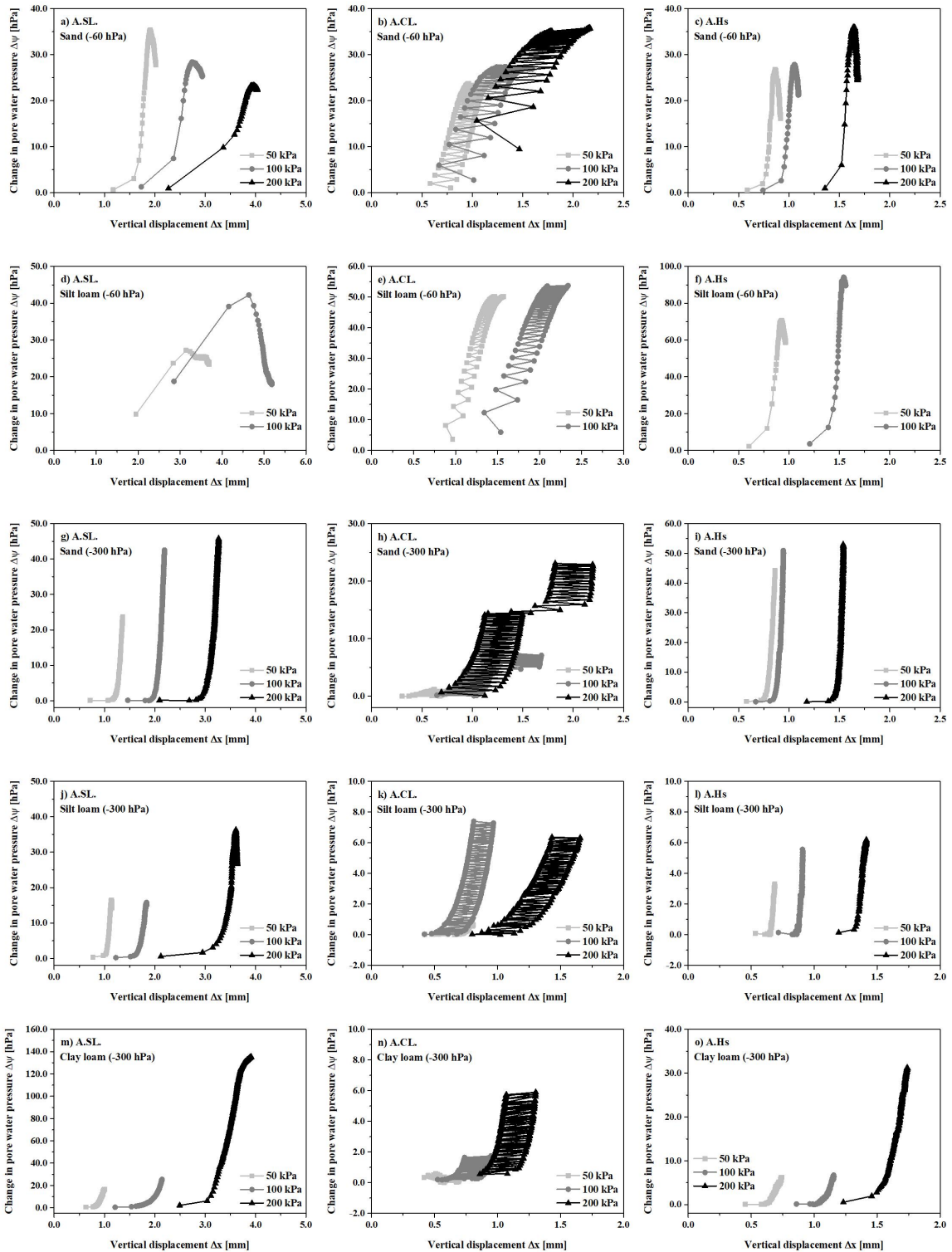


Fig.7-10 Relationship between vertical displacement Δx and the absolute value of the change in pore water pressure $\Delta\psi$ after compaction compared to before under different compaction levels (50, 100 and 200 kPa) for five different treatments (sand soil (-60 hPa), silt loam soil (-60 hPa), sand soil (-300 hPa), silt loam soil (-300 hPa), clay loam soil (-300 hPa)) during static loading (A.SL.), cyclic loading (A.CL.) and static loading with vertical holes (A.Hs).

7 INFLUENCE OF STATIC AND CYCLIC LOADING ON MECHANICAL AND HYDRAULIC PROPERTIES OF SOILS WITH DIFFERENT TEXTURES AND MATRIC POTENTIALS

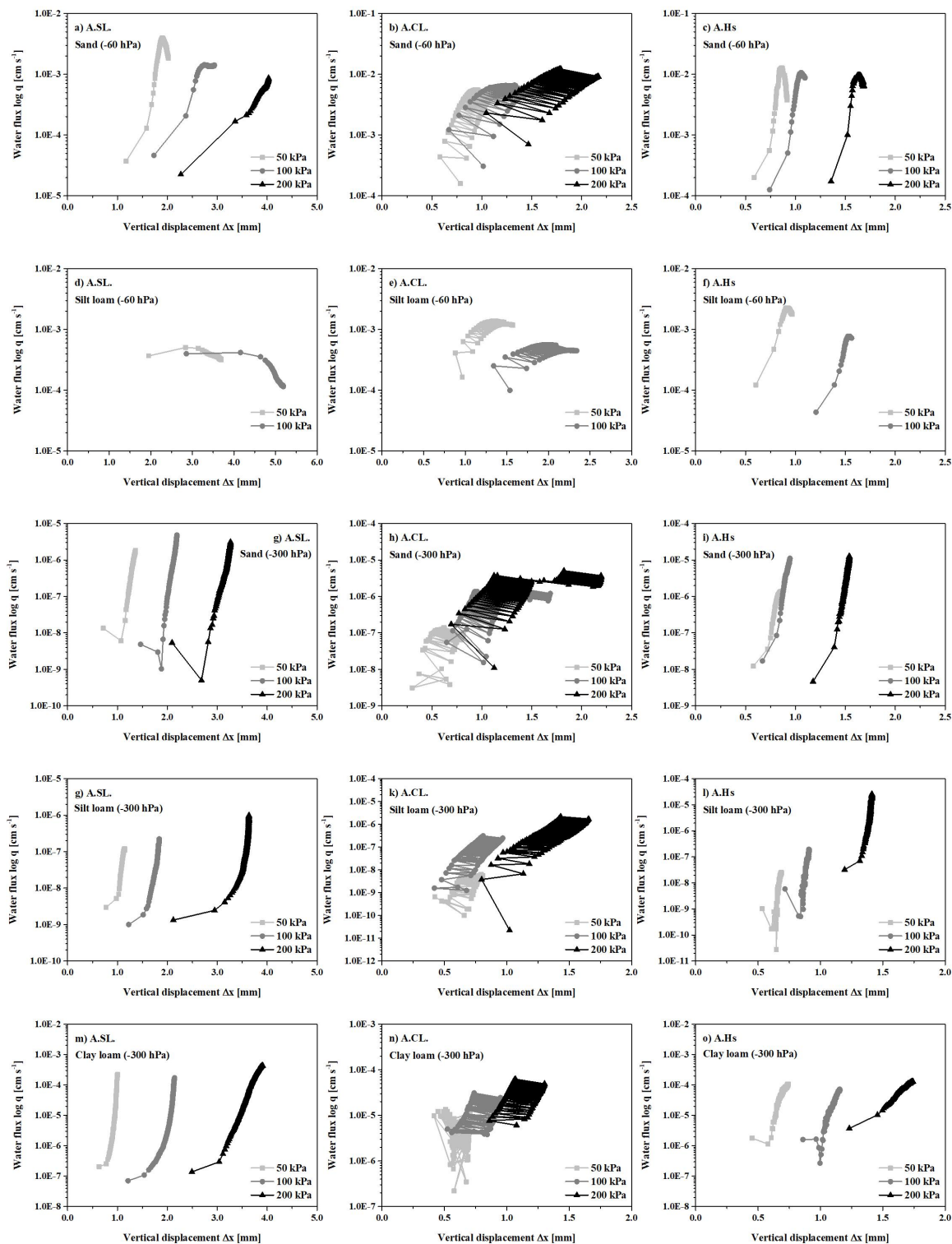


Fig.7-11 Relationship between vertical displacement Δx and water flux q after compaction compared to before under different compaction levels (50, 100 and 200 kPa) for five different treatments (sand soil (-60 hPa), silt loam soil (-60 hPa), sand soil (-300 hPa), silt loam soil (-300 hPa), clay loam soil (-300 hPa)) during static loading (A.SL.), cyclic loading (A.CL.) and static loading with vertical holes (A.Hs).

7.4.5 Consequences of stress application on effective stress

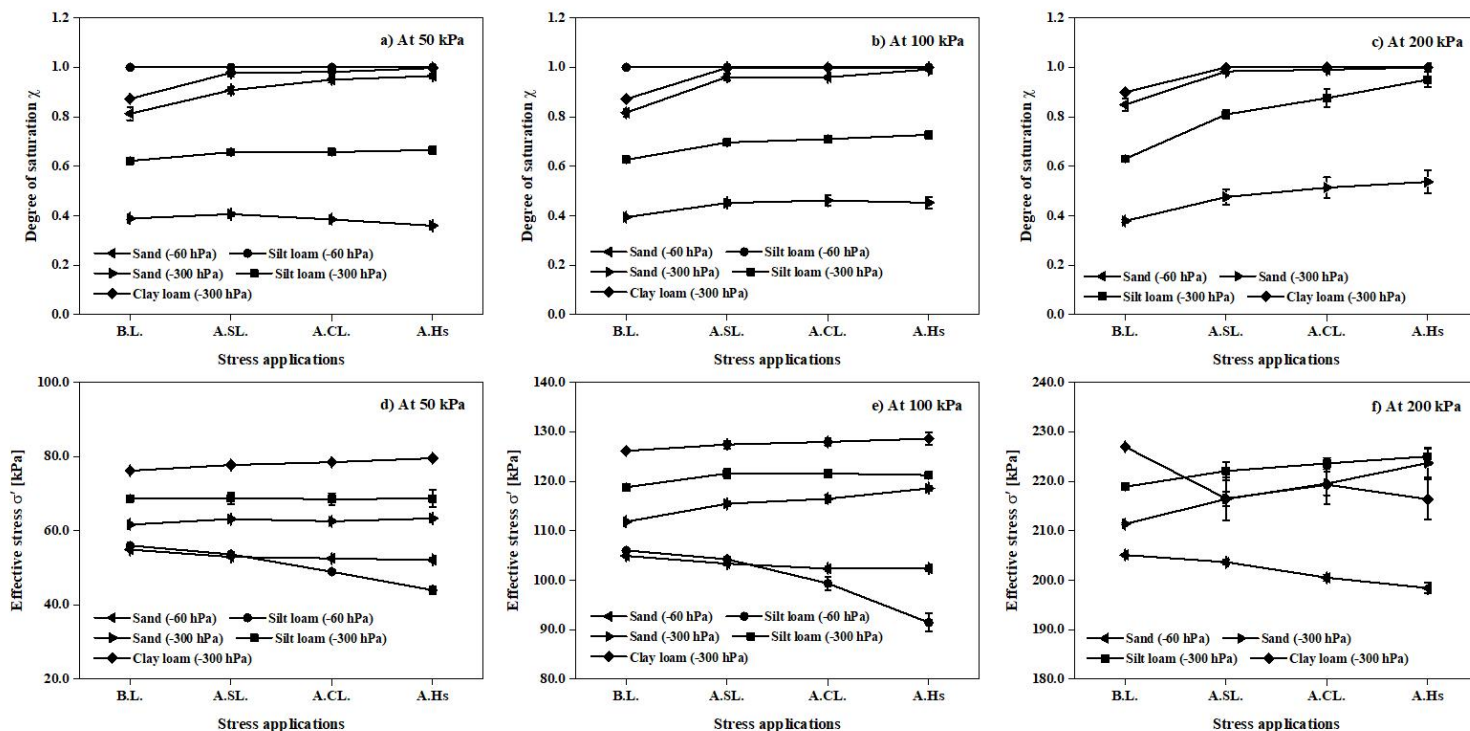


Fig.7-12 Degree of saturation χ (a-c) and effective stress σ' (d-f) as a function of stress applications (before loading (B.L.) and after static loading (A.S.L.), cyclic loading (A.C.L.) and static loading with vertical holes (A.Hs)) for five different treatments (sand soil (-60 hPa), silt loam soil (-60 hPa), sand soil (-300 hPa), silt loam soil (-300 hPa), clay loam soil (-300 hPa)) under different compaction levels (50, 100 and 200 kPa).

The effects of all stress applications on the degree of saturation and effective stress are shown in Fig.7-12, and the extent of changes in the effective saturation, pore water pressure and effective stress for all treatments after stress applications are presented in Table 7-1. At the matric potential of -60 hPa, each stress application resulted in an increased degree of saturation and in pore water pressure values but also in a reduction of effective stress. However, at the matric potential of -300 hPa, both degree of saturation and effective stress increased after each stress application (Fig.7-11). At the same compaction level, the effective stress was lower for treatments at -60hPa matric potential than treatments at -300 hPa matric potential for a given stress application. The effective stress for coarser-textured soils was

higher than for finer-textured soils at -60 hPa matric potential, but the opposite trend was found at -300 hPa matric potential for a given compaction level (Fig.7-11). The extent of change (either decrease or increase) in effective stress was more pronounced for finer-textured soils than for coarser-textured soils for a given matric potential (Table 7-1).

Table 7-1 The extent of changes in effective saturation (S_e), pore water pressure (p) and effective stress (σ') for all treatments after each stress application under all applied stresses (50, 100 and 200 kPa)

Treatments	Compaction levels [kPa]	A.SL.			A.CL.			A.Hs		
		ΔS_e [%]	Δp [%]	$\Delta \sigma'$ [%]	ΔS_e [%]	Δp [%]	$\Delta \sigma'$ [%]	ΔS_e [%]	Δp [%]	$\Delta \sigma'$ [%]
Sand (-60 hPa)	50	9.88	46.55	-3.58	4.69	16.18	-0.69	1.56	12.01	-0.88
	100	16.34	42.26	-1.48	-0.12	46.55	-0.99	3.28	10.90	0.00
	200	19.49	37.48	-0.67	-0.10	76.30	-1.36	1.42	87.15	-1.26
Silt loam (-60 hPa)	50	0.00	39.61	-4.23	0.00	129.78	-8.75	0.00	461.40	-10.13
	100	0.00	29.86	-1.69	0.00	116.20	-4.69	0.00	1156.45	-7.95
Sand (-300 hPa)	50	4.96	-7.89	2.42	-5.36	-0.84	-0.96	-6.56	-13.59	1.23
	100	16.63	-14.18	3.25	2.22	-4.45	0.87	-1.93	-15.56	1.81
	200	22.93	-15.27	2.38	7.91	-10.26	1.45	4.53	-16.83	1.89
Silt loam (-300 hPa)	50	4.94	4.79	0.15	0.02	-0.41	-0.34	1.32	-1.24	0.19
	100	11.24	5.02	2.35	1.95	2.05	-0.01	2.40	-0.73	-0.27
	200	29.35	8.88	1.45	8.16	0.99	0.69	8.53	2.38	0.64
Clay loam (-300 hPa)	50	11.01	5.49	2.02	0.32	-2.34	0.99	1.59	-2.15	1.35
	100	13.30	8.44	1.01	0.01	-1.88	0.42	0.11	-2.33	0.52
	200	13.49	45.03	-4.62	0.00	-16.92	1.29	0.01	15.11	-1.33

Note that positive and negative values define an increase and a decrease after compaction compared to before, respectively. ΔS_e , Δp and $\Delta \sigma'$ represents the ratio of the difference in effective saturation, pore water pressure and effective stress between after and

before compaction to the value before compaction, respectively. A.SL., A.CL., and A.Hs represent after static loading, after cyclic loading and after static loading with vertical holes, respectively.

7.5 Discussion

7.5.1 The effect of loading type on soil deformation for a given compaction level

7.5.1.1 The effect of static loading on time-dependent changes in vertical displacement and pore water pressure

Time dependent processes, such as particle arrangement, breakage of aggregates, chemical bonding and drainage of excess soil water will occur during soil compaction. The intensity of these processes depends on the proportion of soil internal strength to the applied stress. As long as a new equilibrium between the mechanical stress applied and the internal soils strength is still not reached, a further settlement (= strain) occurs, but the strain processes strongly depend on the particle mobility and arrangement during the settlement as well as in water saturated soils each height change coincides with the adequate water loss by drainage. If such a drainage is however prevented by the simultaneously also decreasing hydraulic conductivity, an increasing pore water pressure, starting from the initial values up to even positive values, must be considered as responsible for further internal soil processes. If on the other hand the initially unsaturated soil with air-filled coarse pores is mechanically stressed but remains still unsaturated, even more negative pore water pressure values (= matric potential) can be determined because of newly formed finer but at present still air-filled pores. The disequilibrium results in a redistribution of the actual water and finally results in more negative pore water pressure values (Hartge and Horn 2016; Larson and Gupta, 1980). Once an equilibrium between internal soil strength and the applied stress is achieved, there are no further changes in soil deformation (Horn and Hartge, 1990) and a new equilibrium between applied stress and soil strength is reached, but physical, physico-chemical or biological properties and functions are altered.

During static loading, the vertical displacement in the beginning of stress application can be attributed to the rapid compression of air-filled macropores. Thereafter the vertical

displacement slowed down with increasing loading time for a given applied stress, because the time dependent settlement required time for the rearrangement of particles in a 3 phases system or the hydraulic conductivity dependent drainage off excess soil water if the soil was water saturated during this period. This principle statement was described in Hartge and Horn (2016) and was in agreement with the results by Reszkowska et al. (2011).

The stress induced decrease in pore functionality resulted in the reduction of hydraulic properties and consequently affected the pore water pressure. During static loading, in the case of treatments at -60 hPa, a fast increase in pore water pressure (less negative) was mainly ascribable to an increase in the degree of water saturation due to the preferential reduction of air-filled pores in the beginning of stress application. With increasing the loading time, soil became almost saturated which resulted in higher water flux, and then excess pore water started to be drained off, which can be confirmed by a decrease in volumetric water content after compaction compared to before. Hence, there was a slight decrease in pore water pressure (more negative) during the following of loading time because of excess water drainage. Tang et al. (2009) also found that pore water pressure increased and then decreased with time due to the dissipation process.

In the case of treatments at -300 hPa matric potential, soil compaction only resulted in the loss of air-filled porosity, and no water drainage happened which can be reflected by an increase in volumetric water content after static loading compared to before. Hence, pores filled with water increased during static loading and resulted in an increase in pore water pressure with loading time. This was in agreement with Larson and Gupta (1980). The opposite trend was found in sand soils, because the change in pore water pressure during compaction was also related to change in pore size distribution. Coarser air-filled pores were compressed firstly resulting from static loading, resulting in an increase in the relative volume of smaller pores, and the number of contacts between particles. If a new meniscus formed new contacts in between particles, water was pulled into newly created finer pores, which led to partial drying in other regions. The low hydraulic conductivity and water flux in the soils restricted the rate of water redistribution into these finer pores. Therefore, pore water pressure continuously decreased during static loading, and the hydraulic equilibrium was not achieved at the end of loading. Our results were in agreement with those of Peth et al. (2010), who

stated pore water pressure decreased with time during loading for soils with sand loam to loam texture under 80 kPa.

7.5.1.2 The effect of cyclic loading on time-dependent changes in vertical displacement and pore water pressure

After the 4 hours of static loading, the samples reached a certain equilibrium and the air permeability or gas diffusion declined which was also reported by Zhai and Horn (2018, 2019), and was in agreement with the findings of Keller et al. (2019), Riggert et al. (2019) and Wiermann et al. (1999). However, this equilibrium will be furthermore changed, if shear stresses or cyclic loading events at identical normal stresses are applied. These changes are time dependent as Lipiec et al. (2003) described. They found that vertical deformation was a logarithmic function of the number of passes. Reszkowska et al. (2011) also observed that in the pure cyclic loading test, the settlement was highest during the first loading cycle, and it decreased with increasing number of cycles. Due to rearrangement of soil particles and changes in the spatial distribution of soil water, the highest proportion of the total vertical displacement was obtained after the first loading event. This result was in agreement with the findings of Lipiec et al. (2003), Mordhorst et al. (2012), Reszkowska et al. (2011) and Peth and Horn (2006). A special time-dependent vertical displacement curve occurred for the sand soil at the matric potential of -300 hPa. In the beginning of cycle events (first 34 or 36 cycles) under higher compaction levels and higher soil internal strength resulting from previous static loading led to only a slight decrease in vertical displacement. However, with increasing frequency of loading-unloading cycles, the cumulative effect of cyclic loading on soil deformation was more pronounced and can be explained by a breakage of particle edges and by the spatial rearrangement of soil particles which overall caused a sudden change of vertical deformation in the 35th and 37th cycle event under 100 and 200 kPa. An elastic rebound of vertical displacement during unloading event was observed in our experiment, which was also reported by Reszkowska et al. (2011) and Krümmelbein et al. (2008).

During cyclic loading, the changed pore water pressure due to the height loss can be explained by the combined stress strain and rebound processes, which take place immediately in the samples. Thus, the loading-unloading and rearrangement of particles in dependence of

the actual pore water pressure within the stressed soil induce a higher mobilization of the particles and a weakening of the whole structural system which finally will further collapse at the defined stresses applied. The more this weakening occurs, the higher and longer lasting is the frequency of cyclic loading (Horn, 1976) and the more pore water gets more fluid and causes a more pronounced swelling. These internal processes were also described by Krümmelbein et al. (2009), Fredlund and Rahardjo (1993) and Kézdi and Kinze (1969). Thus, cyclic loading even enhances the increase in pore water pressure (less negative) compared with the static loading. Krümmelbein et al. (2008) described these effects as “water pumping effect under in situ conditions” and the process can be also described as liquefaction (Terzaghi and Jelinek, 1954; Mordhorst et al., 2012; Riggert et al., 2019). Thus, wheeling as a cyclic loading effect must be defined as a combination of static stress application in combination with cyclic loading and shearing because of the particle rearrangement and combined with alterations in pore water pressure in a changing pore system. When the applied stress was removed, water menisci were less curved and thus the shape became more concave, leading to a decrease in pore water pressure (more negative) during unloading. Similar effect was also reported by Peth and Horn (2006), Mordhorst et al. (2012), Reszkowska et al. (2011) and Krümmelbein et al. (2008).

Note also that vertical soil displacement was most pronounced after the first loading-unloading event, but corresponding pore water pressure remained stable in the beginning compared to the following relative changes in pore water pressure caused by successive loading partly due to the tensiometer sensitivity. This result was in agreement with the findings of Peth et al. (2010). They found that the change of pore water pressure became more pronounced with increasing number of loading events, although the soil deformation after the first loading was greatest. For some treatments, time-dependent change in pore water pressure increased with increasing the number of cycles. This possibly suggested that previously air-filled pores were compressed at the beginning of compaction and resulted in a distinct change in vertical displacement followed by a retarded strain when water-filled pores were compressed by the subsequent loading. The longer the loading time, the more time needed for excessive water to drainage or water redistribution to newly formed finer pores out of originally coarser ones. Such changes were also described by Peth et al. (2010) and

Mordhorst et al. (2012).

7.5.1.3 The effect of static loading with vertical holes on time-dependent changes in vertical displacement and pore water pressure

The possibility to ameliorate compressed soils by vertical pores has already been discussed in the past and both the ditch plow approach and the slotting (invented and proofed by Jayawardane and Blackwell (1986)) as well as the review of soil amelioration techniques (Jayawardane and Stewart, 1994) described the positive effect. Previous compaction (static and subsequent cyclic loading) resulted in an increase in soil strength (higher bulk density), which may cause soil becoming more resistant to compaction even during another static loading with artificially vertical holes. These vertical holes remained constant at the identical stresses applied because they were already equilibrated with the major stresses. They were more resistant against vertical stresses which was documented by Zhai and Horn (2018, 2019), Uteau et al. (2013) and Pagenkemper et al. (2014). Hence, vertical holes can be considered as a possibility to even improve the functions of compacted soils, e.g. plow pans concerning better rooting or water infiltration or gas fluxes down to depth.

During static loading, the shape of the time-dependent vertical displacement and pore water pressure curves for a given treatment between before and after having drilled holes was similar, but the extent decreased due to higher internal strength. Noteworthy, in the case of silt loam soil at the matric potential of -60 hPa, previous loading events caused almost fully water saturation, thus the application of subsequent static loading led to a positive pore water pressure. Our data was comparable with those reported by Mordhorst et al. (2012), who observed that substantial high positive pore water pressures (>7 kPa) occurred occasionally in homogenized soils. Seguel and Horn (2005) found that pore water pressure increased to positive values when an external stress > 300 kPa was applied. This situation was more obvious in samples with initial matric potential of -60 hPa than -300 hPa. Nissen (1999) classified the maximum positive pore water pressure values as a function of the aggregate types and reported values up to +70 kPa.

7.5.2 The effect of loading intensity on soil deformation after each stress application

As the compaction levels increased, volumetric water content decreased at higher matric potential (-60 hPa) and increased at lower matric potential (-300 hPa) regardless of stress applications. This result confirmed that there was a decrease in the proportion of larger pores and an increase in the proportion of smaller pores with increasing compaction. Similar observations were reported by Smith et al. (2001), Birle et al. (2008), Hill and Sumner (1967) and Assouline (2006).

Given that the soil sample was restricted by the rigid cylinder wall which resulted in exclusively vertical movements, the change in sample height (i.e. vertical displacement) was directly related to volume change after stress application. Therefore, the corresponding volumetric deformation (a decrease in total porosity and an increase in associated bulk density) took place resulting from soil compaction. For a given treatment, the higher the compaction level, the higher was the soil volumetric deformation or susceptibility to compaction. This was in agreement with the observation of Peng et al. (2004) and Saffih-Hdadi et al. (2009). Therefore, a decrease in total porosity due to soil compaction leads to a change in pore size distribution, which affects the water flow characteristics through the soils. Therefore, higher compaction level tend to have a stronger influence on saturated and unsaturated hydraulic conductivity, which resulted in the more pronounced change in pore water pressure.

7.5.3 What are the consequences on soil strength after each stress application

The effective stress is defined as the force per given area which can stabilize the soil particles against any kind of soil deformation. In the case of treatments at -60 hPa matric potential, lower effective stress was found after each stress application, indicating that the soil strength became weakened to resist the external forces. However, the causes of this situation were different for different textured soils. For coarser-textured soils, soil compaction resulted in vertical displacement, accompanied by an increase in pore water pressure (less negative) and the degree of saturation due to a reduction of pore volume, but the extent of the change in pore water pressure was greater than that in the degree of saturation. Therefore, lower effective stress was found after cyclic loading compared to after static loading. For finer-textured soils, soils were almost saturated before loading, thus there was a minor change in degree of saturation. Therefore, a decrease in effective stress after loading was attributed to

an increase in pore water pressure (less negative). In the case of treatments at -300 hPa, the higher soil's capacity to overcome external stress was observed after each stress application. The reason also depended on pore size distribution and hydraulic properties. For coarser-textured (sand) soils, soil compaction resulted in water redistribution in newly formed finer pores on the expense of coarser air-filled pores, which caused more negative pore water pressure and thus increased effective stress after each stress application. For finer-textured (silt loam and clay loam) soils, although both pore water pressure (less negative) and degree of saturation increased, the extent of change in pore water pressure was lower than that in degree of saturation after compaction compared to before, hence stress applications resulted in soil becoming stronger after compression.

7.6 Conclusions

From our investigations, we can conclude that:

1) The extent of soil deformation on hydraulic properties depend not only on soil internal strength, which is affected by soil texture and initial matric potential, but also on the external stress application (types and magnitude of loading).

2) In the case of static loading, an intensive vertical displacement was observed in the beginning of stress application, and then a constantly slight decline with increasing loading time. Soil mechanical deformation resulted in a decrease or an increase in pore water pressure due to the change in pore functionality and hydraulic properties. In all soil samples stress-induced strain patterns were identical under the same type of loading (static), but in soils with vertical holes smaller additional changes occurred.

3) In the case of subsequent cyclic loading, compaction resulted in the further vertical displacement and pore water pressure increased during loading. A rebound behaviour was observed and pore water pressure decreased during unloading. For a given compaction level, vertical displacement and change in pore water pressure increased with increasing the frequency of loading.

4) For a given stress application, the vertical displacement increased with applied stresses, which resulted in the higher extent of water flux, and finally more pronounced changes in pore water pressure were observed under higher compaction level.

5) After each stress application, soils became either weaker for treatments at -60 hPa matric potential or even stronger for treatments at -300 hPa matric potential, which were reflected by effective stress.

7.7 Acknowledgement

This study was supported by the State Scholarship Fund from the China Scholarship Council (CSC) for Xiafei Zhai (No.201406300027).

7.8 References

- Alaoui, A., Lipiec, J., Gerke, H.H., 2011. A review of the changes in the soil pore system due to soil deformation: A hydrodynamic perspective. *Soil Till. Res.* 115-116, 1-15.
- Assouline, S., 2006. Modeling the relationship between soil bulk density and the hydraulic conductivity function. *Vadose Zone J.* 5, 697-705.
- Baumgarten, W., Horn, R., 2013. Assessing soil degradation by using a scale-spanning soil mechanical approach: A review. *Advances in Geocology*, Catena Verlag.
- Baumgartl, T., Winkelmann, P., Gräsle, W., Richards, B.G., Horn, R., 1995. Measurement of the interaction of soil mechanical properties and hydraulic processes with a modified triaxial test. The 1st International Conference on unsaturated soils. Paris.
- Birle, E., Heyer, D., Vogt, N., 2008. Influence of the initial water content and dry density on the soil-water retention curve and the shrinkage behavior of a compacted clay. *Acta Geotechnica* 3, 191-200.
- Bishop, A.W., 1959. The principle of effective stress. *Teknisk Ukeblad* 106 (39), 859-863.
- Carman, P.C., 1938. The determination of the specific surface of powders. *J. Soc. Chem. Ind. Trans.* 57, 225.
- Carman, P.C., 1956. *Flow of gases through porous media*, Butterworths Scientific Publications, London.
- Destain, M.-F., Roisin, C., Dalcq, A.-S., Mercatoris, B.C.N., 2016. Effect of wheel traffic on the physical properties of a Luvisol. *Geoderma* 262, 276-284.
- Dexter, A.R., 2004. Soil physical quality Part I. Theory, effects of soil texture, density, and organic matter, and effects on root growth. *Geoderma* 120, 201-214.

7 INFLUENCE OF STATIC AND CYCLIC LOADING ON MECHANICAL AND HYDRAULIC PROPERTIES
OF SOILS WITH DIFFERENT TEXTURES AND MATRIC POTENTIALS

- Dörner, J., Dec, D., Feest, E., Vasquez, N., Diaz, M., 2012. Dynamics of soil structure and pore functions of a volcanic ash soil under tillage. *Soil Till. Res.* 125, 52-60.
- Dörner, J., Dec, D., Peng, X., Horn, R., 2010. Effect of land use change on the dynamic behaviour of structural properties of an Andisol in southern Chile under saturated and unsaturated hydraulic conditions. *Geoderma* 159, 189-197.
- Drewry, J.J., Paton, R.J., 2005. Soil physical quality under cattle grazing of a winter-fed brassica crop. *Aust. J. Soil Res.* 43 (4), 525-531.
- Fredlund, D.G., Rahardjo, H., 1993. *Soil Mechanics for Unsaturated Soils*. John Wiley and Sons, New York.
- Gräsle, W., Richards, B.G., Baumgartl, T., Horn, R., 1995. Interaction between soil mechanical properties of structured soils and hydraulic processes: Theoretical fundamentals of a model. 719-725, in: Alonso.E.E. and P.Delage (eds.) *Unsaturated soils*. Balkema Verlag.
- Green, T.R., Ahuja, L.R., Benjamin, J.G., 2003. Advances and challenges in predicting agricultural management effects on soil hydraulic properties. *Geoderma* 116, 3-27.
- Greenwood, K.L., McKenzie, B.M., 2001. Grazing effects on soil physical properties and the consequences for pastures: a review. *Aust. J. Exp. Agric.* 41, 1231-1250.
- Gubiani, P.I., Pértile, P., Reichert, J.M., 2018. Relationship of precompression stress with elasticity and plasticity indexes from uniaxial cyclic loading test.
- Hamza, M.A., Anderson, W.K., 2005. Soil compaction in cropping systems: A review of the nature, causes and possible solutions. *Soil Tillage Res.* 82 (2), 121-145.
- Hartge, K.H., Horn, R., 2016. *Essential Soil Physics, An Introduction to Soil Processes, Functions, Structure and Mechanics*. Schweizerbart Science Publishers.
- Hill, J.N.S., Sumner, M.E., 1967. Effect of bulk density on moisture characteristics of soils. *Soil Sci.* 103, 234-238.
- Horn, R., 1976. Mechanical strength changes due to aggregate formation of a mesocoic clay (in German, PHD Thesis). *Festigkeitsänderungen infolge von Aggregierungsprozessen eines mesozoischen Tones*, Diss. TU Hannover.
- Horn, R., 2003. Stress-strain effects in structured unsaturated soils on coupled mechanical and hydraulic processes. *Geoderma* 116, 77-88.
- Horn, R., 2004. Time dependence of soil mechanical properties and pore functions for arable soils. *Soil*

7 INFLUENCE OF STATIC AND CYCLIC LOADING ON MECHANICAL AND HYDRAULIC PROPERTIES
OF SOILS WITH DIFFERENT TEXTURES AND MATRIC POTENTIALS

- Sci. Soc. Am. J. 68, 1131-1137.
- Horn, R., Fleige, H., 2003. A method for assessing the impact of load on mechanical stability and on physical properties of soils. *Soil Tillage Res.* 73 (1-2), 89-99.
- Horn, R., Hartge, K.H., 1990. Effects of short-time loading on soil deformation and strength of an ameliorated Typic Paleustalf. *Soil Tillage Res.* 15, 247-256.
- Horn, R., Holthusen, D., Dörner, L., Mordhorst, A., Fleige, H., 2019. Research Innovations in Soil Physics-what do we need to know and where to head for a sustainable environment. *Soil Tillage Res.* Under review.
- Horn, R., Smucker, A., 2005. Structure formation and its consequences for gas and water transport in unsaturated arable and forest soils. *Soil Till. Res.* 82, 5-14.
- Horn, R., van den Akker, J.J.H., Arvidsson, J., 2000. *Subsoil Compaction-Distribution, Processes and Consequences.* Catena Verlag.
- Horn, R., Way, T., Rostek, J., 2003. Effect of repeated tractor wheeling on stress/strain properties and consequences on physical properties in structured arable soils. *Soil Till. Res.* 73, 101-106.
- Horton, R., Ankeny, M.D., Allmaras, R.R., 1994. Effects of Compaction on Soil Hydraulic Properties. *Developments in Agricultural Engineering* 11, 141-165.
- Jayawardane, N.S., Blackwell, J., 1986. Effects of gypsum-slotting on infiltration rates and moisture storage in a swelling clay soil. *Soil Use Manage.* 2, 114-118.
- Jayawardane, N.S., Stewart, B.A., 1994. *Subsoil Management Techniques.* Lewis Publishers, Boca Raton.
- Keller, T., Lamandé, M., Peth, S., Berli, M., Delenne, J.-Y., Baumgarten, W., Rabbel, W., Radjaï, F., Rajchenbach, J., Selvadurai, A.P.S., Or, D., 2013. An interdisciplinary approach towards improved understanding of soil deformation during compaction. *Soil Tillage Res.* 128, 61-80.
- Keller, T., Sandin, M., Colombi, T., Horn, R., Or, D., 2019. Historical evolution of soil stress levels and consequences for soil functioning. *Soil Tillage Res.* Submitted.
- Kézdi, Á., Kinze, W., 1969. *Handbuch der Bodenmechanik.* Bd. 1. Bodenphysik. Akadémiai Kiadó .
- Kozeny, J., 1927. Ueber kapillare Leitung des Wassers im Boden. *Sitzungsberichte Wiener Akademie* 136 (2a), 271-306.
- Krümmelbein, J., Peth, S., Horn, R., 2008. Determination of pre-compression stress of a variously grazed steppe soil under static and cyclic loading. *Soil Tillage Res.* 99 (2), 139-148.

7 INFLUENCE OF STATIC AND CYCLIC LOADING ON MECHANICAL AND HYDRAULIC PROPERTIES
OF SOILS WITH DIFFERENT TEXTURES AND MATRIC POTENTIALS

- Krümmelbein, J., Peth, S., Zhao, Y., Horn, R., 2009. Grazing-induced alterations of soil hydraulic properties and functions in Inner Mongolia, P.R. China. *J. Plant Nutr. Soil Sci.* 172, 769-777.
- Krümmelbein, J., Wang, Z., Zhao, Y., Peth, S., Horn, R., 2006. Influence of various grazing intensities on soil stability, soil structure and water balance of grassland soils in Inner Mongolia, P.R. China. *Advances in GeoEcology.* 38, 93-101.
- Larson, W.E., Gupta, S.C., 1980. Estimating critical stresses in unsaturated soils from changes in pore water pressure during confined compression. *Soil Sci. Soc. Am. J.* 44, 1127-1132.
- Lebert, M., Horn, R., 1991. A method to predict the mechanical strength of agricultural soils. *Soil Tillage Res.* 19, 275-286.
- Lipiec, J., Arvidsson, J., Murer, E., 2003. Review of modelling crop growth, movement of water and chemicals in relation to topsoil and subsoil compaction. *Soil Till. Res.* 73, 15-29.
- Martinez, L.J., Zinck, J.A., 2004. Temporal variation of soil compaction and deterioration of soil quality in pasture areas of Colombian Amazonia. *Soil Tillage Res.* 75, 3-17.
- Mentges, M.I., Reichert, J.M., Rodrigues, M.F., Awe, G.O., Mentges, L.R., 2016. Capacity and intensity soil aeration properties affected by granulometry, moisture, and structure in no-tillage soils. *Geoderma* 263, 47-59.
- Mordhorst, A., Zimmermann, I., Peth, S., Horn, R., 2012. Effect of hydraulic and mechanical stresses on cyclic deformation processes of a structured and homogenized silty Luvisol Chernozem. *Soil Tillage Res.* 125, 3-13.
- Naveed, M., Per Schjønning, Keller, T., de Jonge, L. W., Per Moldrup, Lamandé, M., 2016. Quantifying vertical stress transmission and compaction-induced soil structure using sensor mat and X-ray computed tomography. *Soil Tillage Res.* 158, 110-122.
- Nissen, B. 1999. Vorhersage der mechanischen Belastbarkeit von repräsentativen Ackerböden der Bundesrepublik Deutschland-bodenphysikalischer Ansatz. PHD Thesis (Vol. 50). Schriftenreihe des Instituts für Pflanzenernährung und Bodenkunde, CAU Kiel.
- Pagenkemper, S.K., Uteau, D., Peth, S., Horn, R., 2014. Investigation of time dependent development of soil structure and formation of macropore networks as affected by various precrop species. *J. Soil Water Conserv.* 2, 51-66.
- Peng, X., Horn, R., Zhang, B., Zhao, Q.G., 2004. Mechanisms of soil vulnerability to compaction of homogenized and recompacted Ultisols. *Soil Tillage Res.* 76 (2), 125-137.

7 INFLUENCE OF STATIC AND CYCLIC LOADING ON MECHANICAL AND HYDRAULIC PROPERTIES
OF SOILS WITH DIFFERENT TEXTURES AND MATRIC POTENTIALS

- Peth, S., Horn, R., 2006. The mechanical behaviour of structured and homogenized soil under repeated loading. *J. Plant Nutr. Soil Sci.* 169, 401-410.
- Peth, S., Rostek, J., Zink, A., Mordhorst, A., Horn, R., 2010. Soil testing of dynamic deformation processes of arable soils. *Soil Tillage Res.* 106 (2), 317-328.
- Pietola, L., R. Horn, and M. Yli-Halla. 2005. Effects of trampling by cattle on the hydraulic and mechanical properties of soil. *Soil Tillage Res.* 82, 99-108.
- Plagge, R., Renger, M., Röth, C.H., 1990. A new laboratory method to quickly determine the unsaturated hydraulic conductivity of undisturbed soil cores within a wide range of textures. *J. Plant Nutr. Soil Sci.* 153, 39-45.
- Reicosky, D.C., Voorhees, W.B., Radke, J.K., 1981. Unsaturated water flow through a simulated wheel track. *Soil Sci. Soc. Am. J.* 45, 3-8.
- Reszkowska, A., Peth, S., Peng, X., Horn, R., 2011. Grazing Effects on Compressibility of Kastanozems in Inner Mongolian Steppe Ecosystem. *Soil Sci. Soc. Am. J.* 75(2), 426-433.
- Richard, G., Boizard, H., Roger-Estrade, J., Boiffin, J., Guérif, J., 1999. Field study of soil compaction due to traffic in northern France: pore space and morphological analysis of the compacted zones. *Soil Tillage Res.* 51 (1-2), 151-160.
- Richard, G., Cousin, I., Sillon, J. F., Bruand, A., Guerif, J., 2001. Effect of compaction on the porosity of a silty soil: Influence on unsaturated hydraulic properties. *Eur. J. Soil Sci.* 52, 49-58.
- Riggert, R., Fleige, H., Horn, R., 2019. Soil degradation caused by forestry machinery-an assessment scheme for soil ecology and trafficability of skid trails. *Soil Sci.Soc.Amer.J.* In press.
- Saffih-Hdadi, K., Défossez, P., Richard, G., Cui, Y.-J., Tang, A.-M., Chaplain, V., 2009. A method for predicting soil susceptibility to the compaction of surface layers as a function of water content and bulk density. *Soil Tillage Res.* 105 (1), 96-103.
- Semmel, H., 1993. Auswirkungen kontrollierter Bodenbelastungen auf das Druckfortpflanzungsverhalten und physikalisch-mechanische Kenngrößen von Ackerböden
Dissertation, Institut für Pflanzenernährung und Bodenkunde.
- Smith, C.W., Johnston, M.A., Lorentz, S.A., 2001. The effect of soil compaction on the water retention characteristics of soils in forest plantations. *S. Afr. J. Plant Soil* 18(3), 87-97.
- Stange, C.F., Horn, R., 2005. Modeling the Soil Water Retention Curve for Conditions of Variable Porosity. *Vadose Zone J.* 4, 602-613.

7 INFLUENCE OF STATIC AND CYCLIC LOADING ON MECHANICAL AND HYDRAULIC PROPERTIES
OF SOILS WITH DIFFERENT TEXTURES AND MATRIC POTENTIALS

- Tang, A.M., Cui, Y.J., Eslami, J., Défossez, P., 2009. Analysing the form of the confined uniaxial compression curve of various soils. *Geoderma* 148, 282-290.
- Terzaghi, K., Jelinek, R., 1954. *Theoretische Bodenmechanik*. Springer-Verlag, Berlin.
- Uteau, D., Pagenkemper, S.K., Peth, S., Horn, R., 2013. Root and time dependent soil structure formation and its influence on gas transport in the subsoil. *Soil Till. Res.* 132, 69-76.
- van Genuchten, M. T., 1980. A closed-form equation for predicting the hydraulic conductivity of unsaturated soils, *Soil Sci. Soc. Am. J.*, 44, 892-898.
- Wiermann, C., Way, T.R., Horn, R., Bailey, A.C., Burt, E.C., 1999. Effect of various dynamic loads on stress and strain behavior of a Norfolk sandy loam. *Soil Till. Res.* 50, 127-135.
- Zapf, R., 1997. *Mechanische Bodenbelastung durch die landwirtschaftliche Pflanzenproduktion in Bayern*. BLBP, Freising, Germany.
- Zhai, X., Horn, R., 2018. Effect of static and cyclic loading including spatial variation caused by vertical holes on changes in soil aeration. *Soil Tillage Res.* 177, 61-67.
- Zhai, X., Horn, R., 2019. Dynamics of pore functions and gas transport parameters in artificially ameliorated soils due to static and cyclic loading. *Geoderma* 337, 300-310.

8 GENERAL DISCUSSION

8.1 The effect of static loading on soil physical properties

In order to the better understanding of the effects of soil compaction on soil properties and functions, some terms should be defined first. Capacity parameters such as total porosity, air-filled porosity and total pore size distribution are defined as basic soil properties, ignoring soil internal structure and functions, while intensity parameters (i.e. pore continuity and pore tortuosity) quantify soil functions and reflect the dynamic reactions or processes over time and space (Horn and Kutilek, 2009). Generally, each stress application results in changes of capacity and intensity properties due to possible soil pore and structure rearrangement.

For a given treatment, soil deformation depends on the external loading including the intensity and duration of loading. Soil deformation resulting from external forces can lead to serious disturbance of the pore system, both with respect to pore size distribution, average pore diameter, the total number of pores and their functions. If the external pressure exceeds the maximum internal soil strength, firstly the inter-aggregate pore space will be destroyed, while the intra-aggregate pore space remains constant (Horn et al., 1995). Macropores include biopores, shrinkage cracks, other interaggregate pores, and the largest pores within aggregates and peds. These pores are very sensitive to compaction. They are the least stable of all pore size classes, and collapse when they experience stresses higher than the internal soil strength. Therefore, soil compaction when ignoring the shearing effects results in a significant decrease in total porosity primarily caused by the reduction of macropores (Blume et al., 2016; Horn et al., 1995). In our study, if we only consider the effect of static loading on capacity values, both total porosity and air-filled porosity decreased significantly after static loading compared to before, and the extent of reduction increased with increasing the compaction levels.

In term of intensity parameters, pore continuity index (C_2) is defined as the ratio of air permeability (K_a) to air-filled porosity (ϵ_a). The values of C_2 are mostly used as an indicator for similar pore size distributions and pore continuities (Groenevelt et al., 1984; Uteau et al., 2013). Pore tortuosity (τ) reflects the relationship between the length of the average gas transport path and the length of the soil sample. At a given soil sample length, the more

tortuous gas pathways, the higher values of τ are. Low values of intensity properties indicate either that the soil pores are poorly connected or that the soil pores may be well connected but small, both resulting in restricted gas transport. After static loading, the value of C_2 increased for treatments at higher matric potential (-60 hPa), because higher initial water content facilitated the loss of soil water due to drainage during static loading which caused more continuous air-filled pores and then an increase in C_2 . However, the value of C_2 decreased for treatments at more negative matric potential (-300 hPa) after static loading, which was probably related to the reduction of the total volume of soil pores. Ball et al. (1988) found that at -60 hPa matric potential, the pore continuity index decreased in direct drilled clay loam soil after one pass of an unladen tractor applied. Munkholm et al. (2002) observed that at the matric potential of -30 and -100 hPa, pore continuity index decreased significantly after compaction with a 6-8 t tractor, which indicated a relatively poorer continuity of macropores in the compacted soil. However, the experimental data of the effect of compaction on pore tortuosity have yet rarely been documented. In our experiment, a decrease in the value of τ was observed due to the reduction of the water blockage effect after static loading.

For treatments without artificially vertical holes, air-filled porosity is the main determinant factor affecting gas transport. As ϵ_a decreased after static loading, lower K_a and D_s/D_o values were observed. A positive linear log-log relationship between ϵ_a and K_a in all samples was found before having drilled vertical holes. Berisso et al. (2013) found that at three different matric potential and at four different depths, there was a strong positive linear log-log relationship between K_a and ϵ_a in the control and compacted blocks. This result was also supported by Schjønning et al. (2002), Ball et al. (1988) and Dörner and Horn (2006). Both positive linear and exponential relationships between ϵ_a and D_s/D_o were also found in our study. Kuncoro et al. (2014) noticed that the observed decrease in D_s/D_o was reasonably attributed to the reduced values of ϵ_a after compaction. Similar observations were reported in Deepagoda et al. (2011), Hamamoto et al. (2009) and Moldrup et al. (2000).

Besides the volume of macropores, gas transport properties are also controlled by the intensity values (i.e. the quality of air-filled pores). For most of treatments, values of K_a decreased as values of C_2 decreased after static loading. Lower C_2 values indicate that there are less active air-filled pores in soils, which results in restricted air flow. However, this

general statement is not completely true. For coarser-textured soil at less negative matric potential, values of C_2 increased after static loading which was not accompanied by higher values of K_a . This situation was mainly attributable to the reduced values of ε_a . Mentges et al. (2016) found that compared to clayey soils, K_a in sandy soils mostly depends on the volume of macropores, but less correlated with pore continuity. This was in agreement with our findings.

Theoretically, lower τ values indicate the existence of less tortuous pathways for gas transport, thus favoring higher D_s/D_o values. Therefore, for a given stress application, the negative relationship between D_s/D_o and τ was observed after static loading for all treatments, that is, the D_s/D_o values were higher with lower τ values. Papendick and Runkles (1965) observed that at the same ε_a , values of D_s/D_o in wet media were lower than in dry media, due to the increased tortuosity for gas transport. However, for a given treatment, we found that a lower τ value was not always accompanied by a higher D_s/D_o value. For example, for clay loam soil at -300 hPa matric potential, the values of D_s/D_o decreased, even though the lower values of τ was observed after static loading. This might be because the extent of the reduction of ε_a was higher than the reduction of τ , indicating that the number of active air-filled pores increased, but the volume of these pores was smaller after static loading, leading to a decrease in D_s/D_o .

The extent of how far stress application results in a decrease in total pore volume and the alteration of pore size distribution, shape, continuity and tortuosity of soil pores depends not only on the internal soil strength but also on the possible changes with time. Time dependent processes, such as particle arrangement, breakage of aggregates and chemical bonding and drainage of excess soil water will occur during soil compaction. The intensity of these processes depends on the proportion of soil internal strength to the applied stress. Once an equilibrium between soil internal strength and the applied stress is achieved, there is no further changes in soil deformation (Horn and Hartge, 1990). In our study, we found that during static loading an intensive vertical displacement was observed in the beginning of stress application, which was probably caused by the compression of air-filled macropores firstly under compaction, while the vertical displacement tended to be a constantly slight decrease with increasing loading time, because it required time for the rearrangement of

particles or the hydraulic conductivity dependent drainage off the excess soil water when the soil was saturated during this period. This situation was also described by Hartge and Horn (2016) and Reszkowka et al. (2011).

Soil compaction leads to not only soil structural deformation, but also changes in soil hydraulic properties during stress application. Pore water pressure, expressed as matric potential, is the result of changes in soil structure and soil water retention (Larson and Gupta, 1980). Therefore, pore water pressure reflects dynamically the interactive effects of soil structure and water movement as a function of external stress (Peng et al., 2004). During static loading, the time-dependent change in pore water pressure depends on soil texture and initial matric potential. In the case of treatments at the matric potential of -60 hPa, for coarser-textured soils, a fast increase in pore water pressure was mainly ascribable to an increase in the degree of water saturation due to the preferential reduction of air-filled pores in the beginning of stress application, which was accompanied by an intensive vertical displacement. Then, as bulk density increased, an equilibrium between soil internal strength and the applied stress was reached. Therefore, there was no change in pore water pressure during the last of loading time. For the finer-textured soils, a remarkable increase in pore water pressure was observed in the beginning. As the time of loading increased, soil became almost saturated which resulted in higher water flux, and then this peak was followed by a fast decrease due to the dissipation of excess water. Thereafter, a slight decrease in pore water pressure was detected due to lower hydraulic conductivity. In the case of treatments at the matric potential of -300 hPa, soil compaction only resulted in the loss of air-filled pores and no water drainage took place but especially in the coarser-textured soils, air-filled macropores decreased with a simultaneous increase in the number of contacts between soil particles after compaction, and caused additional water menisci newly formed in these finer pores which were still air-filled. Therefore, a decrease in pore water pressure (i.e. more negative) was observed during static loading. For the finer-textured soils, compaction caused a substantial loss of air-filled macropores, and water-filled pores increased due to only a minor dissipation of soil water, which resulted in a constantly increase in pore water pressure up to positive and longlasting values during compaction.

8.2 The effect of the further cyclic loading on soil physical properties

Gas transport parameters are good indicators for identifying soil pore characteristics (Granovsky and McCoy, 1997; Moldrup et al., 2003; Iversen et al., 2001), and soil pore functions in turn affects significantly soil aeration (Schjønning et al., 2002; Deepagoda et al., 2011; Mentges et al., 2016). Air permeability (K_a) is a key parameter representing soil structure and pore network characteristics, which is influenced by soil pore size distribution and the continuity of macropores. Relative gas diffusivity (D_s/D_o) is another important gas transport parameter representing pore tortuosity and connectivity, which is also controlled by the volume of air-filled pore space. Hence, the reduction of values of gas transport parameters after static loading was accompanied by the deterioration of soil pore functions.

Once compacted, soils are assumed to react relatively resistant to further compaction because of the increased proportion of contact points and finer pores at the expense of macropores (Cambi et al., 2015). Although the volume of macropores decreased after the further cyclic loading, the quality of air-filled pores was improved (i.e. an increase in C_2 and a decrease in τ), because the further reduction of soil water content caused less bottle-necks formed by water menisci in the pore system after the further cyclic loading. A combined effect of air-filled porosity (as a capacity indicator) and pore continuity/tortuosity (as an intensity indicator) balanced gas transport properties. Therefore, there was a minor effect of the further cyclic loading on gas transport. Our results are therefore amongst others in agreement with those of Blackwell et al. (1990). They reported that air permeability was greatly reduced by a single trafficking pass, and that further passes of trafficking also decreased air permeability, but in a much smaller magnitude.

Frequency of loading plays an important role in soil deformation. During cyclic loading, soil deformation increased with the number of cycles. This result was in agreement with the findings of Lipiec et al (2003). They found that vertical deformation was a logarithmic function of the number of passes. Only the first loading event had a significant effect on changes in soil stress state, due to the soil strength increase due to the first loading event. This resulted in the highest irreversible changes in soil volume and soil structure, and then a significant deformation occurred, but the following cyclic loading still causes a rearrangement

of particles and changes in the spatial water distribution even if the further deformation is less pronounced. This result was in agreement with the findings of Lipiec et al. (2003), Mordhorst et al. (2012), Reszkowska et al. (2011) and Peth and Horn (2006).

Vertical displacement increased during loading and decreased during unloading (an elastic rebound) in one cycle event. This rebound can be used to quantify the ability of the recovery of the soil pore structure after mechanical disturbance (Zhang et al., 2005). Soil mechanical deformation resulted in changes in hydraulic properties, that is, pore water pressure increased during loading and decreased during unloading. Krümmelbein et al. (2008) described these effects as “water pumping effect under in situ conditions” and the process can be also described as liquefaction (Terzaghi and Jelinek, 1954; Mordhorst et al., 2012; Riggert et al., 2019).

During subsequent cyclic loading, the loading-unloading events induced a higher mobilization and rearrangement of the particles, more excess water drainage off and the more weakening of the whole structural system at a given stress applied. Thus, cyclic loading further resulted in a decrease in pore water pressure (more negative) for sand soil at -300 hPa matric potential, and an increase in pore water pressure (less negative) for other treatments compared to static loading.

8.3 The effect of soil structure (artificially vertical holes) on soil physical properties

The possibility to ameliorate compressed soils by vertical pores has already been discussed before. Both the ditch plow approach and the slotting were invented and proofed by Jayawardane and Blackwell (1986). Jayawardane and Stewart (1994) also described the positive effect of this soil amelioration technique. In our study, we found that there was a minor effect of vertical holes on the volume of macropores (ϵ_a), because the volume of holes (0.40 cm^3) only accounts for 0.2% of the total volume. However, the quality of air-filled pores was improved significantly (an increase in C_2 and a decrease in τ). Based on these limits proposed in Reszkowska et al. (2011), pore continuity index (C_2) varied from very low and low to very high for all treatments with vertical holes. The existence of five continuous, non-tortuous and non-constricted holes also resulted in the reduction of τ by 2.77-75.38%,

particularly for treatments at wet condition (-60 hPa).

Because pore functions were obviously ameliorated by soil structure (artificially vertical holes), gas transport parameters were also enhanced. For a given treatment, even though only a slight increase in ε_a occurred after having drilled vertical holes, K_a significantly increased up to more than one order of magnitude, which was strongly correlated with the significant increase in the pore continuity compared to without vertical holes. This was in agreement with the findings of Mentges et al. (2016), Kuncoro et al. (2014) and Moldrup et al. (2001). A poor correlation between ε_a and K_a in all samples after having drilled vertical holes further confirmed the fact that the value of air permeability is controlled by both the amount of air-filled pores and its configuration. The values of D_s/D_o with vertical holes also increased which was attributed to the decrease in the pore tortuosity compared to without holes. This can be confirmed by Deepagoda et al. (2011).

At a similar air-filled porosity, the average pore diameter was much larger after having drilled vertical holes than before. Air permeability is more dependent than gas diffusion on the radius, length and continuity of the largest pores in the sample and it is less dependent on total air-filled porosity, which is in agreement with the findings of Ball et al. (1988). Since air permeability depends on the fourth power of pore radius and gas diffusion on the square of pore radius, the vertical holes contribute much more to the magnitude of K_a than to the magnitude of D_s/D_o .

When unsaturated soils are compressed, compaction affects porosity and related physical properties such as mechanical properties, and gas and water transport. For most soils, compaction reduces the volume of large pores and consequently affects water retention properties and hydraulic conductivity. After static loading, compaction resulted in the reduction of ε_a , and then lead to restricted gas transport for a given treatment, because air-filled porosity was the main determinant factor affecting soil aeration. The preferential gas flow through macropore networks was rather dominant for mass flow. Artificial vertical pores also reduced water blockage effects. Therefore, there were minor differences in values of K_a among the different treatments, but distinct differences in values of D_s/D_o were observed because it was determined by the total air-filled porosity.

Previous compaction (static and cyclic loading) resulted in an increase in soil strength

(higher bulk density) which may cause soil becoming stronger enough to withstand the applied stress without further failure during another static loading. With the same type of loading (static), a similar trend in vertical displacement and pore water pressure after having drilled vertical holes was found compared to before, but the extent of soil deformation decreased.

8.4 References

- Ball, B.C., O'Sullivan, M.F., Hunter, R., 1988. Gas diffusion, fluid flow and derived pore continuity indices in relation to vehicle traffic and tillage. *J. Soil Sci.* 39, 327-339.
- Berisso, F.E., Schjønning, P., Keller, T., Lamandé, M., Simojoki, A., Iversen, B.V., Alakukku, L., Forkman, J., 2013. Gas transport and subsoil pore characteristics: anisotropy and long-term effects of compaction. *Geoderma* 195-196, 184-191.
- Blackwell, P.S., Ringrose-Voase, A.F., Jayawardane, N.S., Olsson, K.A., McKenzie, D.C., Mason, W.K., 1990. The use of air-filled porosity and intrinsic permeability to characterize macropore structure and saturated hydraulic conductivity of clay soils. *J. Soil Sci.* 41, 215-228.
- Blume, H.P., Brümmer, G.W., Fleige, H., Horn, R., Kandeler, E., Kögel-Knabner, I., Kretschmar, R., Stahr, K., Wilke, B.M., 2016. *Scheffer/Schachtschabel Soil Science*. Springer.
- Cambi, M., Certini, G., Neri, F., Marchi, E., 2015. The impact of heavy traffic on forest soils: A review. *Forest Ecology and Management*, 338, 124-138.
- Deepagoda, T.K.K.C., Moldrup, P., Schjønning, P., De Jonge, L.W., Kawamoto, K., Komatsu, T., 2011. Density-corrected models for gas diffusivity and air permeability in unsaturated soil. *Vadose Zone J.* 10, 226-238.
- Dörner, J., Horn, R., 2006. Anisotropy of pore functions in structured Stagnic Luvisols in the Weichselian moraine region in N Germany. *J. Plant Nutr. Soil Sci.* 169 (2), 213-220.
- Granovsky, A.V., McCoy, E.L., 1997. Air flow measurements to describe field variation in porosity and permeability of soil macropores. *Soil Sci. Soc. Am. J.* 61, 1569-1576.
- Groenevelt, P.H., KAY, B.D., Grant, C.D., 1984. Physical assessment of soil with respect to rooting potential. *Geoderma*, 34, 101-114.
- Hamamoto, S., Moldrup, P., Kawamoto, K., Komatsu, T., 2009. Effect of particle size and soil compaction on gas transport parameters in variably saturated, sandy soils. *Vadose Zone J.* 8 (4),

- 986-995.
- Hartge, K.H., Horn, R., 2016. *Essential Soil Physics, An Introduction to Soil Processes, Functions, Structure and Mechanics*. Schweizerbart Science Publishers.
- Horn, R., Hartge, K.H., 1990. Effects of short-time loading on soil deformation and strength of an ameliorated Typic Paleustalf. *Soil Tillage Res.* 15, 247-256.
- Horn, R., Domżzał, H., Słowińska-Jurkiewicz, A., van Ouwerkerk, C., 1995. Soil compaction processes and their effects on the structure of arable soils and the environment. *Soil Tillage Res.* 35 (1-2), 23-36.
- Horn, R., Kutilek, M., 2009. Editorial: the intensity-capacity concept-How far is it possible to predict intensity values with capacity parameters. *Soil Tillage Res.* 103, 1-3.
- Iversen, B.V., Moldrup, P., Schjønning, P., Loll, P., 2001. Air and water permeability in differently textured soils at two measurement scales. *Soil Sc.* 166(10), 643-659.
- Jayawardane, N.S., Blackwell, J., 1986. Effects of gypsum-slotting on infiltration rates and moisture storage in a swelling clay soil. *Soil Use Manage.* 2, 114-118.
- Jayawardane, N.S., Stewart, B.A., 1994. *Subsoil Management Techniques*. Lewis Publishers, Boca Raton.
- Krümmlbein, J., Peth, S., Horn, R., 2008. Determination of pre-compression stress of a variously grazed steppe soil under static and cyclic loading. *Soil Tillage Res.* 99 (2), 139-148.
- Kuncoro, P.H., Koga, K., Satta, N., Muto, Y., 2014. A study on the effect of compaction on transport properties of soil gas and water I: relative gas diffusivity, air permeability, and saturated hydraulic conductivity. *Soil Tillage Res.* 143, 172-179.
- Larson, W.E., Gupta, S.C., 1980. Estimating critical stresses in unsaturated soils from changes in pore water pressure during confined compression. *Soil Sci. Soc. Am. J.* 44, 1127-1132.
- Lipiec, J., Arvidsson, J., Murer, E., 2003. Review of modelling crop growth, movement of water and chemicals in relation to topsoil and subsoil compaction. *Soil Tillage Res.* 73, 15-29.
- Mentges, M.I., Reichert, J.M., Rodrigues, M.F., Awe, G.O., Mentges, L.R., 2016. Capacity and intensity soil aeration properties affected by granulometry, moisture, and structure in no-tillage soils. *Geoderma* 263, 47-59.
- Moldrup, P., Olesen, T., Komatsu, T., Schjønning, P., Rolston, D.E., 2001. Tortuosity, diffusivity, and permeability in the soil liquid and gaseous phases. *Soil Sci. Soc. Am. J.* 65, 613-623.

- Moldrup, P., Olesen, T., Schjønning, P., Yamaguchi, T., Rolston, D.E., 2000. Predicting the gas diffusion coefficient in undisturbed soil from soil water characteristics. *Soil Sci. Soc. Am. J.* 64, 1588-1594.
- Moldrup, P., Yoshikawa, S., Olesen, T., Komatsu, T., Rolston, D.E., 2003. Air permeability in undisturbed volcanic ash soil: Predictive model test and soil structure finger print. *Soil Sci. Soc. Am. J.* 67, 32-40.
- Mordhorst, A., Zimmermann, I., Peth, S., Horn, R., 2012. Effect of hydraulic and mechanical stresses on cyclic deformation processes of a structured and homogenized silty Luvisol Chernozem. *Soil Tillage Res.* 125, 3-13.
- Munkholm, L.J., Schjønning, P., Kay, B.D., 2002. Tensile strength of soil cores in relation to aggregate strength, soil fragmentation and pore characteristics. *Soil Tillage Res.* 64, 125-135.
- Papendick, R.L., Runkles, J.R., 1965. Transient-state oxygen diffusion in soil: I. The case where rate of oxygen consumption is constant. *Soil Sci.* 100, 251-261.
- Peng, X., Horn, R., Zhang, B., Zhao, Q.G., 2004. Mechanisms of soil vulnerability to compaction of homogenized and recompacted Ultisols. *Soil Tillage Res.* 76 (2), 125-137.
- Peth, S., Horn, R., 2006. The mechanical behaviour of structured and homogenized soil under repeated loading. *J. Plant Nutr. Soil Sci.* 169, 401-410.
- Reszkowska, A., Peth, S., Peng, X., Horn, R., 2011. Grazing Effects on Compressibility of Kastanozems in Inner Mongolian Steppe Ecosystem. *Soil Sci. Soc. Am. J.* 75(2), 426-433.
- Riggert, R., Fleige, H., Horn, R., 2019. Soil degradation caused by forestry machinery-an assessment scheme for soil ecology and trafficability of skid trails. *Soil Sci. Soc. Am. J.* In press.
- Schjønning, P., Munkholm, L.J., Moldrup, P., Jacobsen, O.H., 2002. Modelling soil pore characteristics from measurements of air exchange: the long-term effects of fertilization and crop rotation. *Eur. J. Soil Sci.* 53 (2), 331-339.
- Terzaghi, K., Jelinek, R., 1954. *Theoretische Bodenmechanik*. Springer-Verlag, Berlin.
- Uteau, D., Pagenkemper, S.K., Peth, S., Horn, R., 2013. Root and time dependent soil structure formation and its influence on gas transport in the subsoil. *Soil Tillage Res.* 132, 69-76.
- Zhang, B., Horn, R., Hallett, P.D., 2005. Mechanical resilience of degraded soil amended with organic matter. *Soil Sci. Soc. Am. J.* 69, 864-871.

9 CONCLUSIONS

Investigations of studied soils showed that the changes in soil physical properties are a function of soil texture, matric potential, soil structure (artificially prepared as vertical holes), and type, intensity and duration of loading. It can be concluded, that

1) static loading or cyclic loading can result in on one hand a decrease in total pore volume, which was attributed to the substantial loss of air-filled macropores firstly during compaction if ignoring the shearing effects. On the other hand, the pore size distribution, continuity and tortuosity of soil pores will be altered. Compared to static loading, the further deterioration of pore functionality will occur during the subsequent cyclic loading. For a given stress application, the extent of changes in soil pore functions increased with increasing the compaction levels.

2) Due to the decrease in air-filled porosity, air permeability (K_a) and relative gas diffusivity (D_s/D_o) also decreased after compaction in most cases. However, the effect of soil compaction was not always negative. The values of K_a and D_s/D_o increased sometimes, probably because of the reduction of water blockage effect (an increase in pore continuity and a decrease in pore tortuosity) during compaction. Therefore, besides the volume of soil macropores, soil gas transport parameters are also controlled by the intensity properties (i.e. pore continuity and tortuosity) of pore functions.

3) Pore functions and gas transport are intensely controlled by soil structure (artificially vertical holes). There was a minor effect on air-filled porosity after having drilled vertical holes. Irrespective of this, the ability of soil pore functions (more continuous but less tortuous pores) and gas transport were improved significantly by these five vertical holes. The effect of preferential macropores on values of K_a was more pronounced, while values of D_s/D_o were not. Therefore, artificially vertical holes eliminated the differences in values of K_a among treatments, but the obvious differences in values of D_s/D_o still existed.

4) In the case of static loading, an intensive vertical displacement was observed in the beginning of stress application, followed by a constantly slight decline with

increasing loading time. Soil mechanical deformation resulted in a decrease or an increase in pore water pressure due to the change in pore functionality and hydraulic properties for different treatments. In all soil samples, stress-induced strain patterns were identical under the same type of loading (static), but in soils with vertical holes smaller additional changes occurred. In the case of subsequent cyclic loading, compaction resulted in the further vertical displacement and an increase in pore water pressure (less negative) during loading. A rebound behaviour was observed and pore water pressure decreased (more negative) during unloading.

5) For a given stress application, the vertical displacement increased with applied stresses, which resulted in the higher extent of water flux, and finally more pronounced changes in pore water pressure were observed under higher compaction level. However, for a given compaction level, vertical displacement and change in pore water pressure increased with increasing the frequency and duration of loading.

6) The alternation of soil strength under compaction is reflected by the effective stress, which depends on the change in pore water pressure and degree of saturation. In our experiment, we found that as the stress application advanced, the effective stress decreased (i.e. soils became more sensitive against external stress) for treatments of -60 hPa matric potential, and increased (i.e. soils became more stable to compaction) for treatments of -300 hPa matric potential for a given compaction level.

ACKNOWLEDGEMENT

First of all, I would like to extend my sincere gratitude to my supervisor, Prof. Rainer Horn, who has offered me valuable suggestions in the academic studies. I do appreciate his patient instruction, insightful criticism and expert guidance during the writing of this dissertation.

The fund support of my study by the State Scholarship Fund from the China Scholarship Council (CSC) for Xiafei Zhai (No.201406300027) is gratefully acknowledged.

I am also deeply thankful colleagues of Kiel University who I worked with. Many thanks to Pia Heibach, Thomas Neugebauer who helped me to collect soil samples in the fields, Jens Rostek, Veronika Schroeren, Anneka Mordhorst and Christoph Haas who taught me how to use the experimental instruments I needed. Also many thanks to other colleagues who provided good study environments and were willing to help me when I met with some difficulties.

Last but not the least, I am indebted to my beloved parents and my fiancé Luo Chao for their continuous care and encouragement through all these years. Due to their support without a word of complaint, I can do whatever I want to do without any burdens.

Xiafei Zhai

28 Apr. 2019

Kiel University, Germany

CURRICULUM VITAE

PERSONAL DETAILS

Name: Xiafei Zhai

Place of birth: Henan, China

Date of birth: 22.07.1989

Nationality: Chinese

Marital status: Engaged

Office address: Institute of Plant Nutrition and Soil Science, Kiel University,
Olshausenstr. 40, 24118 Kiel, Germany

Email: x.zhai@soils.uni-kiel.de or xiafeizhai@gmail.com

EDUCATIONS

10/2014-06/2019 PhD Study
Institute of Plant Nutrition and Soil Science, Kiel University,
Germany
Supervisor: Prof. Dr. Rainer Horn

09/2011-06/2014 Master Degree
College of Natural Resources and Environment, Northwest A&F
University, China
Supervisor: Prof. Dr. Zhao Ying

09/2007-07/2011 Bachelor Degree
College of Natural Resources and Environment, Northwest A&F
University, China

